

國立臺灣大學公共衛生學院環境衛生研究所



博士論文

Institute of Environmental Health

College of Public Health

National Taiwan University

Doctoral Dissertation

發光二極體做為室內照明光源對視網膜影響之大鼠研究

Light Emitting Diode (LED) lighting as domestic light  
source and retina injury in rat models

商育滿

Yu-Man Shang

指導教授：王根樹 博士

楊長豪 博士

Advisor: Gen-Shuh Wang, Ph.D.

Chang-Hao Yang, MD. Ph.D.

中華民國 106 年 2 月

February, 2017

# **Light Emitting Diode (LED) lighting as domestic light source and retina injury in rat models**



A dissertation prepared by

Yu-Man Shang

Submitted to

**The Institute of Environmental Health**

**College of Public Health**

In partial fulfillment of the requirements for the degree of  
Doctor of Philosophy in the subject of **Environmental Health**

**National Taiwan University**

Taipei, Taiwan

February, 2017



## Dedication

This thesis is the rich accumulation of sweat from hard work, tears from obstruction, and inevitable sleepless nights which every graduate student endures. But more importantly, it is the memories of all accomplishments and the joy of finding my true courage toward an ultimate goal on this journey. It is for you, ones that I love, that I dedicate this piece of my life.

Thank you, Mom, Dad in heaven, Miles, Dr. Cheng, Tim, Zoe, and all my dear friends along the way.



## Acknowledgements

I am blessed to have many great mentors who guide my way through the journey of this research.

Dr. Gen-Shuh Wang who is my advisor deserves the deepest appreciation for finishing this study. He paves every step of my path to success throughout the courses of my doctoral study. He gives me the freedom to create a vision, offers his wise advices when I am troubled, and brings laughs to the room when I am depressed. He is always generous in time for my requests during his extremely tight schedule. He has faith in me, and that empowers me to do anything which might seem impossible to others from the beginning. I would like to express my tremendous appreciation and gratitude to him for his help and steadfast encouragement in all my professional endeavors.

I also deeply thank Dr. Chang-Hao Yang for his prodigious knowledge in ophthalmology and his guidance to my experiments. Thank him for the technical training and resource sharing as well as the amity throughout the years. He strengthens my passion of pursuing a scientific career with rigorous practices.

Deep appreciation is also given to Dr. David H. Sliney who guides me the way to conquer the toughest challenges and introduces me to many professional conferences and committees. He demonstrates the contagious enthusiasm of a noble scholar and earns my highest respect for all his compassion and decency.

Countless gratitude is also given to Dr. Li-Ling Lee who provides tremendous resources and advices from many aspects. She brightens up my days when the light is out. For all the greetings and encouragements during my tough times, thank her for the unrequited supports.

Many thanks are also given to the other members of my dissertation committee: Dr. Dan-Pai Feng, Dr. Luke Long-Kuang Lin, Dr. Pau-Chung Chen, Dr. Yaw-Huei Hwang, Dr. Chin-Pao Cheng, and Dr. Tzu-Chau Chang. I have benefited remarkably from their professional comments and valuable suggestions.

Finally, I would like to thank all the members from Dr. Yang's retinal research lab and Dr. Lee's LED research lab, especially for the countless discussions and technical assistances from Ms. Zi-Yun Weng, Mr. Eric Wang, Mr. Bo-Lin Feng, Mr. Kevin Lin and many others.

I am forever indebted to you all.

## 中文摘要



照明是生活的基本需求，人工光源也由照亮空間的基本要求，延伸至人因工程所關注的健康與舒適考量。近來各界積極推動節能照明，發光二極體 (Light Emitting Diode, LED) 照明以環保節能的優勢深獲期許，其中室內照明以白光 LED 做為替代光源頗具潛力與代表性。而 LED 屬固態發光 (Solid State Lighting, SSL) 的一種，是由半導體材料所製成的發光元件，不同材料與製程可發出不同的波長，視覺系統藉此感受到不同顏色的光。LED 的發光特性與光學表現適合應用於指示性的用途，當轉型發展成為一般照明，目前符合經濟效益且成為主流的白光 LED，大多為藍色晶片搭配黃色螢光粉的 (phosphate-conversion, PC) 的型態，而其光譜有一大區間落於 400 nm – 550 nm，屬於視網膜藍光危害區，且其中尖銳的藍光波峰所呈現的單點強度，可能對視網膜產生傷害而未被人眼察覺，長期低劑量的暴露也可能對黃斑部產生累積性的負面效應而不自覺。因此 LED 照明如何呈現最適合生理機轉的光學表現，有待醫學及公衛體系的專業研究並加以定義。

本研究之目的在探討以白光 LED 為室內照明光源時，其所含不同波長光線對於視網膜的潛在影響。有別於前人研究多以短時間（數秒至數天）的方式進行，本研究針對白光 LED 作為室內照明光源之波長與頻譜分佈進行長期低暴露分析，透過大鼠動物實驗，以視網膜電波圖 (electroretinogram, ERG) 檢查視網膜功能上所受的衝擊，同時以多種組織切片觀察感光細胞形貌上的改變，以及透過生化分析觀察細胞受到氧化壓力而引發的凋亡和壞死狀況，探討視網膜光傷害的機轉，研析白光 LED 照明對使用者視網膜生理結構的影響。為達成此研究目的，整體研究架構以二階段實驗方式進行。

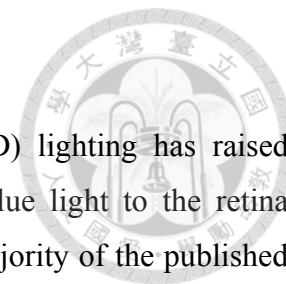
第一階段以藍光 LED (460 nm) 以及全頻譜的白光 LED (CCT 6500) 搭配相對應的螢光燈管 (CFL, CCT 6500) 和黃光 (CFL, CCT 2700) 對大鼠進行照光暴露實驗，以證實在參數相同的暴露環境中，LED 比 CFL 更容易誘發視網膜的光傷害。接著第二段實驗以三種不同波段的 LED 光源，包括藍光 (460 nm)、綠光 (530 nm) 及紅光 (620 nm) 進行比對，透過更深入的生化分析工具，觀察 LED 所誘發的視網膜光傷害是否存在波長的劑量效應關係，以及其傷害機轉。實驗結果證實大鼠視網膜

感光細胞在不同光源的暴露下產生的光化學危害 (photochemical injury)，細胞結構變化是由氧化壓力所引發，且呈現波長的劑量效應關係。相同暴露參數下，波長越短造成的傷害越強，因而推論在大鼠實驗中，做為室內照明的白光 LED 光源中，藍光對視網膜的危害貢獻最多。

以環境衛生的角度，本研究結果提醒以 LED 做為室內照明時，必須特別留意頻譜中藍光的比重分佈。同時也提供予相關產業於產品研發時挹注健康的考量因子，並呼籲使用者注意暴露風險與防範措施。然而以風險評估的觀點而言，此動物實驗結果並無法直接定義人類的使用風險，尚須經過適當的評估或甚至進一步的人體暴露分析才能得到具體結論，未來應有更多學者延續此主題的研究。

**關鍵詞：**視力;視網膜;光傷害;照明;氧化壓力;發光二極體;藍光危害

## Abstract



The rapid development of white light-emitting diode (LED) lighting has raised serious retinal hazard concerns. LED delivers higher levels of blue light to the retina compared to conventional domestic light sources. However, the majority of the published retinal blue light injury studies are either in anesthetized animals or *in vitro* with high exposure intensity for acute injury assessment. The significance of the blue component in LED lighting contributing to the injury needs further study in a free-running animal model with chronic exposure setting.

This study intends to assess the potential adverse effects from exposure to the domestic LED lights with different wavelengths. Two sets of LED-induced retinal neuronal cell damage in the Sprague-Dawley rat models through functional, histological, and biochemical measurements were completed. In the first part of study, blue LED (460 nm) and full-spectrum white LED (CCT 6500) coupled with matching compact fluorescent lamps (CFL) were used for exposure treatments. The results suggested that the LED white light has a higher chance to induce retinal photochemical injury (RPI) than does the conventional CFL white light. The results raise questions related to adverse effects on the retina from chronic LED light exposure compared to current lamp sources that have less blue light. To further assess the risk, LED induced RPI with wavelength dependency and its mechanism were focused on the second part of study.

Although there has been a wealth of studies describing the RPI associated with wavelength dependency previously, the experimental settings were focused on high intensity light exposure over a short period of time (a few seconds to 3 days) for acute or subacute toxicity assessments. The tested animals were anesthetized or forced to stare into the lights in most of the cases, and the light sources varied due to contemporary technology availability. Thus, in the second part of study, blue (460 nm), green (530 nm), and red (620 nm) LEDs were investigated to measure how specific bands were responsible for retinal phototoxic effects under the same irradiance level at  $102 \mu\text{W}/\text{cm}^2$ . Both functional and histopathological results indicated blue light-induced RPI. The oxidative stress and iron-related molecular markers suggested that blue LED exposure increased retinal toxicity compared with longer wavelength LEDs. Biochemical assays on lipid, protein, and DNA also showed higher oxidative expressions after blue LED exposure.

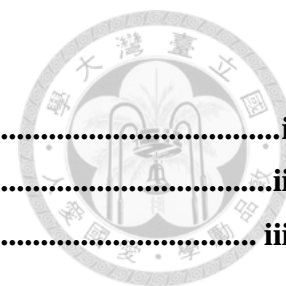
LED light-induced retinal injury could be due to oxidative stress through iron overload. Several biomarkers confirmed the greater risk of LED blue-light exposure in awake, task-oriented rod-dominant animals.

Based on the study results, it is concluded that LED light exposure may induce RPI through oxidative stress with a wavelength-dependent effect. More importantly, the long-term effects of exposure to low doses of domestic lighting may lead to serious retinal degenerative diseases. Several functional, morphological, and biochemical measurements were applied to characterize the exposure results associated with this injury. The wavelength-dependent effect should be considered carefully when switching to LED domestic lighting applications. However, the exact mechanism underlying these effects will be the subject of ongoing investigation with more analytical methods. The interpretation from the animal study to human applications should also be carefully considered based on the risk assessment perspective.

**Keywords: LED, light damage, retina, eye, retinal light injury, blue light, oxidative stress**



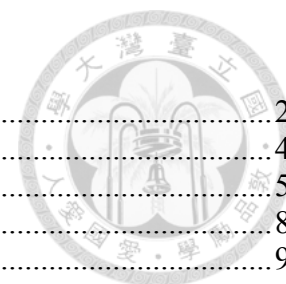
# Table of Contents



<b>Dedication</b> .....	<b>i</b>
<b>Acknowledgements</b> .....	<b>ii</b>
<b>中文摘要</b> .....	<b>iii</b>
<b>Abstract</b> .....	<b>v</b>
<b>Table of Contents</b> .....	<b>vii</b>
<b>List of Figures</b> .....	<b>ix</b>
<b>List of Tables</b> .....	<b>x</b>
<b>Abbreviations</b> .....	<b>xi</b>
<b>1 INTRODUCTION</b> .....	<b>1</b>
<b>1.1 Background</b> .....	<b>1</b>
1.1.1 Light affects daily living through vision.....	1
1.1.2 Artificial light sources .....	1
1.1.3 Energy saving lighting .....	3
1.1.4 Learning from the history .....	3
<b>1.2 Objectives</b> .....	<b>4</b>
1.2.1 Direct outcome.....	5
1.2.2 Indirect influence .....	6
<b>2 LITERATURE REVIEW</b> .....	<b>7</b>
<b>2.1 Light</b> .....	<b>7</b>
2.1.1 Light Source.....	7
2.1.1.1 Light Properties .....	7
2.1.2 Light Measurement .....	8
2.1.2.1 Color Temperature .....	8
2.1.2.2 Intensity.....	11
2.1.3 Solid State Lighting (SSL).....	14
2.1.3.1 Solid State Light Segments .....	14
2.1.3.2 LED Light Characteristics.....	14
2.1.3.3 LED Light for Lighting.....	16
2.1.3.4 White Light LED Performance Diversification.....	20
<b>2.2 Retinal Physiopathology</b> .....	<b>22</b>
2.2.1 Retina React with Light .....	22
2.2.2 Retina Light Injury.....	24
2.2.3 Action Spectrum of Retinal Light Injury .....	26
2.2.4 Progress of Photoreceptor Light Induced Injury.....	27
2.2.5 Animal Model for Retinal Light Injury .....	28
<b>2.3 Potential retinal injury induced by chronic exposure to LED light</b> .....	<b>30</b>
2.3.1 Data Collection and Selection.....	30
2.3.2 Retinal Light Injury vs. LED Lighting .....	31
2.3.3 Retinal Light Injury Mechanisms .....	32
2.3.4 Principal of the domestic lighting exposure.....	33
<b>3 RESEARCH DESIGN AND METHODS</b> .....	<b>34</b>
<b>3.1 Hypotheses of photochemical injury</b> .....	<b>34</b>
<b>3.2 Animal handling and light exposure plan</b> .....	<b>35</b>
3.2.1 Animals and rearing conditions .....	35
3.2.1.1 For the comparison of CFL vs. LED .....	35
3.2.1.2 For the comparison of RGB LEDs .....	37
3.2.2 Light source .....	37

3.2.2.1	For the comparison of CFL vs. LED .....	37
3.2.2.2	For the comparison of RGB LEDs .....	39
3.2.3	Light exposure .....	40
3.2.3.1	For the comparison of CFL vs. LED .....	40
3.2.3.2	For the comparison of RGB LEDs .....	41
<b>3.3</b>	<b>Sample pretreatment.....</b>	<b>42</b>
<b>3.4</b>	<b>Analytical Methods.....</b>	<b>43</b>
3.4.1	Electroretinography (ERG).....	43
3.4.2	Hematoxylin and eosin (H&E staining).....	45
3.4.3	Transmission electron microscopy (TEM) analysis.....	46
3.4.4	Terminal deoxynucleotidyl transferase dUTP nick end labeling (TUNEL) .....	48
3.4.5	Immunohistochemistry (IHC).....	48
3.4.6	Free radical assay (reactive oxidative species, ROS) .....	49
3.4.7	Western blotting (WB).....	49
3.4.8	Hydrogen peroxide (H <sub>2</sub> O <sub>2</sub> ) assay .....	50
3.4.9	Total iron and ferric (Fe <sup>3+</sup> ) assay .....	51
<b>3.5</b>	<b>Statistical analysis.....</b>	<b>51</b>
<b>4</b>	<b>RESULTS AND DISCUSSION .....</b>	<b>52</b>
<b>4.1</b>	<b>White LED at domestic lighting level to induce retinal injury.....</b>	<b>52</b>
4.1.1	Electrophysiological response shows photoreceptor cell function loss .....	52
4.1.2	Retinal histology–H&E staining showing layer damages.....	54
4.1.3	Apoptosis Detection - TUNEL staining detects nuclear apoptosis .....	56
4.1.4	TEM demonstrations on the cellular injury .....	58
4.1.5	Immunohistochemistry (IHC) staining results indicating retinal light injury .....	60
4.1.6	Oxidative Stress -- superoxide anion O <sub>2</sub> <sup>-</sup> shows the injury .....	62
<b>4.2</b>	<b>Mechanism of LED induced retinal injury and its wavelength dependency.....</b>	<b>64</b>
4.2.1	Functional and morphological alterations.....	64
4.2.2	RPI oxidative stress markers expression.....	70
4.2.3	Iron metabolism and superoxide products .....	73
<b>4.3</b>	<b>Discussion .....</b>	<b>78</b>
4.3.1	Retinal light injury susceptibility between human and experimental animals.....	78
4.3.2	Oxidative stress induced injury.....	79
4.3.3	Low-intensity chronic exposure.....	79
4.3.4	LED-induced RPI is wavelength-dependent.....	80
4.3.5	Oxidative stress and photon absorption-stimulated RPI .....	80
4.3.6	Iron-related RPI oxidative pathway .....	82
4.3.7	Wavelength (hue) discrimination and specie differences .....	82
4.3.8	Environmental health perspectives .....	83
<b>5</b>	<b>CONCLUSION .....</b>	<b>85</b>
<b>5.1</b>	<b>LED lighting induces retinal light injury .....</b>	<b>85</b>
<b>5.2</b>	<b>Blue light makes the most contribution to retinal light injury .....</b>	<b>86</b>
<b>5.3</b>	<b>The way ahead .....</b>	<b>86</b>
<b>6</b>	<b>REFERENCES.....</b>	<b>89</b>
<b>7</b>	<b>APPENDIX.....</b>	<b>95</b>

## List of Figures



<b>Figure 1 Artificial light source branches</b> .....	2
<b>Figure 2 Illuminance recommendations fluctuations since 1930</b> <sup>5, 6</sup> .....	4
<b>Figure 3 Study Objectives</b> .....	5
<b>Figure 4 Electromagnetic radiation ranges</b> .....	8
<b>Figure 5 Example of LED color temperature correlation</b> .....	9
<b>Figure 6 CIE 1931 chromaticity diagram</b> <sup>8</sup> .....	11
<b>Figure 7 (A) LED in details and (B) illustration of LED electron convert to photons</b> ....	15
<b>Figure 8 Light and heat emission direction (A) incandescent lamp; (B) LED chip</b> <sup>9</sup> ....	15
<b>Figure 9 White light LED converting methods</b> <sup>11, 12</sup> .....	17
<b>Figure 10 Spectral representations of white light using LEDs</b> <sup>4</sup> .....	18
<b>Figure 11 LED spectral power distribution in different color temperature models</b> <sup>4</sup> ....	19
<b>Figure 12 Spectrum distribution for three domestic light sources</b> <sup>4</sup> .....	21
<b>Figure 13 Light path within the retina layers</b> <sup>15</sup> .....	23
<b>Figure 14 Light absorption and transmittance in the eye</b> <sup>4, 18, 19</sup> .....	24
<b>Figure 15 Action spectrum of retinal light damage</b> <sup>17</sup> .....	27
<b>Figure 16 Scheme of the photoreceptor light induced injury progress</b> .....	28
<b>Figure 17 Sprague-Dawley (SD) rats acute and chronic retinal light injury</b> <sup>27</sup> .....	29
<b>Figure 18 Literature relation map</b> .....	31
<b>Figure 19 Timeframe of the experimental design</b> .....	36
<b>Figure 20 Light source spectral power distribution (SPD) curves</b> .....	38
<b>Figure 21 Custom made LED light strip</b> .....	39
<b>Figure 22 LED light source spectral power distribution (SPD) curves</b> .....	40
<b>Figure 23 Diagram of light exposure setting</b> .....	42
<b>Figure 24 (A) Eye enucleation and (B) retina tissue removal</b> .....	43
<b>Figure 25 ERG operation</b> .....	44
<b>Figure 26 Diagram of retina response components to ERG stimulation</b> <sup>15</sup> .....	45
<b>Figure 27 Specimen of a retina slice</b> .....	47
<b>Figure 28 TEM observation instrument (JEOL JEM-1400)</b> .....	47
<b>Figure 29 ERG responses after light exposure</b> .....	53
<b>Figure 30 Retinal light injury after 9 d or 28 d of exposure analyzed by H&amp;E staining</b> 55	
<b>Figure 31 Light-induced retinal cell apoptosis tested by TUNEL labeling</b> .....	57
<b>Figure 32 Retinal cellular injury studied by TEM</b> .....	59
<b>Figure 33 Retinal light injury labeling after 9 d of exposure by IHC</b> .....	61
<b>Figure 34 A reactive oxygen species assay after 3 d and 9 d of light exposure</b> .....	63
<b>Figure 35 Electroretinography (ERG) responses</b> .....	66
<b>Figure 36 Histological analysis</b> .....	67
<b>Figure 37 Retinal cellular injury studied by transmission electron microscopy (TEM)</b> 68	
<b>Figure 38 Molecular apoptotic marker detection</b> .....	69
<b>Figure 39 Retinal light injury molecular labeling by immunohistochemistry (IHC)</b> .....	71
<b>Figure 40 Western blot (WB) assay of anti-oxidant enzymes</b> .....	72
<b>Figure 41 Western blot (WB) assay of iron metabolism markers</b> .....	75
<b>Figure 42 Iron metabolism and superoxide products</b> .....	76
<b>Figure 43 Light source registration at California energy commission</b> .....	84

## List of Tables

<b>Table 1 The photometric quantities</b> .....	13
<b>Table 2 photometric and radiometric units</b> .....	13
<b>Table 3 Exposure groups allocation</b> .....	37



## Abbreviations



1. age-related macular degeneration (AMD)
2. analysis of variance (ANOVA)
3. American National Standards Institute (ANSI)
4. Association for Research in Vision and Ophthalmology (ARVO)
5. Certification Body Testing Laboratory (CBTL)
6. correlated color temperature (CCT)
7. ceruloplasmin (CP)
8. chemiluminescence (CL)
9. compact fluorescent lamp (CFL)
10. Commission Internationale de l'Eclairage (International Commission on Illumination, CIE)
11. distilled water (DW)
12. electromagnetic (EM)
13. electroretinography (ERG)
14. ferric ( $\text{Fe}^{3+}$ )
15. ferritin (Ft)
16. ferroportin (Fpn)
17. ferrous ( $\text{Fe}^{2+}$ )
18. full width at half maximum (FWHM)
19. ganglion cell layer (GCL)
20. glutathione peroxidase (GPx1)
21. hematoxylin and eosin (H&E) staining
22. hemeoxygenase-1 (HO-1)
23. hydrogen peroxide ( $\text{H}_2\text{O}_2$ )
24. hydroperoxyl radical ( $\text{HO}_2$ )
25. Kelvin (K)
26. hydroxyl radicals ( $\text{OH}\cdot$ )
27. Institutional Animal Care and Use Committee (IACUC)
28. immunohistochemical (IHC)
29. inner nuclear layer (INL)
30. light-emitting diode (LED)
31. lipid electron donors (LH)
32. lipid hydroperoxide ( $\text{LO}_2\cdot$ )
33. lipid radical ( $\text{L}\cdot$ )
34. manganese superoxide dismutase (MnSOD)
35. organic light-emitting diodes (OLED)
36. outer nuclear layer (ONL)
37. outer segment (OS)
38. oxygen ( $\text{O}_2$ )
39. personal protective equipment (PPE)
40. phosphate buffered saline (PBS)
41. phosphate-conversion (PC)
42. photoreceptor inner segment (PIS)
43. polymer light-emitting diodes (PLED)
44. photoreceptor outer segment (POS)
45. poly (ADP-ribose) polymerase-1 (PARP-1)
46. radioimmunoprecipitation assay (RIPA)
47. reactive oxygen species (ROS)

48. rod outer segment (ROS) membranes
49. red, green, and blue (RGB)
50. retinal photochemical injury (RPI)
51. retinal pigment epithelium (RPE)
52. scientific committee on emerging and newly identified health risks (SCENIHR)
53. spectral power distribution (SPD)
54. Sprague–Dawley (SD) rats
55. superoxide anion ( $O_2^-$ )
56. superoxide dismutase (SOD2)
57. solid-state lighting (SSL)
58. terminal deoxynucleotidyl transferase dUTP nick end labeling (TUNEL)
59. transferrin (Tf)
60. transferrin receptor (TrfR)
61. transmission electron microscopy (TEM)
62. ultraviolet (UV)
63. western blotting (WB)



# 1 INTRODUCTION



## 1.1 Background

### 1.1.1 Light affects daily living through vision

It is estimated that over 80% of the information processed in the human brain is directly or indirectly interpreted by the visual system. Because of the nature of print and near-work function involved, the task of reading requires particular greater accuracy <sup>1</sup>. To perform this function, the light source is necessary and essential to ocular system. The complex interactions within the ocular system provide the ability to interpret photic stimulus into visual information. When light enters the eye, and reaches the retina, the visual perception is initiated by transforming the radiant energy into visual transduction signals. This transformation also creates toxic potential and the eyes have developed several protective mechanisms defending light-induced injury. However, the injury may still occur under certain conditions which has been intensively reported in clinical and basic science literature <sup>2</sup>.

### 1.1.2 Artificial light sources

The burning or heated light source (incandescence) has been essentially used for many centuries. Some flame-operated lamps (namely kerosene, carbide and gas lamps) and candles are still practical to some situations. Those lamps were generated through chemical reaction to heat materials. The emitted spectrum is continuous with low correlated color temperature (CCT) due to the limited irradiating component and poor luminous efficacy <sup>3</sup>. According to a 2012 report by European Commission-scientific committee on emerging and newly identified health risks (SCENIHR), there are still approximately 1.6 billion

people who do not have access to electrical grid and being forced to rely on flame-operated lamps in everyday life. Alternatively, artificial light can also be generated without lighting up a fire (luminescence). Incandescent and luminescent lamps are two artificial lighting technologies in use today. The end category can be further divided into discharge / fluorescence lamps and solid state lighting (SSL) devices, respectively, as shown in Figure 1.

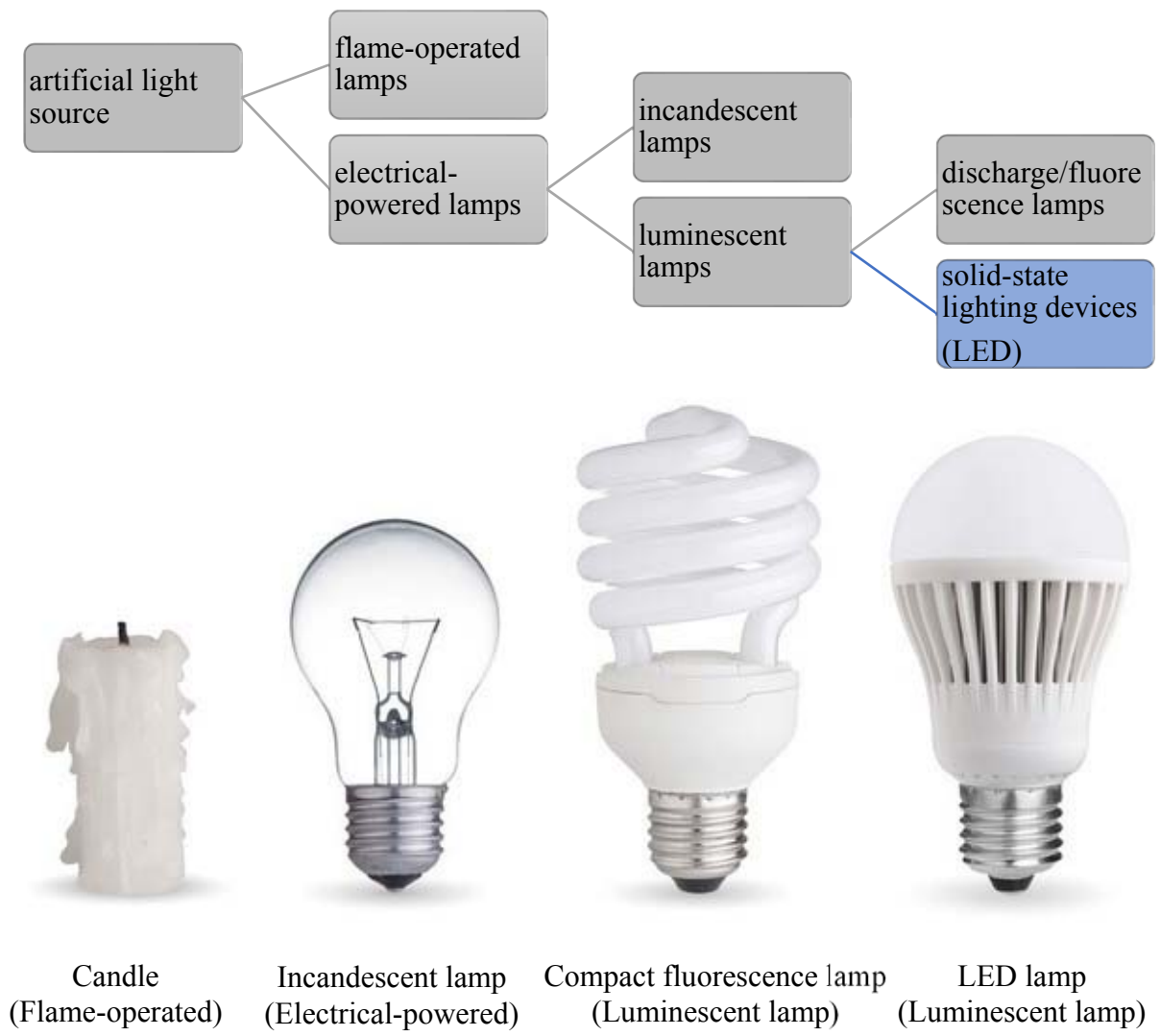
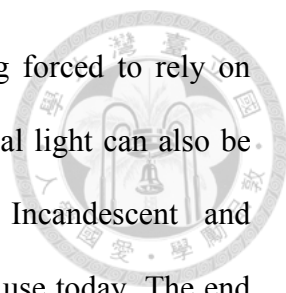


**Figure 1 Artificial light source branches**

Pictures from the web source: <http://54.204.81.18/news/stories/311024-brandpost-the-evolution-is-here-moving-beyond-log-centric-siem>



### 1.1.3 Energy saving lighting

Among a wide variety of artificial lighting selections, the most recognized branch of SSL, light-emitting diodes (LED), is promoted by the energy conservation trend globally. With the announcement of LED for indoor lighting since 2009, the technology improvement in all aspects surged rapidly. However, LEDs emit higher levels of blue light compared to conventional light sources. This is also the first time that humans have experienced such extensive blue-light exposure in the history<sup>4</sup>. From an environmental health perspective, retinal light injury and the potential risks for chronic exposure from using LEDs as a domestic light source require assessment before further development of this important, energy-saving technology.

### 1.1.4 Learning from the history

Learning from the history (see Figure 2 and text explain in Appendix), oscillations which are solely social-economical driven on the illuminance recommendations for several decades. The health factor was not even the concern in some periods of time. However, researchers are now able to evaluate the full scope of new lighting developments with the knowledge and awareness available. Therefore, it is necessary to include the health concern along with the excitement of LED lighting for general applications.

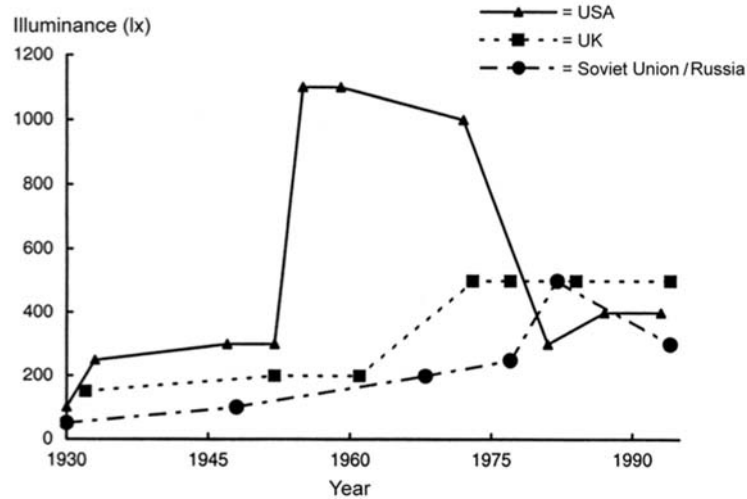


**Figure 2 Illuminance recommendations fluctuations since 1930** <sup>5,6</sup>

## 1.2 Objectives

As shown in Figure 3, the objective of this study is to investigate the ocular safety (majorly retina) of white light LED to be used as a constant domestic light source in a pathophysiological perspective. The core is to develop a scientific assessment report for further expansion. There is an urgent need for a better evaluation of potential light toxicity, depending on the different artificial light sources available, and upon chronic exposure of different populations to define clear guidelines for manufacturers and associated regulation officials.

## Objective

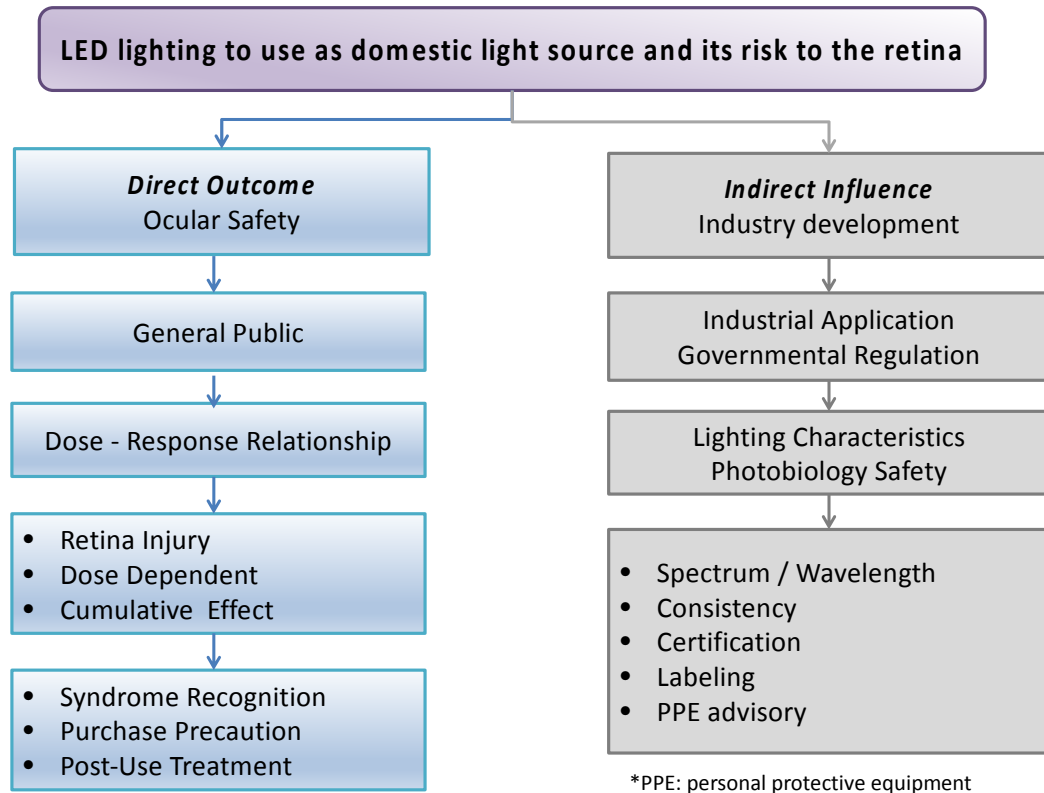


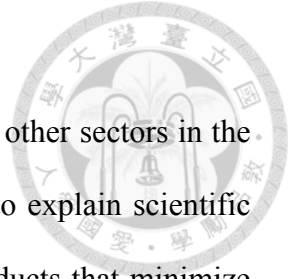
**Figure 3 Study Objectives**

### 1.2.1 Direct outcome

Adapting LED lighting era, the availability of new imaging technology and constant improving analytical instrumentation for ocular research expands the understanding of the light-induced injury. The first aim of this study is to identify the injury pattern and its mechanisms in order to define intervention suggestions for general users. Among many risk factors affecting the severity of this type of injury, cumulative effect and dose dependent relationship of light intensity, spectrum distribution, and exposure duration are the main objectives of this study.

### 1.2.2 Indirect influence

It is also a further hope to bring continuous influences to other sectors in the path of LED lighting development. This study is expected to explain scientific findings for manufactures to design better LED lighting products that minimize the risk to retina function. It may further urge a need for regulation updates on the photobiology safety concern. Some critical health-related lighting characteristics including CCT, spectrum distribution, and consistency should be properly certificated and labeled. Additionally, personal protective equipment (PPE) should be created and advised for inevitable occupational exposure situations.



## 2 LITERATURE REVIEW

### 2.1 Light

#### 2.1.1 Light Source

Light exposure is necessary for the visual sensory operation and also essential for entraining the circadian system. However, light exposure can have both positive and negative effects on human health. Some impacts that can be recognized instantly after exposure and some prolonged after many years <sup>5</sup>.

##### 2.1.1.1 Light Properties

As shown in Figure 4, light is a part of electromagnetic (EM) radiation in the range from 400 nm to 780 nm or some say 700 nm (1 nm equals to  $10^{-9}$  m) that is visible to human eye. Similar to EM radiation, light is emitted by quantum state transition when excess energy is to be released in this specific wavelength range. Nature light sources occurs by heat, inelastic collisions and nuclear reactions involving atomic/electronic de-excitation activities <sup>5,7</sup>.

According to Boyce <sup>5</sup> and Held <sup>7</sup>, examples include: “(1) *the glowing appearance of fires, flames and other sources such as volcanic hot material, where thermal radiation is released;* (2) *the photochemical light generation of animals such as the glow-worm;* (3) *the Nordic light (aurora borealis) when sprinklings of elementary particles are trapped by the earth’s magnetic field and hit the outer atmosphere;* (4) *the bright sensation of the electric discharge through the air in lightning, and last but not least* (5) *the light emitted by the sun, which emerges from the hot plasma induced by hydrogen to helium fusion.*”



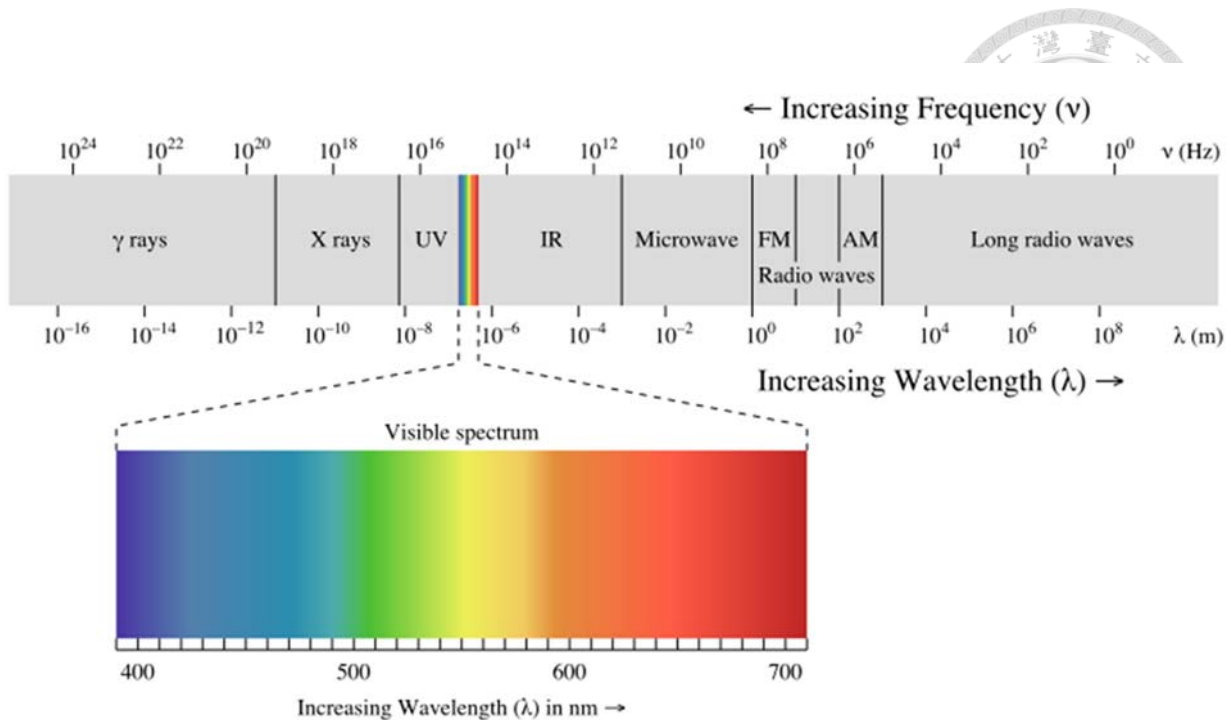


**Figure 4 Electromagnetic radiation ranges**

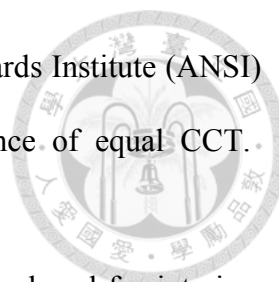
Picture from the web source: <https://publiclab.org/wiki/revisions/sample-curriculum-all-about-light>

## 2.1.2 Light Measurement

### 2.1.2.1 Color Temperature

Color temperature is the most important characteristic that describes how “cool” (bluish) or how “warm” (yellowish) of a light defined by CCT. The CCT metric, given in Kelvin (K), relates the appearance of a light to the color of a theoretical black body heated to certain temperatures. As temperature rises, the black body becomes red, orange, yellow, white, and finally blue<sup>3</sup>. Additionally, K characterizes the color of the emitted light, not the color of illuminated objects.

The CCT metric theorizes a complex spectral power distribution (SPD) to a particular amount. However, this conversion may produce discrepancy between numerical measurements and human perception. In some cases, two light sources with the same CCT can look very different, one appearing greenish and



the other appearing pinkish. Thus, American National Standards Institute (ANSI) further references Duv to quantify the chromaticity distance of equal CCT. ANSI has also set Duv tolerances for LED white lights <sup>8</sup>.

White LED light with any specific CCTs can now be produced for interior and exterior lightings (see Figure 5). Moreover, higher-CCT LEDs work more efficiently than lower-CCT ones due to quantum efficiency differences. Hence, some advance LED products created with dynamic CCT adjustment feature to increase control flexibility.

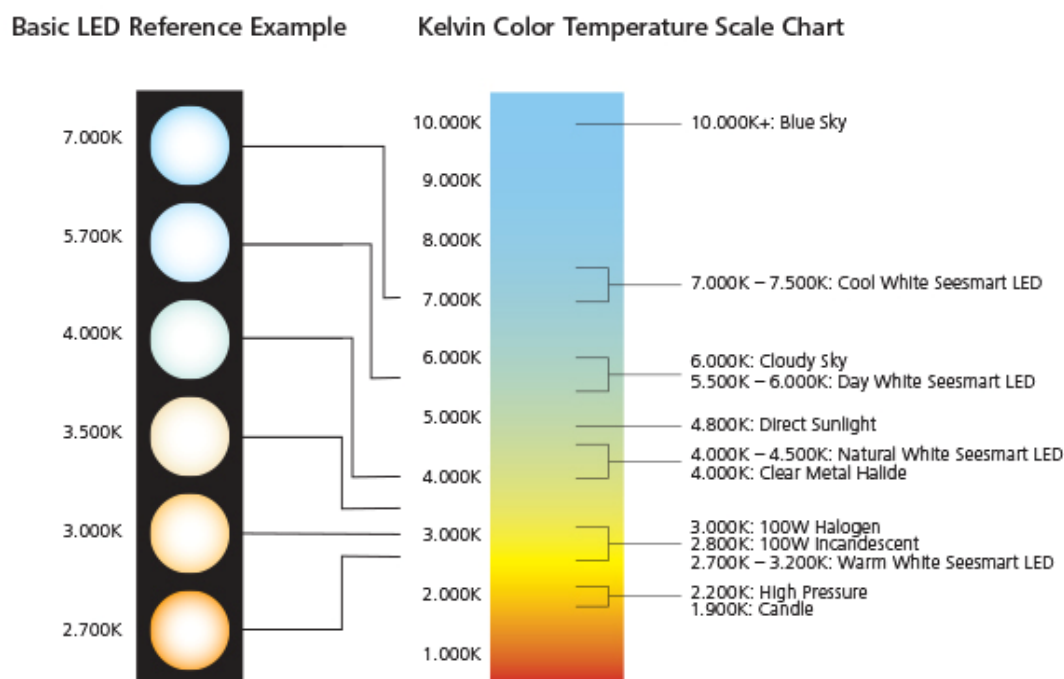
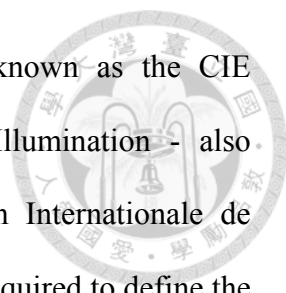


**Figure 5 Example of LED color temperature correlation**

Picture from the web source: <http://www.ledacademy.net/1-2-led-basic-parametres/>

Furthermore, chromaticity coordinates can also characterize the color of the light emitted by a light source. In this system, the spectral emission of a black body is defined by famous Planck's radiation law (see Figure 6) and is a function of its temperature only.



As shown in Figure 6, the values  $x$ ,  $y$ , and  $z$  are known as the CIE chromaticity coordinates. (International Commission on Illumination - also known as the CIE from its French title, the Commission Internationale de l'Eclairage). As  $x + y + z = 1$ , only  $x$  and  $y$  coordinates are required to define the chromaticity of a color. When a color can be represented by two coordinates, all colors can be represented on a two-dimensional surface. All pure colors with single wavelength should lie on the outer curved border (or so called spectrum locus). According to CIE definition, the straight line joining the ends of the spectrum locus is the purple boundary and is the locus of the most saturated purples obtainable. At the center of the diagram, there is a point called the equal energy point. That is the point where a colorless surface will be located. Close to the equal energy point is a curve called the Planckian locus. This curve passes through the chromaticity coordinates of objects that operate as a black body, i.e. the spectral power distribution of the light source is determined solely by its temperature.



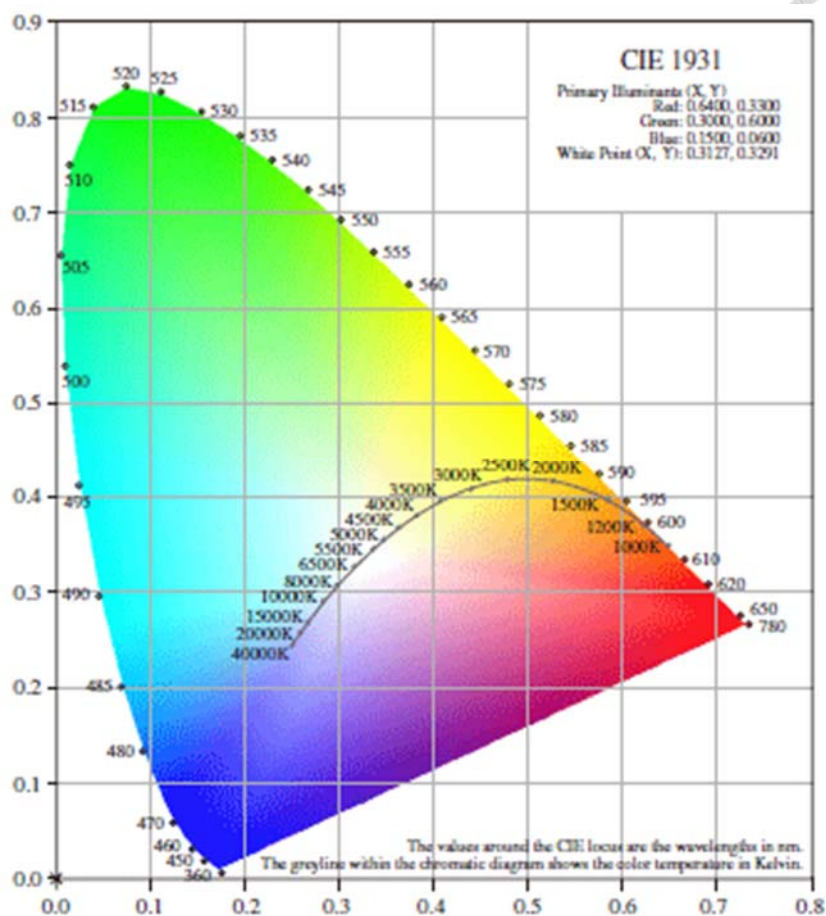
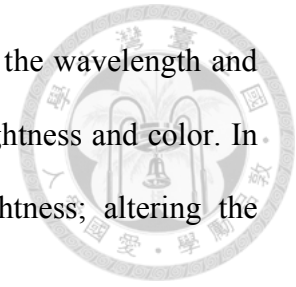


Figure 6 CIE 1931 chromaticity diagram <sup>8</sup>

### 2.1.2.2 Intensity

Explained in the book of human factors in lighting <sup>5</sup>, human visual system does not response constantly at all wavelengths in the range 380 nm - 780 nm (some say 400 nm - 700 nm). Thus, besides the electromagnetic spectrum quantified by radiometric, the spectral sensitivity of human visual system should be measured as well. The spectral sensitivity measurement is equivalent to visual effect that principled in perception of brightness. Any wavelength within the visible range (380 nm -780 nm) can be perceived in both brightness and color. Therefore, both wavelength and radiance should be considered and measured to complete a visual effect evaluation. For example, when two fields have the same wavelength but different radiances, the fields will appear differently. The one

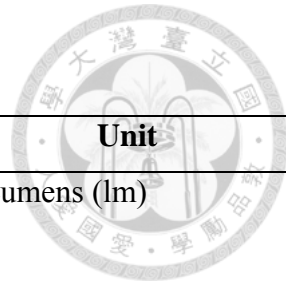
with higher radiance will be perceived brighter. When both the wavelength and radiance are different, the two fields will have different brightness and color. In this situation, changing the radiance can adjust the brightness; altering the wavelength can control the color of the light.



The relationship between the amount of light incident on a surface and the amount of light reflected from the same surface should be recognized. The total light output of a light source in all directions can be quantified by luminous flux. Moreover, the luminous flux emitted in a given direction can be measured by luminous intensity. In other words, luminous intensity is the luminous flux emitted per unit solid angle, in a specified direction. The unit of luminous intensity is the candela (cd), which is equivalent to a lumen per steradian. Luminous intensity is usually used to quantify the distribution of light from a luminaire.

The luminous flux falling on unit area of a surface is called the illuminance ( $\text{lm}/\text{m}^2$  or lux), which is the primary unit this study will adapt for light measurement. The luminous intensity emitted per unit-projected area of a source in a given direction is the luminance ( $\text{cd}/\text{m}^2$ ). The illuminance incident on a surface is the most widely used electric lighting design criterion. The luminance of a surface is correlate to its brightness. Table 1 summarizes some of the important photometric quantities, and Table 2 lists some of the photometric and radiometric measurement units that commonly used.

**Table 1 The photometric quantities**



<b>Measure</b>	<b>Definition</b>	<b>Unit</b>
Luminous flux	That quantity of radiant flux which expresses its capacity to produce visual sensation.	Lumens (lm)
Luminous intensity	The luminous flux emitted in a very narrow cone containing the given direction divided by the solid angle of the cone.	Candela (cd)
Illuminance	The luminous flux/unit area at a point on a surface.	Lumen/ meter <sup>2</sup> (lux)
Luminance	The luminous flux emitted in a given direction divided by the product of the projected area of the source element perpendicular to the direction and the solid angle containing that direction,	Candela/ meter <sup>2</sup> (nit)

**Table 2 photometric and radiometric units**

<b>Radiometry</b>		<b>Photometry</b>	
<b>Quantity</b>	<b>Units</b>	<b>Quantity</b>	<b>Units</b>
Radiant Energy	J	Luminous Energy	lm s
Radiant flux	W	Luminous Flux	lm
Irradiance	W/m <sup>2</sup> or mW/cm <sup>2</sup>	Illuminance	lm/m <sup>2</sup>
Radiant Intensity	W/sr	Luminous Intensity	lm/sr
Radiance	W/(m <sup>2</sup> sr)	Luminance	lm/(m <sup>2</sup> sr)



### 2.1.3 Solid State Lighting (SSL)

#### 2.1.3.1 *Solid State Light Segments*

Solid-state lighting (SSL) includes light converted by semiconductor light-emitting diode (LED), organic light-emitting diode (OLED), and polymer light-emitting diode (PLED) contrast to electrical filaments, plasma (used in arc lamps / fluorescent lamps), or gas. The concept of SSL comes from the solid-state electroluminescence, which differ from incandescent bulbs (use thermal radiation) and fluorescent tubes. SSL produces visible light with reduced heat generation and parasitic energy loss, compare to incandescent lamps. Among three SSL branches, LED is the most popular one in the current market. Following the same principle of fluorescent lamps, white LED lights are generated by photoluminescence approach.

SSL is largely promoted for many traffic related applications (namely traffic lights, vehicle lights, street and parking lot lights), building exteriors, and expanding to indoor lightings in the past decade.

#### 2.1.3.2 *LED Light Characteristics*

A LED (see Figure 7A) is principally monochromatic and the emitting wavelength determines its conversion efficiency. The value of the energy gap between the conduction and valence bands determines the dominant wavelength emitted by the semi-conductor junction (see Figure 7B). Additionally, the junction temperature controls the full width at half maximum (FWHM) value on the emitted spectral line. The LED was made and commercialized in red first, and a variety of colors can be created in today's technology <sup>4</sup>.

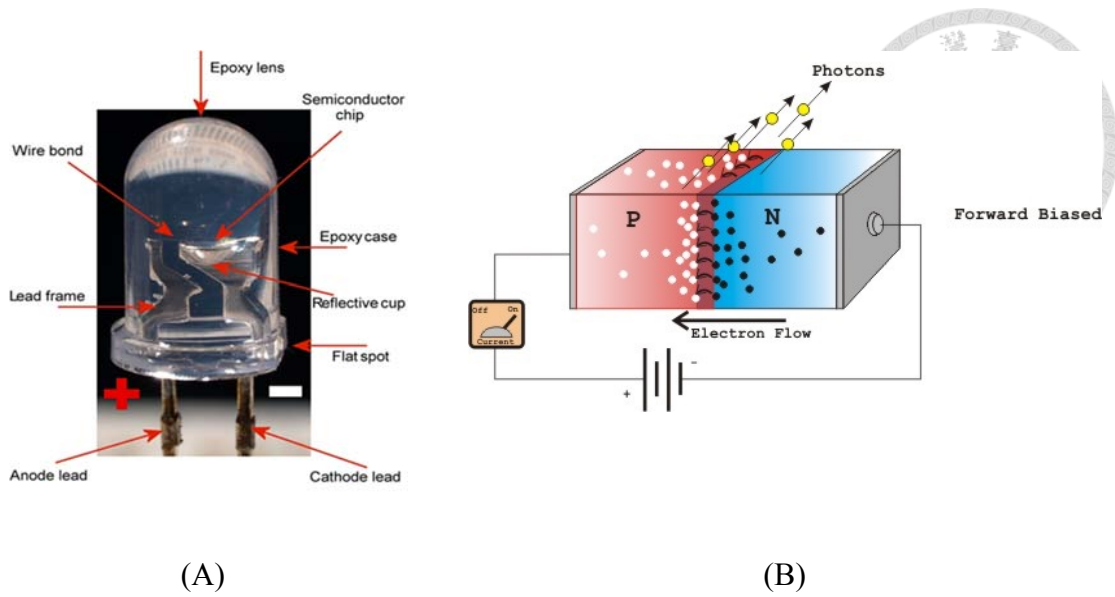


**Figure 7 (A) LED in details and (B) illustration of LED electron convert to photons**

Pictures from the web source: <http://www.imagesco.com/articles/photovoltaic/photovoltaic-pg4.html>

Besides the light intensity, the spectral distribution and unwanted heat transformation are other aspects dominating the lighting industry development. As illustrated in Figure 8A and 8B, the directions (angle) of light emission may result in very different illumination characteristics and efficacy.

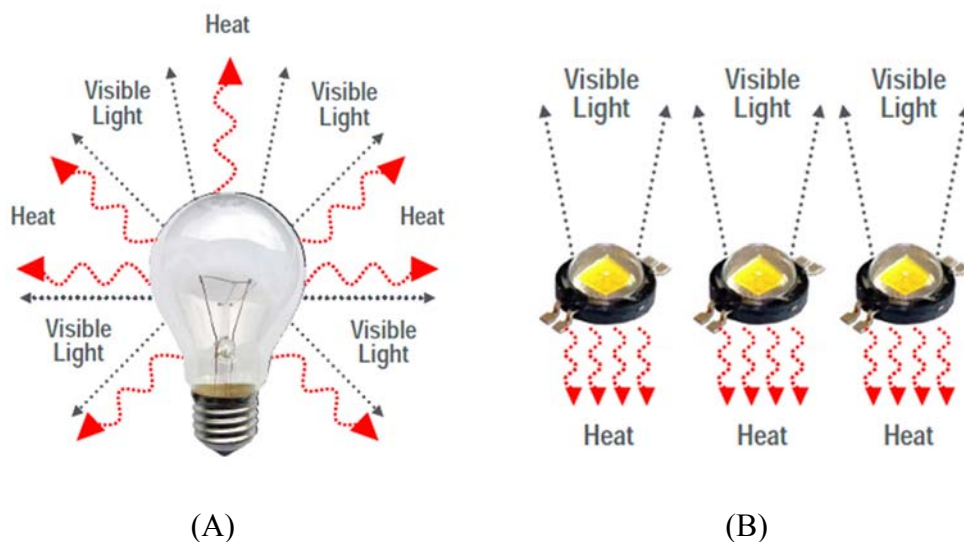


**Figure 8 Light and heat emission direction (A) incandescent lamp; (B) LED chip <sup>9</sup>**

### 2.1.3.3 LED Light for Lighting

The rising of LED in architecture and various of indoor lighting applications raises the concern of LED lighting quality <sup>9</sup>. LED lighting has already leading the industry by its advantages of energy efficiency, durability, versatility, and color control. LED lighting is forecasted to take 46% of general illumination lumen-hour sales by 2030, contributing 3.4 quads of energy savings annually <sup>10</sup>.

Creating “high power efficient white LED” is the key issue for LEDs to deeply penetrate the general lighting market. As shown in Figure 9, there are three color matching methods on either LED-based or LED-phosphor-based to generate white light listed below; each of these methods offers different advantages and drawbacks <sup>4,9</sup>.

1. *Di-chromatic white source*: combine diode emitting at short wavelength  $\lambda_1$  (blue) with a phosphor emitting or the other diode at a larger wavelength  $\lambda_2$  (yellow).
2. *Tri-chromatic white source*: combine red, green, and blue (RGB) three diodes; or use a diode, emitting in the near ultraviolet (UV), coupled with one or several phosphors.
3. *Tetra-chromatic white source*: use three diodes (at least) emitting at different visible wavelength which then combine themselves to produce white light; or combination of diodes and phosphors to produce white light.

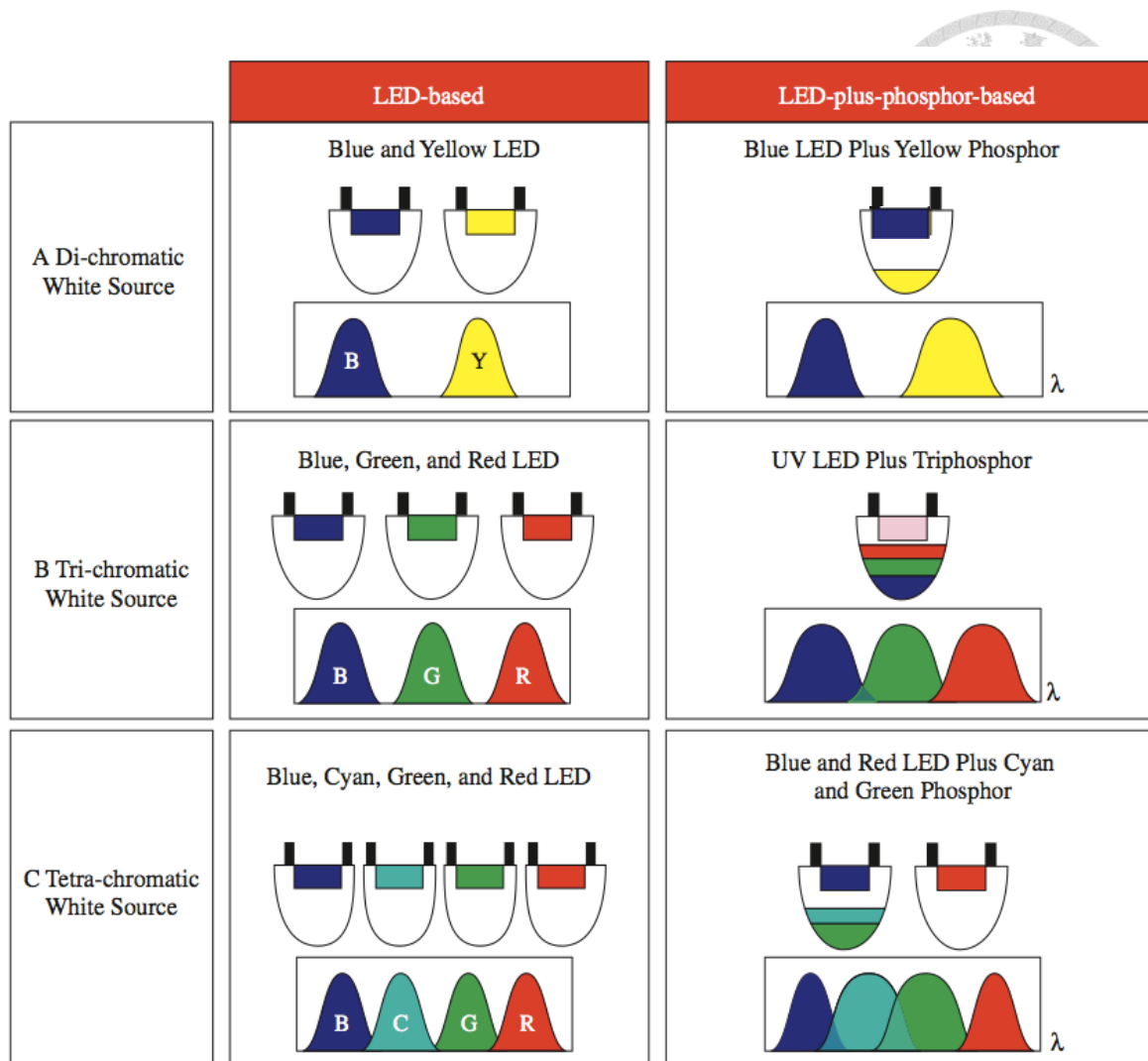


**Figure 9 White light LED converting methods** <sup>11, 12</sup>

However, the first method (LED-phosphor-based) is totally dominating the white LED market promoted by its good luminous efficiency, overall optical performance, and cost effective concern. A diode generating a short wavelength is covered with a layer of phosphor, which absorbs a few short wavelength photons to convert them into longer wavelength photons. As shown in Figure 10, two complementary-wavelength-photons simultaneously reach the human retina creating a white light sensation, and to be perceived as a beam of white light <sup>4, 9</sup>.

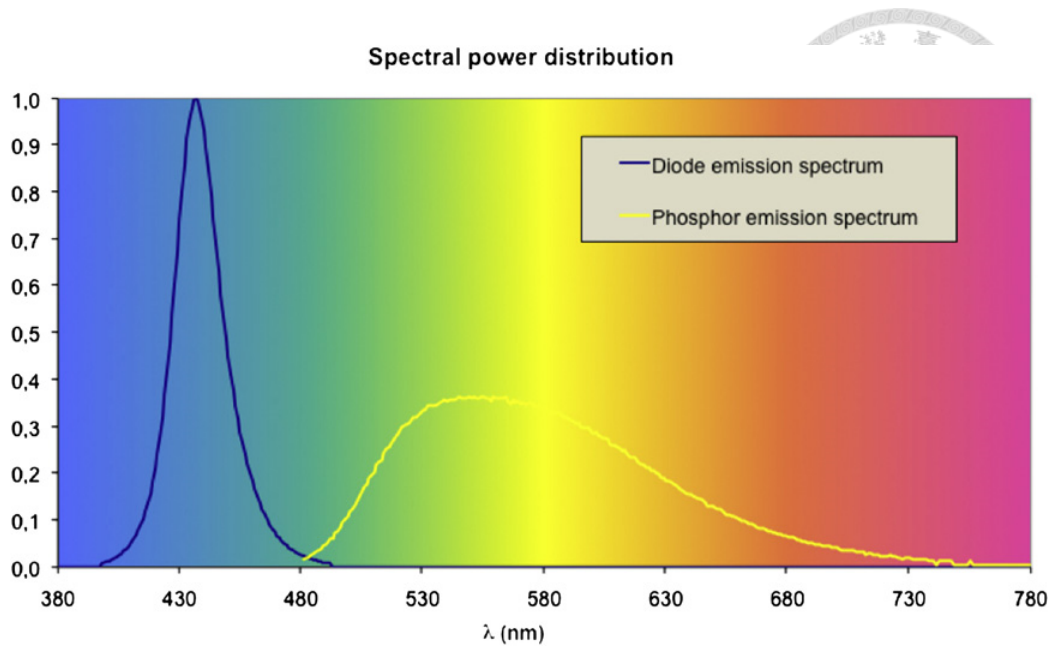


**Figure 10 Spectral representations of white light using LEDs <sup>4</sup>**

For white LED mass-production (CCT above 5500 K), blue emitting diodes based on InGaN or GaN crystals and combined with a yellow phosphor (YAG: Ce or similar) are generally applied. An additional layer of phosphor that emitting red light is included for “warm-white” (CCT near 3200 K) LED mass-production. However, this added layer will significantly reduce LED luminous efficacy. More importantly as shown in Figure 11, regardless the CCT value (or the color of LED white light), the blue light element is always heavily overlapping the black curve representing the blue light hazard.



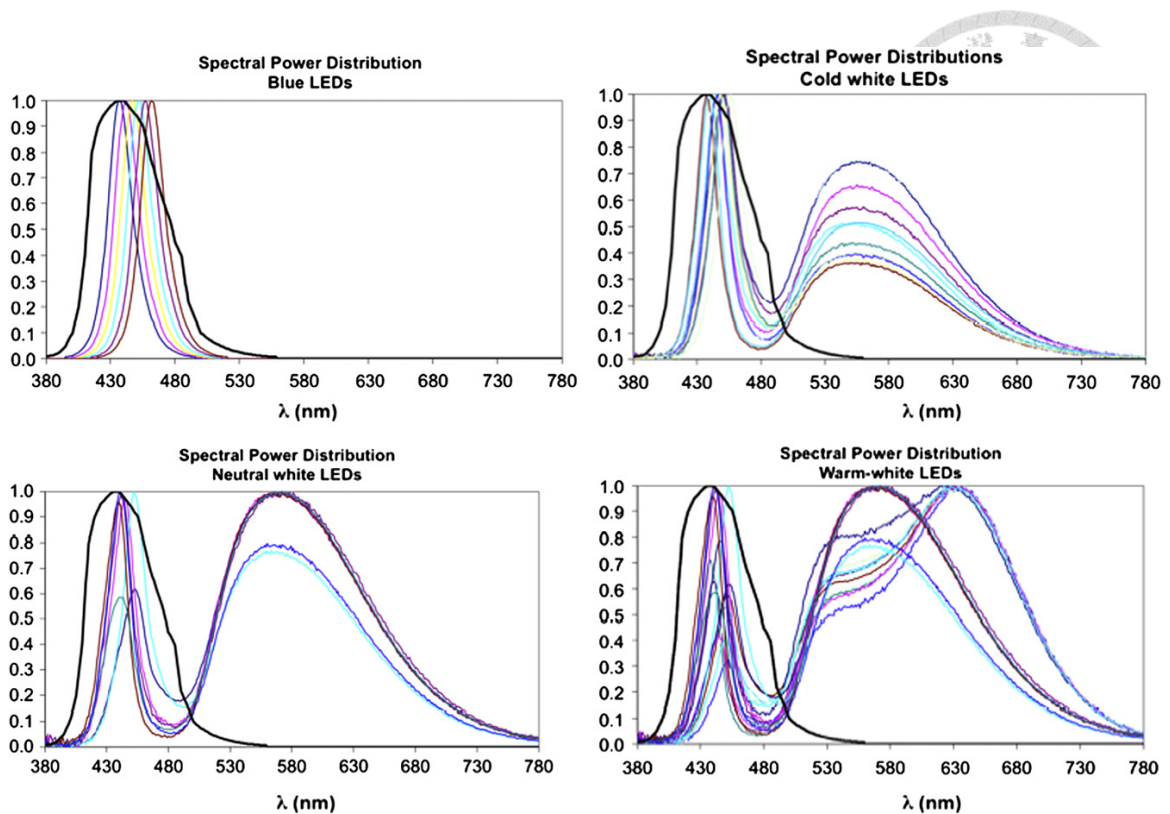


**Figure 11 LED spectral power distribution in different color temperature models <sup>4</sup>**

The second method in Figure 9 is similar to fluorescent lamp production. For mass-production purpose, a short wavelength diode emitting near ultraviolet light combined with one or multiple layers of phosphor converting the UV radiations into visible white light. This approach can produce high quality white light with good color rendering. However, it is basically away from the emission of “blue light” which is excluded from this research.

The third approach in Figure 9, additive multiple color creates white light with desired CCT. More than three sources are normally applied for more color shades obtaining or reaching an accurate color point. Some unique colors (cyan, amber or red orange) can be added to further improve the color rendering for special lighting requirements with higher cost.

The first method surpasses the other two based on economical and practical

concerns, and it is the primary mass-production practice in the current market. Therefore, it is the major LED white light manufacture technique that will be discussed in this risk assessment.



#### 2.1.3.4 *White Light LED Performance Diversification*

Monochromatic LED light is generated by an individual chip that emits a narrow range of light. By combining multiple spectral components produced by LED chip directly or through phosphor conversion as techniques mentioned above, LED lamps and luminaires deliver white light in different CCTs to the human eye. As illustrated in Figure 12, incandescent lamps (upper left) have a broad spectral distribution, and fluorescent lamps (lower left and right) base on a particular set of phosphors to present specific emission characteristics. The exact color temperature (CCT) can be adjusted by controlling the deposition of fluorescent powder. Although they also cover the full spectrum, the irregular spectral distributions are demonstrated by their serrated curves. Differently, the spectrum of the LED light shows a big blue peak along with a larger yellow peak (upper right).

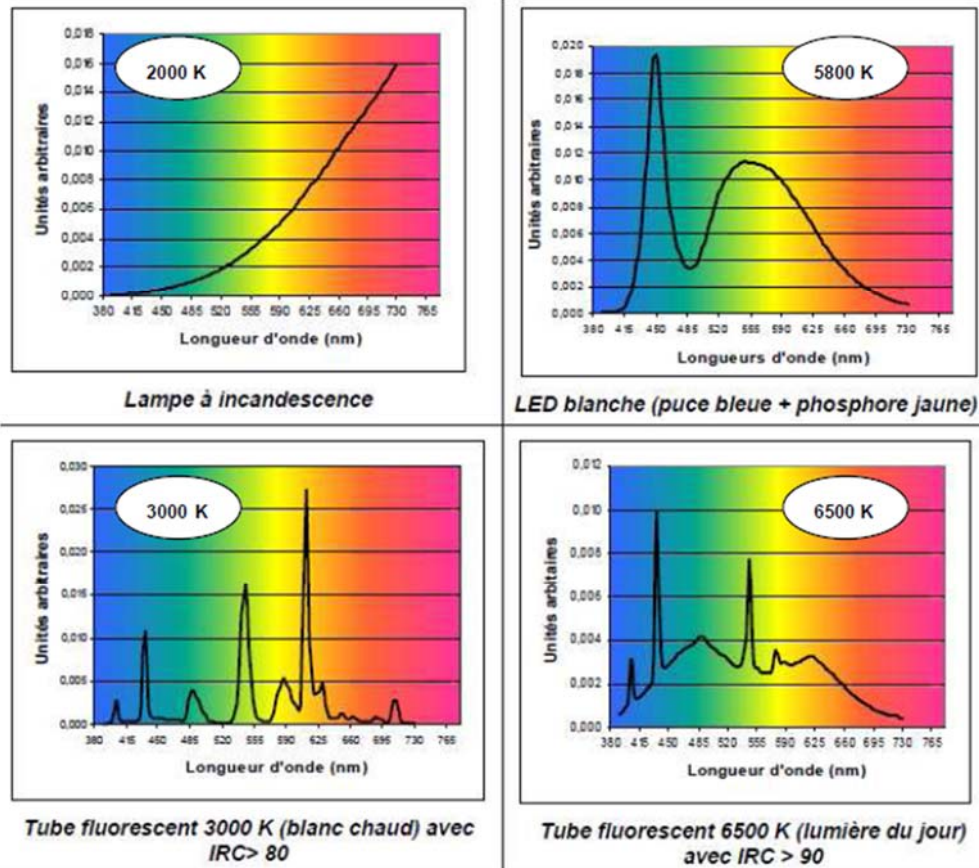



**Figure 12 Spectrum distribution for three domestic light sources <sup>4</sup>**

Theoretically, mixed LED light source means higher efficiency, longer life, and dynamic color control. In fact, they are generally have less color consistency, require complicated mixing optical system, and therefore raising the production cost <sup>13</sup>. The phosphor conversion LED (PC-LED) have a better overall performance than mixed LEDs in terms of efficacy for general lighting applications. Furthermore, each product should be evaluated individually considering the performance variations resulting from the materials, components, and production procedures applied, regardless the manufacturer or technology offered.

## 2.2 Retinal Physiopathology

### 2.2.1 Retina React with Light



There are 10 layers in the retina <sup>2, 14, 15</sup>, listing from the light path as follows: internal limiting membrane, nerve fiber layer, ganglion cell layer, inner plexiform layer, inner nuclear layer (INL), outer plexiform layer, outer nuclear layer (ONL), external limiting membrane, photoreceptor (rod and cone) layer, retina pigment epithelium (RPE). *“Photoreceptor cells are differentiated postmitotic retinal neurons uniquely adapted for the efficient capture of photons and for the initiation of visual transduction”* <sup>16</sup> (see Figure 13). In order to perform these functions, photoreceptors are being maintained in an oxygen rich environment and interact with high levels of incident light. The rod outer segment (ROS) membranes also contain high levels of polyunsaturated fatty acids, which stand a high potential for cell injury. *“Yet, normally, most visual cells survive into the seventh decade and beyond”* <sup>17</sup>. The constant renewal of ROS, disk displacement and phagocytosis activities in the RPE layer may help ROS membrane turnover every nine to ten days <sup>15</sup>. *“Photoreceptors also have the ability to adapt electrophysiologically to a wide range of incident light and metabolically to long-term environmental light conditions”* <sup>15</sup>. Additionally, repair mechanisms may also greatly prevent cell death. The delicate balance between the light interaction and overload-self-protecting mechanism determines the photoreceptor’s survival or irreversible damage.

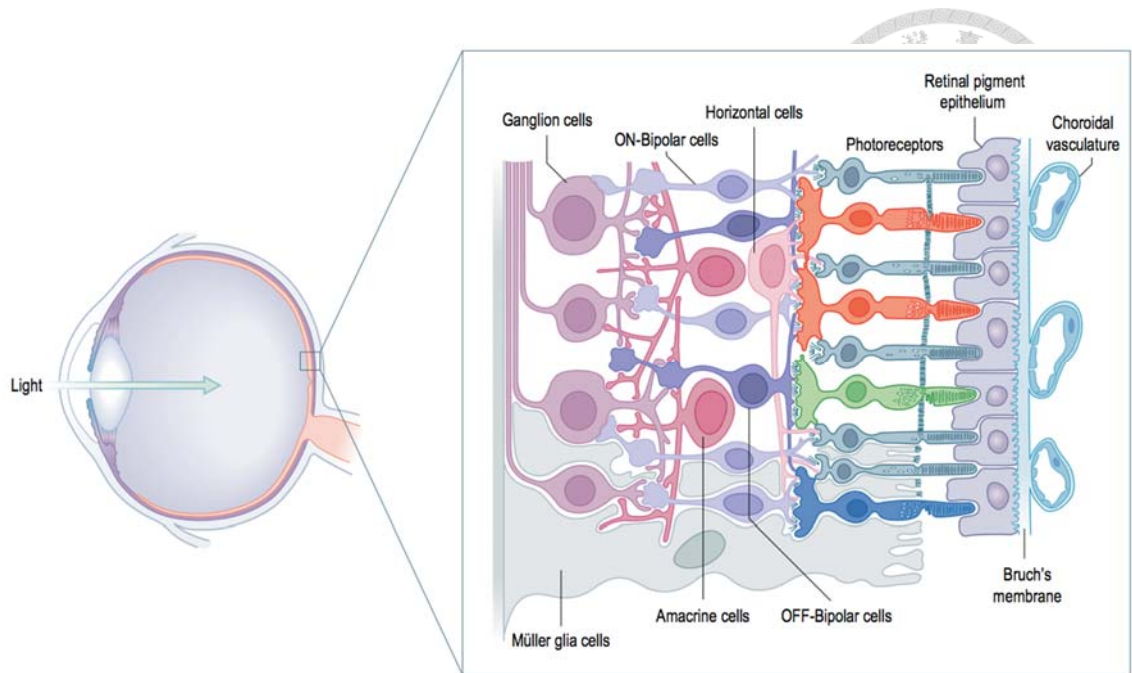


**Figure 13 Light path within the retina layers**<sup>15</sup>

Moreover, specific wavelength has its different light absorption and transmittance rates for each tissue. Demonstrating in Figure 14<sup>4</sup>, While the retinal transmission extends from 400 to 1200 nm, the retinal absorption peaks between 400 and 600 nm, which is the PC-LED white light dominated region. Although the outer ocular tissues (such as cornea and lens) absorb majority of the toxic UV lights, it is another research subject and therefore is excluded from this report.

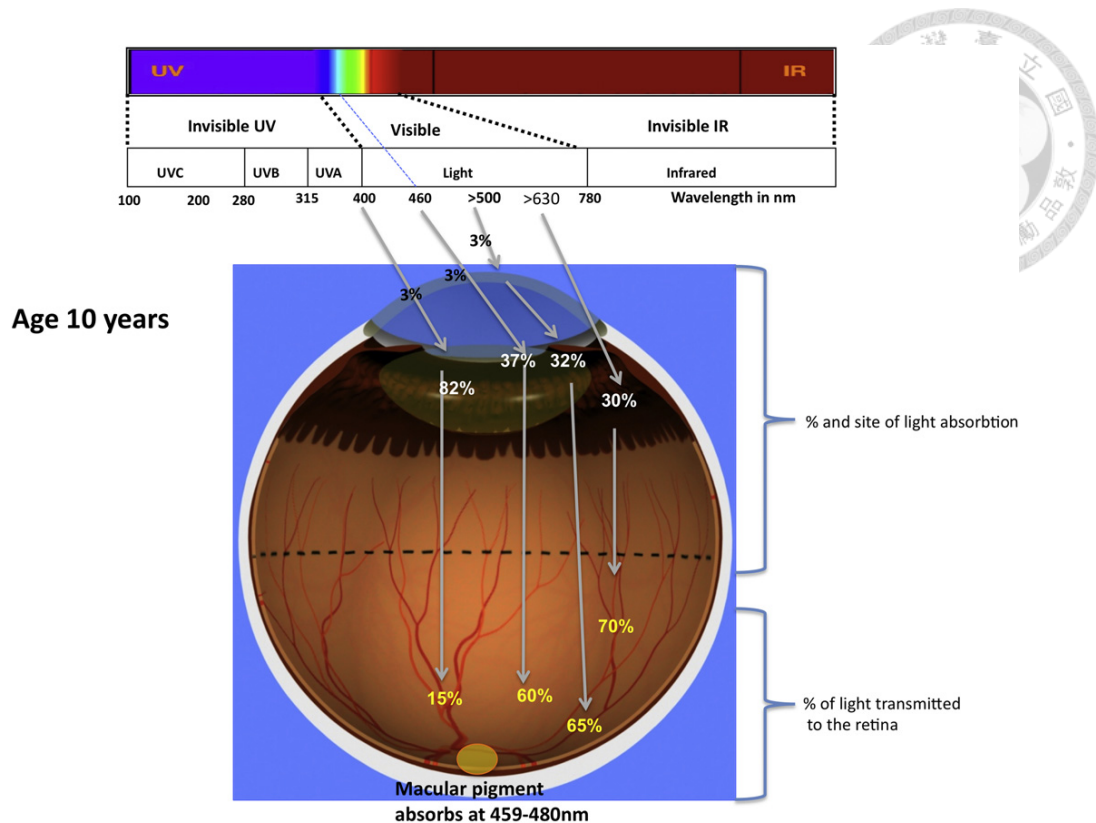


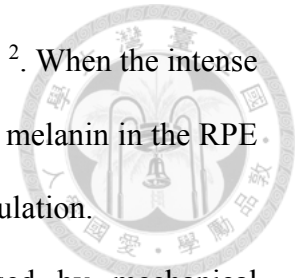
**Figure 14 Light absorption and transmittance in the eye** <sup>4, 18, 19</sup>

### 2.2.2 Retina Light Injury

The retinal light injury induced by environmental light exposure was first described in 1966 <sup>20</sup>. Many associated investigations have been added to researcher's understanding of its pathological process since. The initial intention of this type of study was to determine and define the injury, and it has expanded to more recent mechanism oriented pathological analyses. The light interacts with visual system through different mechanisms. Some of the ocular tissues or pigments are designed to absorb photons to reduce retinal exposure as a self-defense function. Moreover, some other ocular structures can increase oxidative stress and lead to retinal injuries through photochemical and photodynamic effects. Three mechanisms have been categorized: photothermal-, photomechanical-, and photochemical light induced retinal injury <sup>2, 16, 21</sup>.

(1). Photothermal injury: the tissue damage is caused by “the transfer of

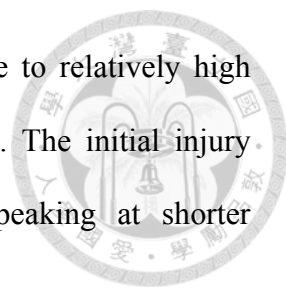
*radiant energy, a photon, from light to the retinal tissue”*<sup>2</sup>. When the intense light is converted into heat, the pigmented tissue (mostly melanin in the RPE and choroid) raises its temperature and causes photocoagulation.



- (2). Photomechanical injury: the tissue damage is caused by mechanical compressive or tensile forces that generated by rapid introduction of energy into RPE melanosomes. Is occurred when extremely high retinal irradiances (typically laser beam) cause tissue heating and expansion that triggers instant retina alteration and bleeding.
- (3). Photochemical injury: the tissue damage is caused by free radicals that generated from light exposure. This type of injury associates with both long-duration and short-wavelength light exposure<sup>22,23</sup>. When the retinal intrinsic protective mechanism is overdoing by defending the light insult, the retinal injury may occur.

Noell et al. suggested this hypothesis in 1966, after learning that the albino rat retinas were irreversibly injured by continuous exposure to ambient light. This finding motivated extensive studies, further elucidating this mechanism different from mechanical and thermal retinal injury. This also is the most common type of retinal light injury with two classes<sup>16, 24</sup>. According to Kremers and his colleagues' research in 1988, these two classes of retinal injury have been shown in both rodent and primate models<sup>24</sup>.

- (a) Class I injury is characterized as exposure to white light (irradiance below 1 mW/cm<sup>2</sup>) for hours to weeks. Despite there are some debates on the initial site of injury from low-level light exposure, it is generally believed the initial injury site starting at photoreceptor outer segment (POS) rather than RPE.



(b) Class II injury is characterized as exposure to relatively high irradiance white light (above 10 mW/cm<sup>2</sup>). The initial injury site at the RPE with action spectrum peaking at shorter wavelengths.

### 2.2.3 Action Spectrum of Retinal Light Injury

It is well recognized that retinal light injury is determined by the exposure duration and light intensity reaches the retina (retinal irradiance). The wavelength dependency is also convinced with action spectra in its pathological process. As shown in Figure 15, the action spectrum of retinal light injury ranges from 400 nm to 580 nm and peaked around 480 nm to 500 nm. This action spectrum closely overlapping the PC white light LED emitting range and signifying a warning for ONL injury.

As mentioned previously, LED is becoming the primary light sources for many lighting applications. White LEDs make retina exposure to violet, indigo and blue light at much higher levels than in conventional light sources. This is the first time in history that human will be exposed to such substantial bright light regardless day or night. Moreover, photochemical injuries usually progressively induce photoreceptor loss long after the initial exposures. Therefore, when evaluating all the knowledges and risks on blue-light hazard, its cumulative effect should also be carefully considered for this unavoidable chronic exposure.



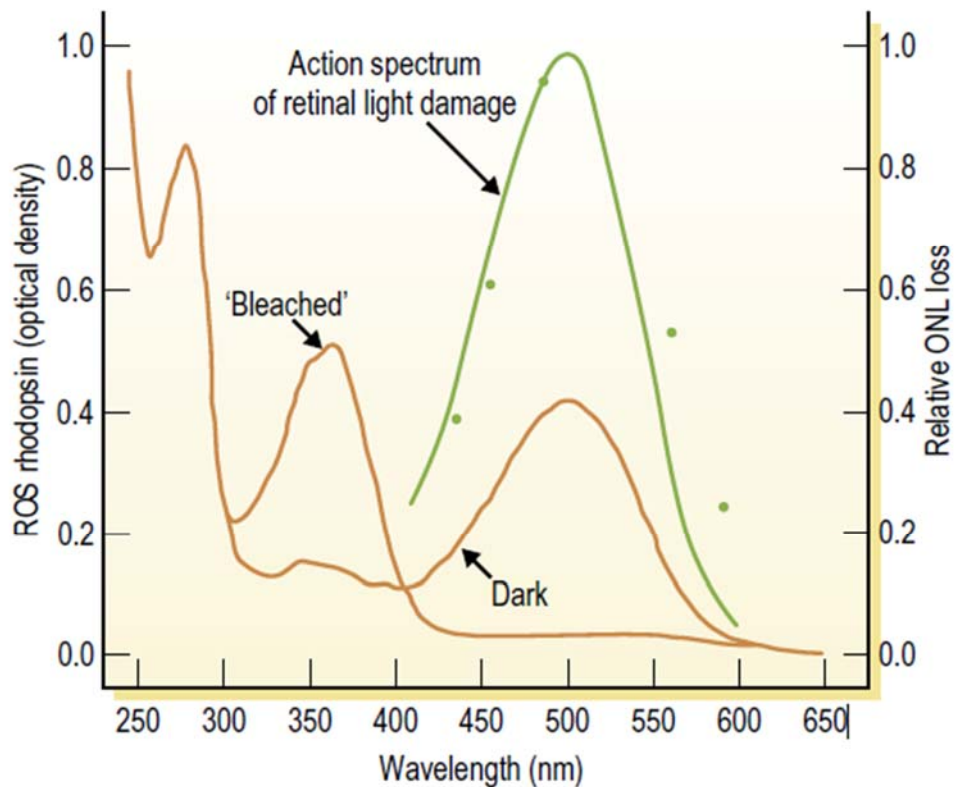


**Figure 15 Action spectrum of retinal light damage** <sup>17</sup>

#### 2.2.4 Progress of Photoreceptor Light Induced Injury

As demonstrating on Figure 16, a typical development of retinal injury by light exposure is shown schematically <sup>25</sup>. As first explained by Kuwabara and Gornss in a 1968 publication, only the tip of photoreceptor shows vacuoles at stage 1. At stage 2, outer segment is tortuous and swollen. Myelin membranes are separated from each other and form vesicular and tubular structures. The pathological changes can be found at the synaptic end of photoreceptive cells. Pigment epithelium also shows clear increase in myeloid bodies. At stage 3, damaged outer segment is isolated from inner segment and becomes large round or pear-shaped body filled with tubular material, followed by cellular degeneration at stage 4 and complete adhesion of pigment epithelium and

Müller's cell at stage 5.

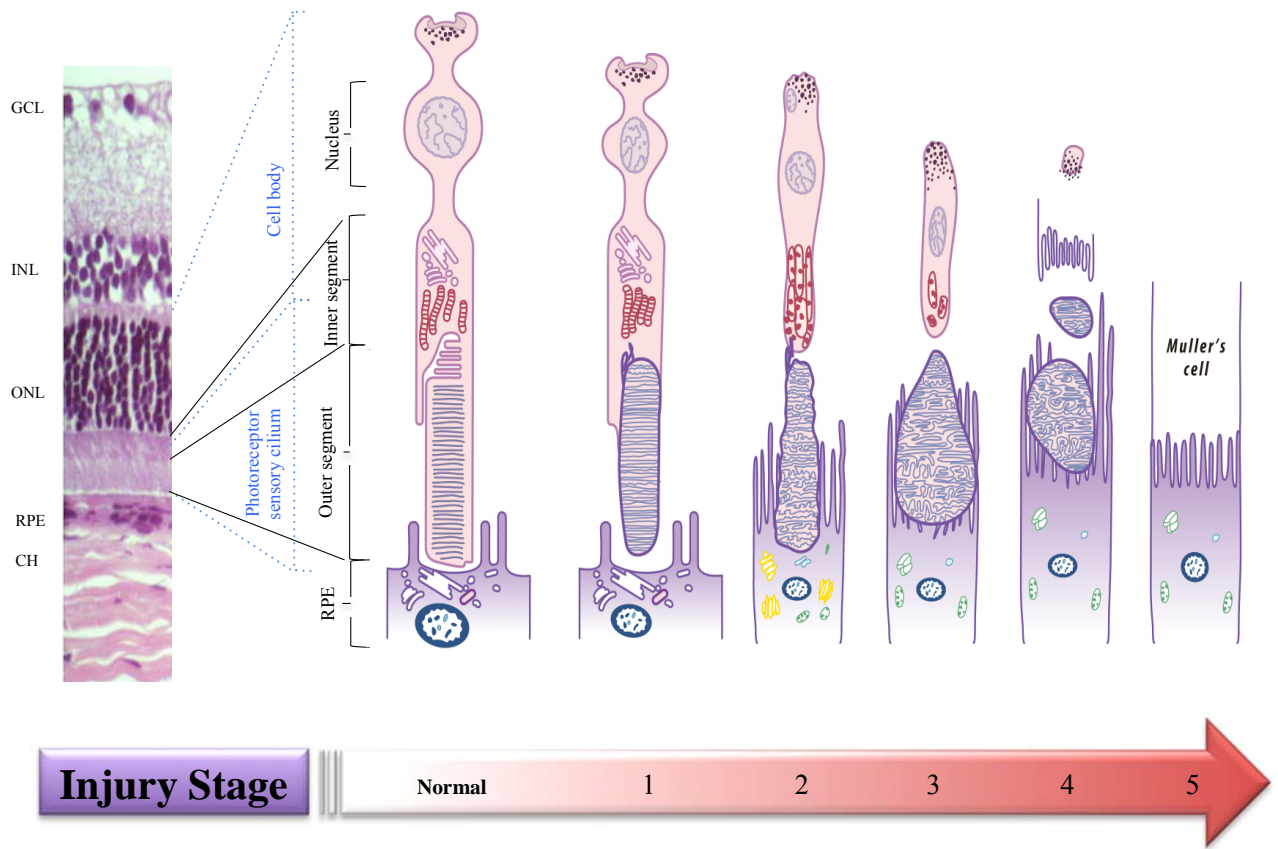


**Figure 16 Scheme of the photoreceptor light induced injury progress**

Diagram concept modified from (Kuwabara and Gornss)<sup>25</sup>

### 2.2.5 Animal Model for Retinal Light Injury

Animal models is frequently used for light-induced retinal degeneration and mechanisms analysis. Rodent retina is a good alternative, if primate is not available for light induced retina degeneration study. To test the light induced retina injury in rodent species became the most convenient model due to its accessibility, capacity to induce photoreceptor-specific cell death, oxidative stress recognition, blood-retina barrier breakdown, and other inflammation marker identification<sup>26</sup>.

Two types of light induced retinal injury have been studied and recognized by many animal models. The first type of the injury is short-bright-light

exposure associated (acute); the second type of the injury is induced by less-bright-cyclic light exposure (chronic). Despite both types can lead to serious retinal degeneration, their injury mechanisms and phenotypes can be very different. Giving the credit to professor Mandal <sup>27</sup>, Figure 17A shows the typical retinal injury by acute light exposure in a Sprague Dawley (SD) rat. The photoreceptor cell death can easily be observed (white arrows) juxtaposing by those normal-appearing cells (yellow arrow). On the other hand, the chronic light injured retina appears to be “normal” morphologically as shown in Figure 17B. Its ONL is thinning gradually without regional differences. The gentle ONL thinning process could protect the retina from massive retina destruction <sup>27</sup>. This is a strategical self-defense mechanism so called “retina remodeling”, which should be observed closely and interpreted systematically.

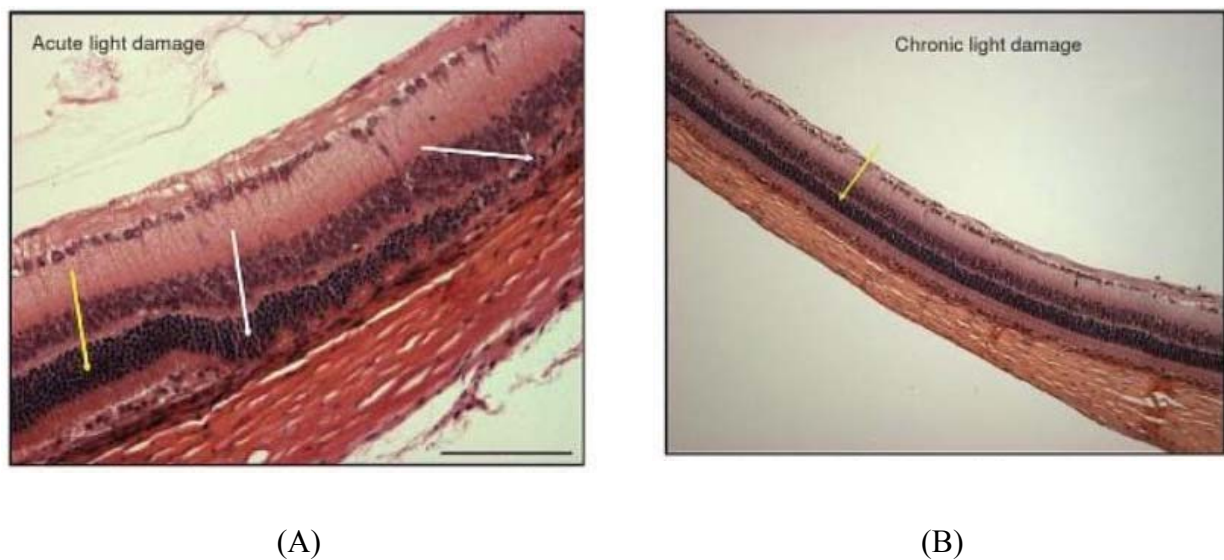


**Figure 17 Sprague-Dawley (SD) rats acute and chronic retinal light injury <sup>27</sup>**

## 2.3 Potential retinal injury induced by chronic exposure to LED light

### 2.3.1 Data Collection and Selection

Increased use of LED applications may increase irreversible retinal injury. This study was designed to systematically review the reports of retinal injury induced by LEDs, and identified 26 articles from 1707 published studies that associated with retinal light injury between 1966 and 2016. As shown in Figure 18, it presented a well-diversified research path and some with very limited light source descriptions. In this reviewing process, the type of light source prioritized the data screening. The majority of the included studies elucidated LED blue light hazard and confirmed the mechanism and retinal health effects. The results inform a systematic approach of research findings that greater control of blue light exposure from domestic LED lighting is required. This may be of particular concern for aging populations with pre-existing vision impairment.

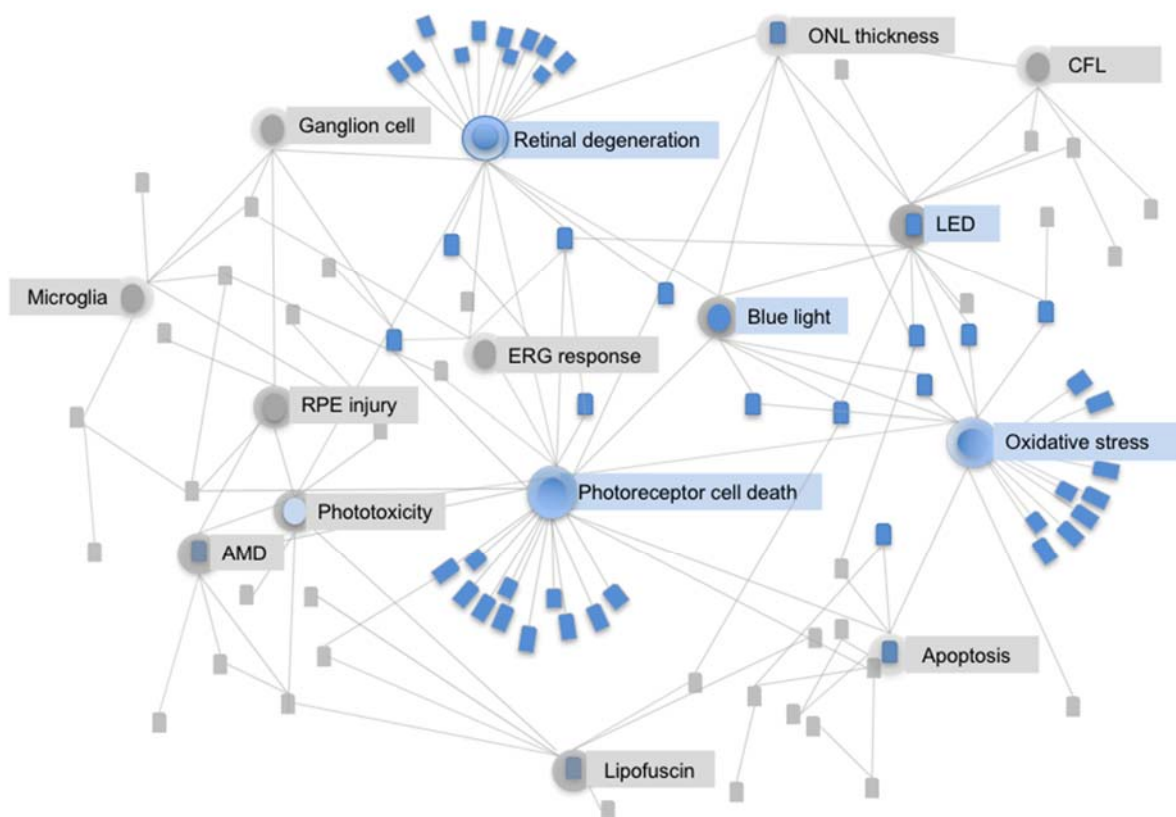




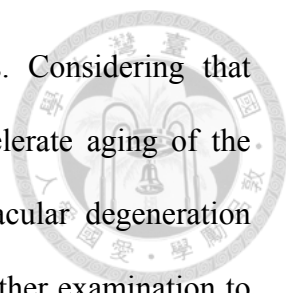
**Figure 18 Literature relation map**

### 2.3.2 Retinal Light Injury vs. LED Lighting

Retinal light injury was studied intensively after Noell<sup>20</sup> first described the retinal injury caused by environmental fluorescent light exposure and numerous studies have reported that high-intensity blue light causes acute retinal injury<sup>28, 29</sup>. However, few studies have focused on retinal injury caused by exposure to relatively low-intensity blue light under chronic exposure conditions<sup>30</sup>.

The most popular LED lighting product, a phosphate-conversion (PC) LED, is a LED chip that emits blue light passing through a yellow phosphor-coating layer to generate the ultimate white light<sup>31</sup>. Although the white light generated from LEDs appears normal to human vision, a strong peak of blue light ranging from 460 to 500 nm is also emitted within the white light spectrum and corresponds to a known spectrum for retinal hazards<sup>4</sup>. Because LED (or solid-state) lighting sources are designed to emit all energy within the wavelength range of human vision, it is the most energy-efficient commercially manufactured light; however, many current “white-light” LED designs emit much more blue light than conventional lamps, which has a number of health implications, including disruption of circadian rhythms<sup>32</sup>.

Moreover, the composition of the white-light spectrum differs among LED products, and their light qualities change over time. Although it is robust in the beginning, a PC-LED progressively releases more short-wavelengths (blue light) when LED lumen depreciation occurs because of phosphor degradation. The quality of the light deteriorates after the lights pass the 70% lumen maintenance level (L70)<sup>33</sup>. These characteristics suggest that a white LED can cause more

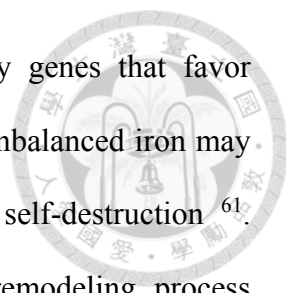


blue light exposure than other domestic lighting sources. Considering that cumulative exposure to blue light has been argued to accelerate aging of the retina and may play an etiological role in age-related macular degeneration (AMD) <sup>4</sup>, domestic lighting with high blue light requires further examination to determine its potential retinal effects.

### 2.3.3 Retinal Light Injury Mechanisms

Photochemical retinal injury resulting from a cumulative effect is caused by free radicals generated from retinal tissue through continuous light exposure <sup>23</sup>. When exposure surpasses the protective capability, unfavorable free radicals and reactive oxygen species may form <sup>16,34</sup>. This enhances the oxygenated products and provides conditions favorable for photodynamic damage of photoreceptors and other retinal tissues <sup>35</sup>. However, susceptibility to retinal photochemical injury (RPI) is multifactorial <sup>17</sup>, and wavelengths certainly play an important role<sup>36</sup>. According to Planck's relation ( $E = h/\lambda$ , where  $E$  = energy,  $h$  = the Planck constant, and  $\lambda$  = wavelength), a photon corresponding to blue light is more energetic <sup>17</sup> than photons of longer wavelengths, such as green or red light. Furthermore, blue light has the greatest potential to induce PRI, which has been reconfirmed both by *in vitro* <sup>37-44</sup> and *in vivo* studies <sup>45-50</sup>.

Blue light could induce the formation of reactive oxygen species (ROS) in RPE mitochondria that leads to retinal apoptosis has been reported by cell culture studies <sup>38, 41, 43, 44, 51-54</sup> and animal models <sup>46, 49, 55, 56</sup>. The initial injuries involve a series of processes, including signaling molecules released from outer retinal cells, oxidatively damaged biomolecules <sup>57</sup>, dysfunction and death of outer retinal cells, and removal of apoptotic debris by activated retinal microglia and systemic macrophages <sup>58</sup>. This injury is also site-specific and depends on the



iron concentration in the retina <sup>59, 60</sup>. The iron regulatory genes that favor increased iron uptake were altered after photic injury. The unbalanced iron may further accelerate oxidative stress in a cycle of cellular self-destruction <sup>61</sup>. Moreover, the injury possibly corresponds to a retinal remodeling process following the light injury <sup>62, 63</sup>. However, the wavelength-dependent effect and its influences on white LED light-induced retinal degenerations remain unknown. Some epidemiological studies have suggested that short-wavelength light exposure is a predisposing cause for AMD <sup>16</sup>. Animal models have also been used to determine that excessive exposure to blue light is a critical factor in photochemical retinal injury targeting photoreceptors and the retinal pigment epithelium (RPE) <sup>64</sup>.

#### 2.3.4 Principal of the domestic lighting exposure

Although there has been a wealth of studies describing the RPI and some of them even discussed the wavelength dependency, the experimental settings were focused on high intensity light exposure over a short period of time (a few seconds to 3 days) for acute or subacute toxicity assessments. The tested animals were anesthetized or forced to stare into the lights in most of the cases, and the light sources varied due to contemporary technology availability.

Therefore, a study focusing on subchronic risk assessment is needed. The animals in the experiments were allowed to move freely in the cage during the exposure. The light sources were critically designed to meet the updated industrial development. The exposure conditions were also created to simulate the domestic lighting environments in the most possible way. To investigate how specific wavelengths in LED domestic lighting were responsible for retinal phototoxic effects under long term exposure form the principal of this research.

### 3 RESEARCH DESIGN AND METHODS



#### 3.1 Hypotheses of photochemical injury

The ability of light to cause injury to the retina has been shown both clinically and experimentally. It is now well established that prolonged light exposure can lead to photoreceptor cell injury by non-thermal mechanisms. It is also clear that light injury involves a complex series of events which depend upon the duration and intensity of light, its wavelength and the characteristics and distribution of absorbing chromophores within the retina. Although light injury results in visual cell death in a number of animal models, the initial events may differ.

While neurosensory retina and RPE are protected from light-induced exposure by the absorption profile of the surrounding ocular structures, including the cornea, crystalline lens, and macular pigments, as well as the ability of the retinal photoreceptors to regenerate its outer segments, photic injury is still possible. The principles of photomechanical, photothermal, and photochemical injury to the retina provide a framework for understanding and photic injury to the retina. However, this study mainly focuses on the class I photochemical injury (described previously on 2.2.3) to reflect the white light LED as reading light source features.



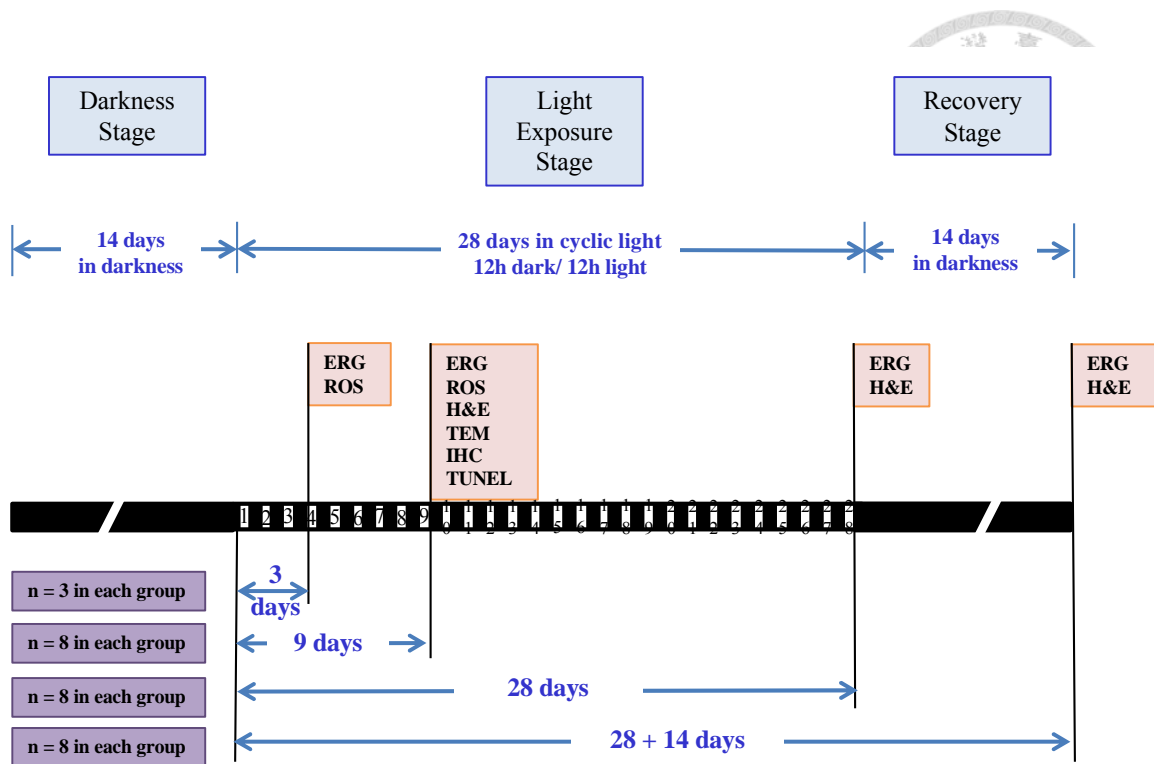
## 3.2 Animal handling and light exposure plan

### 3.2.1 Animals and rearing conditions

#### 3.2.1.1 *For the comparison of CFL vs. LED*

In total, 120 adult male Sprague–Dawley rats were purchased from BioLasco Taiwan Co., Ltd at 8 weeks of age and stored in a dark environment for 14 days to clear the light exposure effect from their previous rearing environment. Twelve normal rats served as controls without exposure, and the other 108 rats received programmed light exposure, as shown in Figure 19. The groups were randomly allocated during the experiment and/or when assessing the outcome. The animals would be excluded from the analysis if animals were died during the experiments. The temperature of the exposure environment (both the room and individual cages) was maintained at 22-23°C with humidity between 50% and 70%. All animals received food and water *ad libitum*. The use of rats in this study conformed to the ARVO statement for the Use of Animals in Ophthalmic and Vision Research and Laboratory Animal Resource Committee guidelines at National Taiwan University. This study received the animal use approval (affidavit of approval of animal use protocol #20110568) from National Taiwan University College of Medicine and College of Public Health Institutional Animal Care and Use Committee (IACUC). The animals were treated humanely and with regard to the alleviation of suffering.



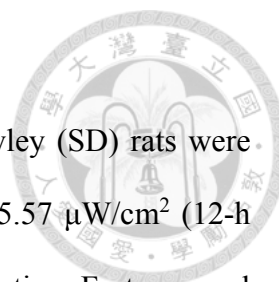


		Number of animals in each group				
		Blue LED	White LED	White Florescent	Yellow Florescent	Total
Treatments of light exposure	Control	3	3	3	3	12
	3 days	3	3	3	3	12
	9 days	8	8	8	8	32
	28 days	8	8	8	8	32
	28 +14 days	8	8	8	8	32
	<b>Total</b>	<b>30</b>	<b>30</b>	<b>30</b>	<b>30</b>	<b>120</b>

**Figure 19** Timeframe of the experimental design

ROS: Reactive oxygen species. ERG: Electroretinography. H&E: hematoxylin and eosin staining. TEM: Transmission electron microscopy. IHC: Immunohistochemistry. TUNEL: Terminal deoxynucleotidyl transferase dUTP nick end labeling stain.

After 14 days of dark maintenance, the rats were divided into 4 groups and exposed to different light sources. During the exposure and recovery stages, certain analytical techniques (red boxes in the figure) were performed at the end of various exposure durations.



### 3.2.1.2 For the comparison of RGB LEDs

In total, 202 adult male eight-week-old Sprague–Dawley (SD) rats were purchased from BioLasco Taiwan Co., Ltd and housed at 15.57  $\mu\text{W}/\text{cm}^2$  (12-h cyclic CFL, CCT 6500) for 10 days for environmental adaptation. Forty normal rats served as controls without exposure (remained in 15.57  $\mu\text{W}/\text{cm}^2$  12-h cyclic CFL light), and the other 162 rats received programmed light exposure, as shown in Table 3.

**Table 3 Exposure groups allocation**

	<b>Control</b>	<b>Blue LED</b>	<b>Green LED</b>	<b>Red LED</b>
<b>Wavelength</b>		(460 nm)	(530 nm)	(620 nm)
	Number of animals in each group			
<b>3 days</b> (ERG / H&E / WB / ROS / Iron)	12	18	18	18
<b>9 days</b> (ERG / H&E / TEM / TUNEL / IHC / WB / ROS / Iron)	16	24	24	24
<b>28 days</b> (ERG / H&E / TEM / WB)	8	12	12	12
(Total n=198)	<b>36</b>	<b>54</b>	<b>54</b>	<b>54</b>

## 3.2.2 Light source

### 3.2.2.1 For the comparison of CFL vs. LED

As shown in Figure 20, single-wavelength blue LEDs ( $460 \pm 10$  nm) and blue LED with yellow PC white LEDs were custom made for the exposure experiments. The PC-LED had a correlated color temperature (CCT) of 6500 K (see Figure 21). One group of white compact fluorescent lamps (CFL) also matched the CCT at 6500 K (Chuanshih, ESE27D-EX, Taiwan), whereas the

other group of yellow CFL was set at 3000 K (Chuanshih, ESE27L-EX, Taiwan). Each light source was programmed for 40 measurements in an integrating sphere. The spectrum distributions and total intensities for all light sources were tested by the Industrial Technology Research Institute of Taiwan, a Certification Body Testing Laboratory (CBTL).

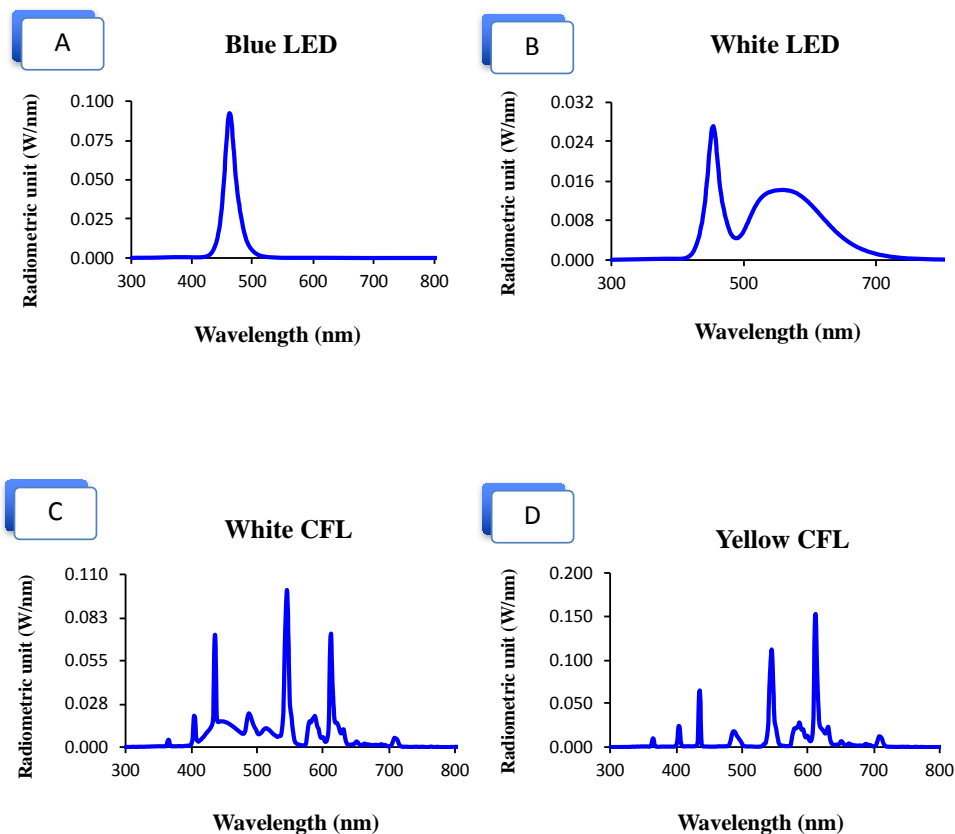


**Figure 20 Light source spectral power distribution (SPD) curves**

(A) Single-wavelength blue light LED peaked at 460 nm with 0.1 W/nm in radiometric units. (B) Yellow phosphor-converted white LED to exhibit CCT at 6500 K; the first peak appeared at 460 nm with 0.028 W/nm showing the blue content and the second peak with a bell shape presenting a large portion of yellow content. (C) Compact fluorescent lamp with CCT at 6500 K showing several sharp peaks across the spectrum; the blue peak is relatively shorter than the yellow or red peaks, and the full width at half maximum (FWHM) is smaller than that in (A) and (B). (D) Similar to the condition in (C) with CCT at 3000 K, the highest peak is presented in yellow. Although all light sources contain blue light peaks, the area under the curve variation leads to a total intensity difference.



**Figure 21 Custom made LED light strip**

*3.2.2.2 For the comparison of RGB LEDs*

LED lights with varying spectral characteristics were used as the sources for primary exposure treatments. As shown in Figure 22, single-wavelength blue LEDs (460 nm,  $102.3 \mu\text{W}/\text{cm}^2$ ), green LEDs (530 nm,  $102.8 \mu\text{W}/\text{cm}^2$ ), and red LEDs (620 nm,  $102.7 \mu\text{W}/\text{cm}^2$ ) were custom-made for the exposure experiments (BlueDog Technology Corporation Ltd., Taipei, Taiwan). Each light source was pretested in an integrating sphere and programmed for 40 measurements on site.

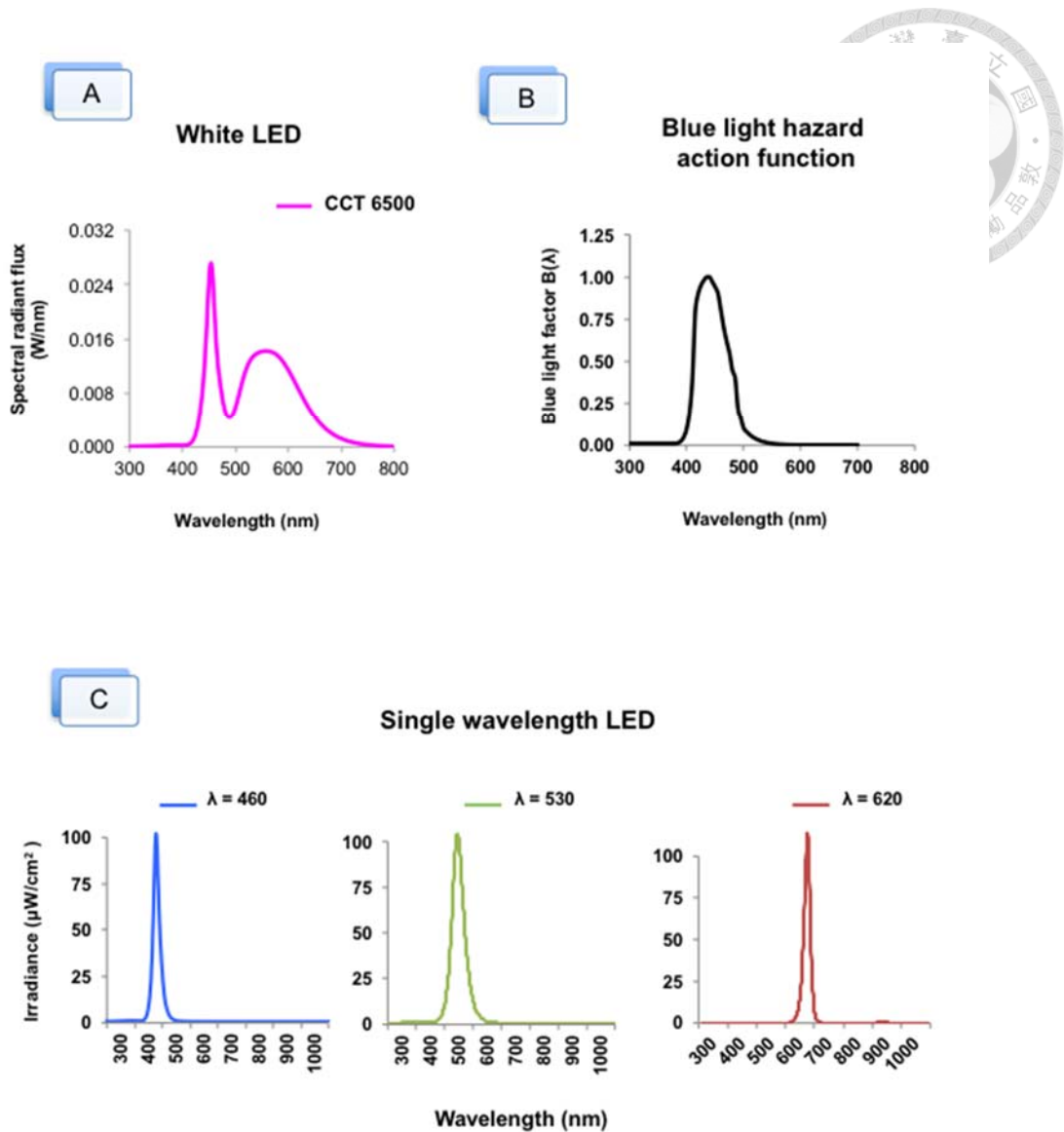
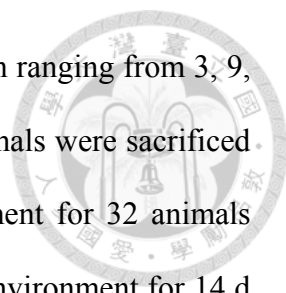


**Figure 22 LED light source spectral power distribution (SPD) curves**

### 3.2.3 Light exposure

#### 3.2.3.1 For the comparison of CFL vs. LED

As shown in Figure 19. The animals were divided into 4 groups, and each rat was stored in an individual transparent cage with a dimension of 45 x 25 x 20 (cm). Each cage was placed in the center of a rack shelf with dimensions of 75 x 45 x 35 (cm). The light sources were set on the top of each shelf and were measured 20 cm away from each source to acquire the common domestic luminance level at 750 lux. After 14 d of dark maintenance, the light exposure



started at 6:00 PM of Day 15 with the total exposure duration ranging from 3, 9, to 28 d under 12 hr dark/12 hr light cyclic routines. The animals were sacrificed for analysis after light exposure. However, a special treatment for 32 animals was performed, 8 from each group were returned to a dark environment for 14 d of recovery after 28 d of exposure. The objective of the recovery stage was to allow for possible removal of necrotic photoreceptor cell debris.

### 3.2.3.2 *For the comparison of RGB LEDs*

As shown in Table 2, the animals were randomly divided into 3 exposure groups, and each rat was housed in an individual transparent cage with dimensions of 45 x 25 x 20 (cm). As shown in Figure 23, each cage was placed in the center of a rack shelf with dimensions of 75 x 45 x 35 (cm). Each rack, equipped with 6 layers of shelving, was covered with a black curtain to keep the light intensity and quality separate. The light sources were set at the top of each shelf and were measured at 20 cm from each source to acquire the irradiance at the level of the cornea at 102.3  $\mu\text{W}/\text{cm}^2$ , 102.8  $\mu\text{W}/\text{cm}^2$ , and 102.7  $\mu\text{W}/\text{cm}^2$  for blue, green, and red, respectively. After 10 days of environmental adaptation, the light exposure was initiated at 6:00 PM on Day 11, with the total exposure duration ranging from 3 days to 9 days to 28 days under a 12 h-dark/12 h-light cyclic routine. The animals were sacrificed for analysis after light exposure.

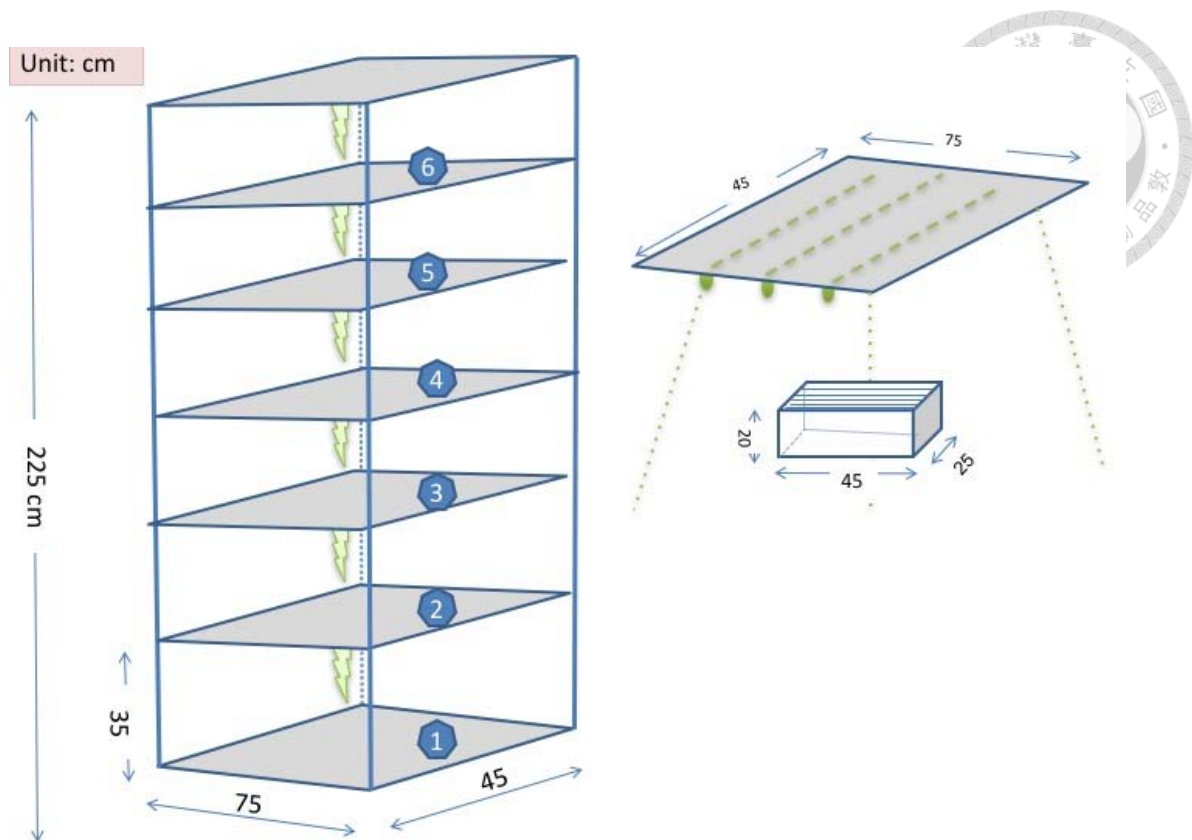


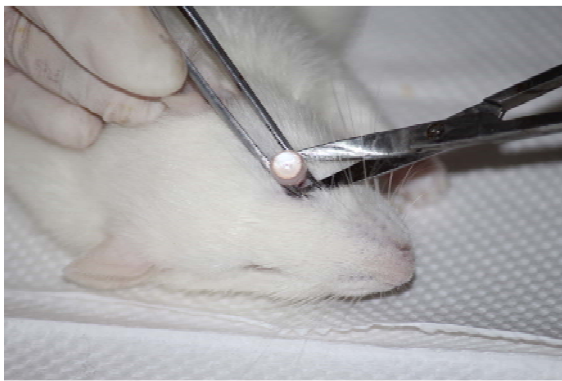
**Figure 23 Diagram of light exposure setting**

### 3.3 Sample pretreatment

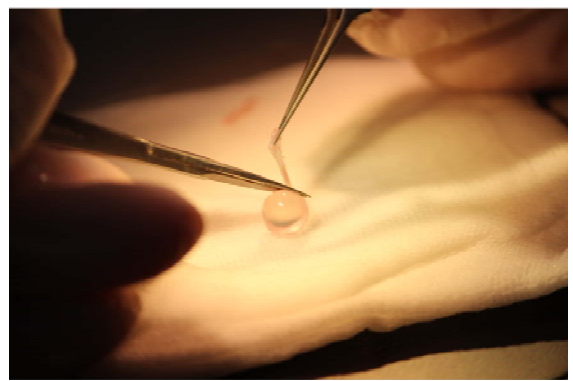
The animals were anesthetized, and both eyes were scanned using electroretinography (ERG) after completing the light treatment. They were sacrificed with pentobarbital sodium (> 60 mg/kg, intraperitoneal) immediately after the ERG scans. For hematoxylin and eosin (H&E) staining and terminal deoxynucleotidyl transferase dUTP nick end labeling (TUNEL) staining, enucleated eyes were immersion-fixed in 4% paraformaldehyde in 0.1 M phosphate buffered saline (PBS) at pH 7.4 overnight before being embedded in paraffin. For the transmission electron microscopy (TEM) analysis, the eyeballs were immersion-fixed in 2.5% glutaraldehyde in PBS for 2 h before further processing. For the immunohistochemistry (IHC) stains, the eyeballs were frozen immediately in liquid nitrogen after enucleation. Cryosections of 4  $\mu\text{m}$



thickness were made in the glass slide and maintained at  $-80^{\circ}\text{C}$  until analysis. The mid-superior aspect of the retina was examined using H&E, TUNEL, TEM, and IHC. For the superoxide anion ( $\text{O}_2^{\cdot-}$ ) assay, the eyeballs were frozen immediately in liquid nitrogen after enucleation. The eyeballs were ground with saline (500  $\mu\text{L}$  saline per eye) for extraction. Additionally, for the western blot (WB), the hydrogen peroxide ( $\text{H}_2\text{O}_2$ ) assay, and the iron assays, retinal tissues were taken immediately for protein extraction after the eyes were enucleated (as Figure 24). As reported previously<sup>65</sup>, the proteins were extracted from the retinal homogenates using radioimmunoprecipitation assay (RIPA) lysis buffer, which contained 0.5 M Tris-HCl (pH 7.4), 1.5 M NaCl, 2.5% deoxycholic acid, 10% NP-40, 10 mM EDTA, and 10% protease inhibitors (Complete Mini; Roche Diagnostics Corp., Indianapolis, IN, USA).



(A)



(B)

**Figure 24 (A) Eye enucleation and (B) retina tissue removal**

### 3.4 Analytical Methods

#### 3.4.1 Electroretinography (ERG)

As shown in Figure 25 and Figure 26, ERG was performed as described previously with modification<sup>66</sup>. Retinal electrical responses were recorded for

all rats before and after light exposure using ERG (Acrivet, Hennigsdorf, Germany). After 18 h of dark adaptation, rats were anesthetized using an intramuscular injection of 100 mg/kg ketamine and 5 mg/kg xylazine (WDT eG, Garbsen, Germany). One drop of tropicamide (0.5%) (Mydriaticum Stulln, Pharma Stulln, Germany) was applied for pupil dilation before ERG measurement. One drop of Alcaine (0.5%) (proxymetacaine hydrochloride; Alcon Pharmaceuticals Ltd, Puurs, Belgium) was applied for local anesthesia before placing the active electrode onto the cornea (see Figure 25). Two subcutaneous needle electrodes (Ambu Neuroline Twisted Pair Subdermal, Bad Nauheim, Germany) served as the reference and ground electrodes. The reference needle was subcutaneously inserted between the eyes, and the ground needle was subcutaneously inserted between the rear legs to obtain the proper impedance levels, which were less than 10 k $\Omega$  at 25 Hz. LED flashes were stimulated without background illumination, and the flash interval was 1 s with a flash duration of 3 ms. The weighted average of 10 stimulations was computed by the program to produce the final detection values.

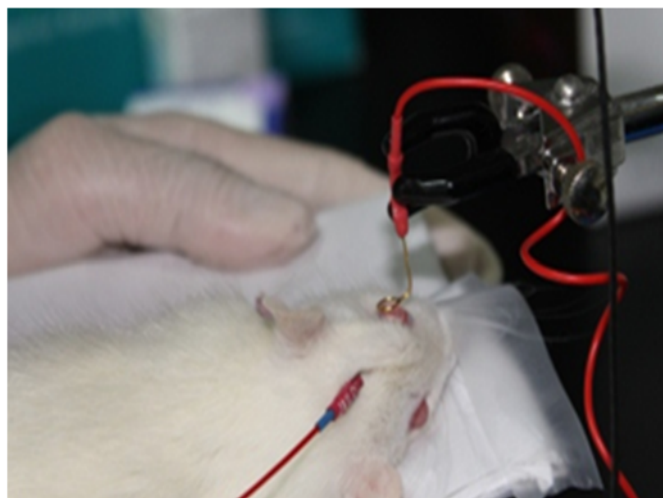


**Figure 25 ERG operation**

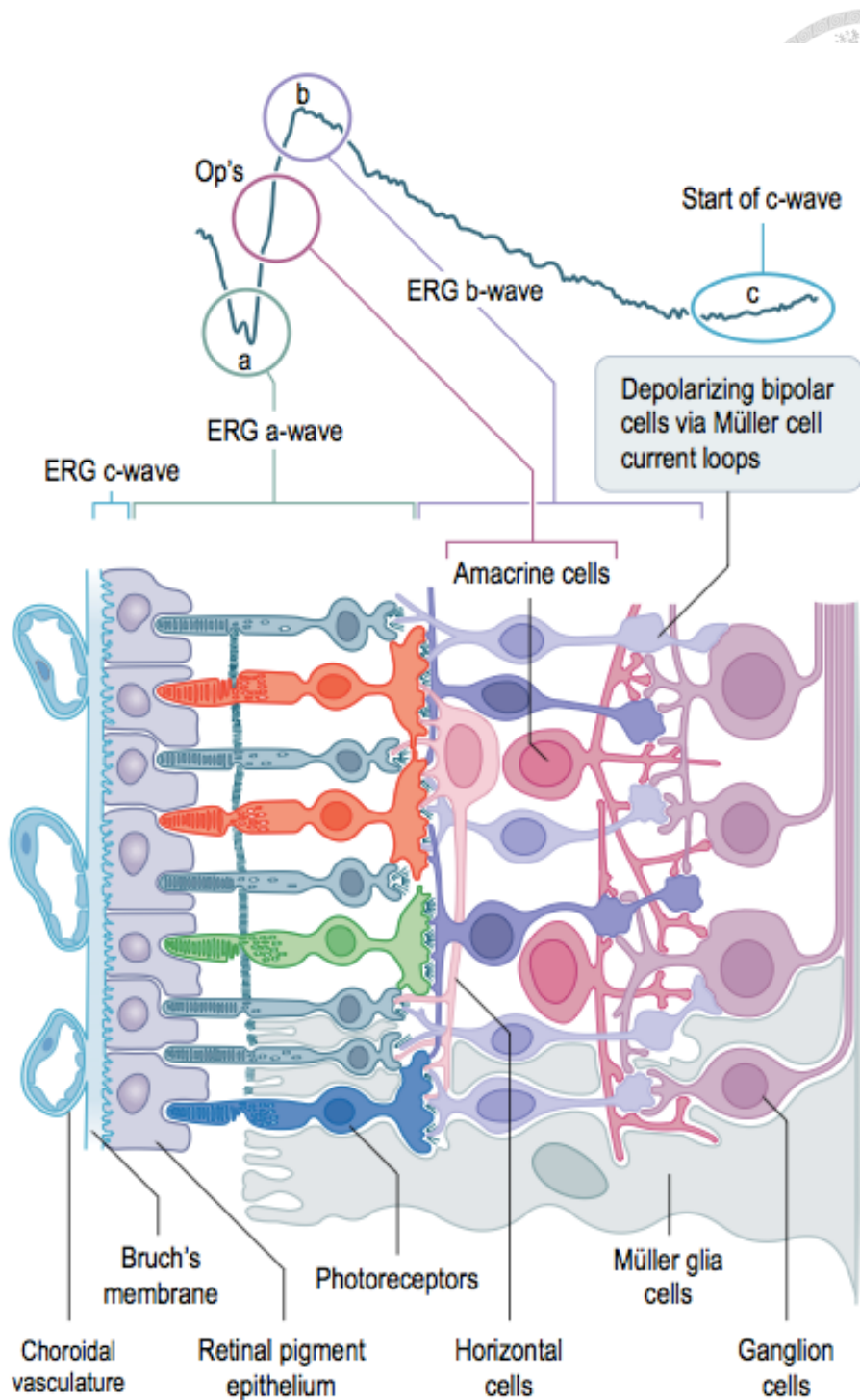
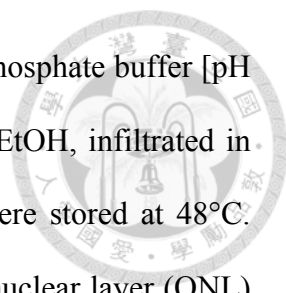


**Figure 26 Diagram of retina response components to ERG stimulation** <sup>15</sup>

### 3.4.2 Hematoxylin and eosin (H&E staining)

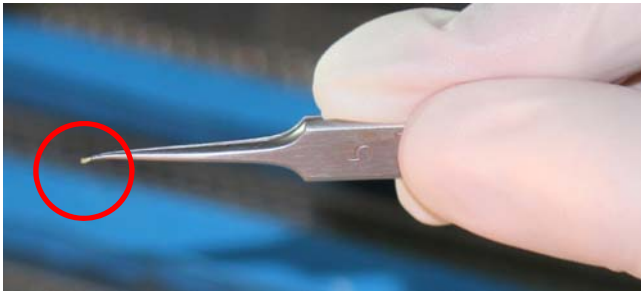
Retinal histology was performed as described previously with modifications <sup>67</sup> after 9, 28, 28+14 d of light exposure. In brief, after pretreatment, paraffin



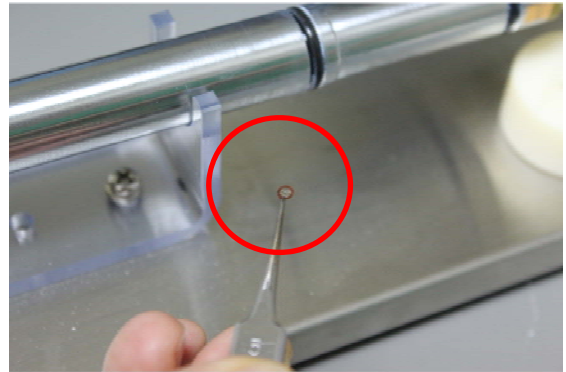
sectioning was performed (4% paraformaldehyde in 0.1 M phosphate buffer [pH 7.4] for 1 h at 48°C), and the eyeballs were dehydrated in EtOH, infiltrated in xylene, and embedded in paraffin. Radial 5 μm sections were stored at 48°C. The histologic analysis included quantification of the outer nuclear layer (ONL) and retina morphology alteration using a light microscope. The midsuperior aspect of the retina was examined for all histological analyses in this study.

### 3.4.3 Transmission electron microscopy (TEM) analysis

TEM was performed as described previously<sup>64</sup> after 9 d of light exposure. The processes were performed at the Electron Microscopy Facility at the Department of Pathology at National Taiwan University Hospital (Taipei, Taiwan). Retina slices of 1 mm (Figure 27A) were prefixed in 2.5% glutaraldehyde in PBS, postfixed with 2% osmium tetroxide, and dehydrated for 10 min each in sequential baths of 30%, 50%, 70%, 90%, and 100% ethanol. The specimens were placed into propylene oxide for 30 min, followed by a mixture of propylene oxide and epoxy resin for an additional 1 h; the samples were subsequently embedded into a gelatin capsule with epoxy resin at 60°C for one day. Subsequently, 80 to 90 nm ultrathin sections were obtained using an ultramicrotome. The sections were stained with 2% tannic acid in distilled water (DW) for 5 min, followed by 2% uranyl acetate in DW for 15 min and a lead-staining solution for 5 min. In the final step, the sections were coated with a thin copper grid-film and placed in a vacuum chamber for scanning (Figure 27B). As shown in Figure 28A, the specimens were examined using TEM with a high-resolution instrument at 80 kV (JEOL JEM-1400, Peabody, MA, USA), and images were captured in real time (Figure 28B).



(A)



(B)

**Figure 27 Specimen of a retina slice**



(A)



(B)

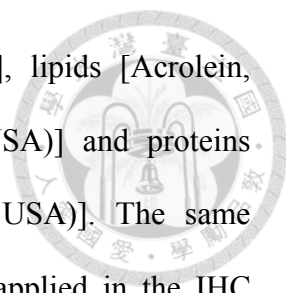
**Figure 28 TEM observation instrument (JEOL JEM-1400)**

#### 3.4.4 Terminal deoxynucleotidyl transferase dUTP nick end labeling (TUNEL)

The TUNEL assay was performed using a FragEL™ DNA fragmentation detection kit (Calbiochem, Darmstadt, Germany) following the standard protocol with a minor modification to detect apoptotic cells after 9 d of light exposure. Tissue sections were deparaffinized, rehydrated, and blocked using endogenous peroxidase with H<sub>2</sub>O<sub>2</sub> for 30 min. Antigen retrieval was achieved by pressure-cooking in a 0.1 M citrate buffer at pH 6 for 10 min followed by cooling at room temperature before incubation with the enzyme. The TUNEL enzyme (1 h at 37°C) and peroxidase converter (30 min at 37°C) were applied to the 10 µm sections after incubation for 5 min in a permeabilizing solution of 0.1% Triton-X in 0.1% sodium citrate. The tissues were counter-stained with DAPI, and the DNA strand breaks were labeled with fluorescein FITC-Avidin D. The fluorescent signals were obtained by adding FITC-Avidin, which bound to the biotinylated-dU of the damaged DNA. After staining, image analysis was used to quantify the relative fluorescence intensity of the TUNEL-positive cells, with the number of TUNEL-stained nuclei quantified in 4 random slides per sample. Sections were visualized on a fluorescent microscope over the entire retina excluding the RPE layer (Nikon Instruments Inc., NY, USA). The number of TUNEL-positive cells for each section was counted by Image-Pro Plus software (v.6.0).

#### 3.4.5 Immunohistochemistry (IHC)

Immunohistochemistry was performed as described previously<sup>67, 68</sup> after 9 d of light exposure. In brief, cryosections of the retina samples were incubated overnight at 48°C with specific primary antibodies. Three antibodies were used for detection of oxidative/nitrative modifications of DNA [8-hydroxy-2'-



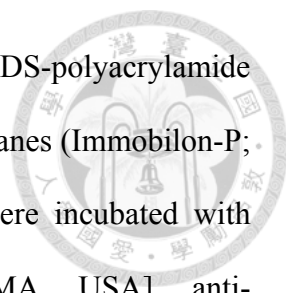
deoxyguanosine (8-OHdG) (1:50, JAICA, Tokyo, Japan)], lipids [Acrolein, (1:200, Advanced Targeting Systems, San Diego, CA USA)] and proteins [nitrotyrosine, (1:200, Abcam, Millipore Billerica, MA, USA)]. The same quantification method used for the TUNEL analysis was applied in the IHC analyses. The relative fluorescence intensity corresponding to the number of IHC-positive cells for each section was measured and quantified by Image-Pro Plus software (v.6.0).

#### 3.4.6 Free radical assay (reactive oxidative species, ROS)

Measurement of reactive oxygen species in the retina was performed as described previously<sup>68</sup> after 3 or 9 d of light exposure. In brief, 0.2 mL of homogenized extraction was loaded with 0.1 mL of 0.9% saline onto a 3-cm dish with a stir bar placed at the center. The dish was placed into the chemiluminescence analyzer chamber (Tohoku CLA-FS1, Miyagi, Japan). The ROS were quantified after adding the enhancer Lucigenin to the chemiluminescence analyzer. After 60 s of background detection, 1 mL of a Lucigenin (bis-N-methylacridinium nitrate) solvent (2.5 mg of Lucigenin dissolved in 50 mL 0.9% saline) was added for stimulation. The stimulated O<sub>2</sub><sup>-</sup> and total oxidative products were captured every 10 s and computed for 7 min after 1 min of baseline detection.

#### 3.4.7 Western blotting (WB)

Total protein was extracted from the retina by lysing the sample in radioimmunoprecipitation assay (RIPA) buffer [0.5 M Tris-HCl (pH 7.4), 1.5 M NaCl, 2.5% deoxycholic acid, 10% NP-40, 10 mM EDTA] and protease inhibitors (Complete Mini; Roche Diagnostics Corp., Indianapolis, IN, USA). The extract and Laemmli buffer were mixed at a 1:1 ratio, and the mixture was



boiled for 5 min. A 100-mg sample was separated on 10% SDS-polyacrylamide gels and then transferred to polyvinylidene difluoride membranes (Immobilon-P; Millipore Corp., Billerica, MA, USA). The membranes were incubated with anti-hemeoxygenase-1 [(HO-1); Abcam, Cambridge, MA, USA], anti-ceruloplasmin [(CP); Santa Cruz Biotechnology, Dallas, Texas, USA], anti-cytosolic glutathione peroxidase [(GPx1); Abcam, Millipore Billerica, MA, USA], anti-poly (ADP-ribose) polymerase-1 [(PARP-1); Cell Signaling Technology Inc., Danvers, MA, USA], anti-superoxide dismutase [(SOD2); Santa Cruz Biotechnology Inc., Dallas, Texas, USA], and anti- $\beta$ -actin (Abcam, Millipore Billerica, MA, USA) antibodies. The membranes were incubated with horseradish peroxidase-conjugated secondary antibody and visualized by chemiluminescence (GE Healthcare). The density of the blots was determined using image analysis software after scanning the image (Photoshop, ver.7.0; Adobe Systems, San Jose, CA, USA). The optical densities of each band were evaluated by comparison with the density of the  $\beta$ -actin bands.

#### 3.4.8 Hydrogen peroxide (H<sub>2</sub>O<sub>2</sub>) assay

The assay was performed using a hydrogen peroxide colorimetric/fluorometric assay kit (BioVision, Milpitas, CA, USA) following the standard protocol to detect H<sub>2</sub>O<sub>2</sub> concentrations after 3 days of light exposure. In brief, total protein was extracted from the retina and centrifuged for 15 min immediately after the extraction. Each well was loaded with 20  $\mu$ l samples and brought to a volume of 50  $\mu$ l with assay buffer. Reagents and H<sub>2</sub>O<sub>2</sub> standards were mixed and then incubated for 10 min. A background detection was performed, and an H<sub>2</sub>O<sub>2</sub> standard curve was plotted. Sample readings were compared to the standard curve for the concentration calculations.



#### 3.4.9 Total iron and ferric (Fe<sup>3+</sup>) assay

The assay was performed using a QuantiChrom Iron Assay (DIFE-250) Kit (BioAssay Systems, Hayward, CA, USA) following the standard protocol to detect total iron concentrations after 3 days of light exposure. In brief, total protein was extracted from the retina, and 50 µl of the extraction was loaded into a 96-well plate. Then, 200 µl of working reagent was added and incubated for 40 min at room temperature, followed by an optical density reading at 510–630 nm. Sample readings were compared with the standard curve to calculate the concentrations.

#### 3.5 Statistical analysis

Data are presented as the mean ± SD unless otherwise stated. Data were evaluated using an analysis of variance (ANOVA) with Tukey's post hoc tests to show differences between the groups. A *p* value less than 0.05 was considered statistically significant.

## 4 RESULTS AND DISCUSSION



### 4.1 White LED at domestic lighting level to induce retinal injury

#### 4.1.1 Electrophysiological response shows photoreceptor cell function loss

The representative ERG response curves of rats are shown in Figure 29A. The normal retina showed a high b-wave peak, but the injured retina curved a low b-wave peak as a result of cell function loss. As shown in Figure 29B. Two LED groups and the white CFL group all demonstrated a significant decrease of b-wave amplitude at day 9 and day 28 after light exposure (ANOVA followed by Tukey post hoc test  $p < 0.001$ ). The b-wave amplitude of the yellow CFL group did not decrease significantly at day 9; however, it had 21% of decrease at day 28 after light exposure. The data from each of the four exposure groups was not statistically different at 28+14 d as compared to 28 d of exposure, and this trend was also applied to the H&E staining results (data not shown). No significant development was found after 3 d of light exposure, and therefore data were not shown as well.\*

---

\* The results in section 4.1 has been published by *Environmental Health Perspectives* with the citation information as: Shang YM, Wang GS, Sliney D, Yang CH, Lee LL. White Light-Emitting Diodes (LEDs) at Domestic Lighting Levels and Retinal Injury in a Rat Model. *Environ. Health Perspect.* 2014;122(3):269-76. doi:10.1289/ehp.1307294.

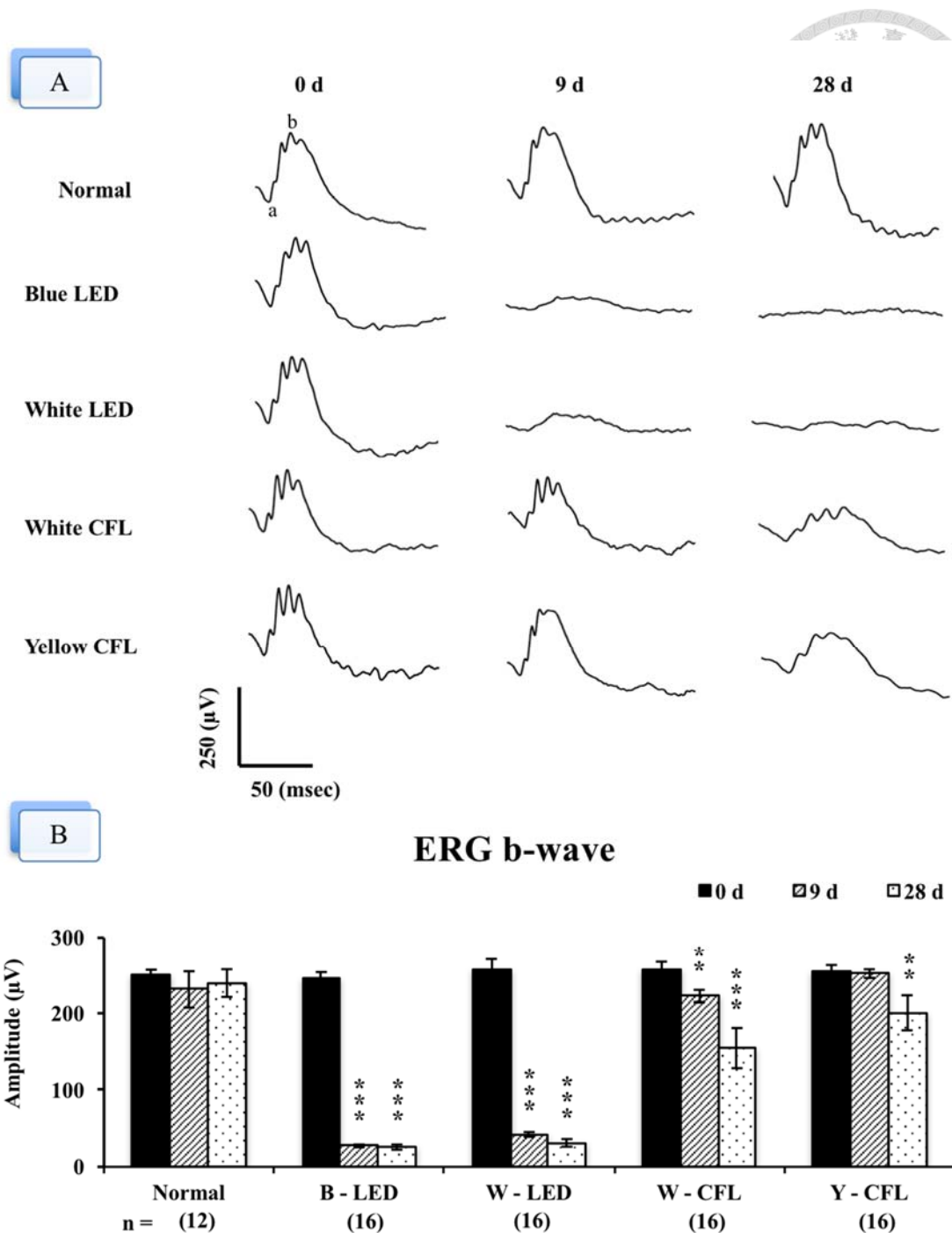


**Figure 29 ERG responses after light exposure**

Both LED groups demonstrated a significant decrease of b-wave amplitude at day 9 and day 28 after light exposure. The fluorescent lamp groups developed severe loss of b-wave amplitude until 28 d of light exposure.  $n = 3$  for controls,  $n = 3$  for 3 days of exposure groups, and  $n = 8$  for each exposure group at each time of exposure (Curve scale: amplitude = 250  $\mu\text{V}$  and stimulation = 50 msec). (\*\*, \*\*\*  $p < 0.01, 0.001$ , respectively, compared to the “normal” group by ANOVA with the Tukey post hoc test).



#### 4.1.2 Retinal histology–H&E staining showing layer damages

As shown in Figure 30a-b. White LED light exposure can lead to morphologic alterations in the rat retina. The group that was exposed to 750 lux white LED light for 28 d exhibited the adverse effect of light exposure including the pyknotic photoreceptor nuclei (arrow), swelling of the inner segment (arrow head), and a disorganized outer segment (asterisk). As shown in Figure 30c-f. The ONL thickness of white and blue LED groups decreased significantly at day 9 and day 28 (data not shown) after light exposure (ANOVA followed by Tukey post hoc test  $p < 0.01$ ), whereas, the ONL thickness of the white and yellow CFL groups did not decrease significantly at day 9 after light exposure.

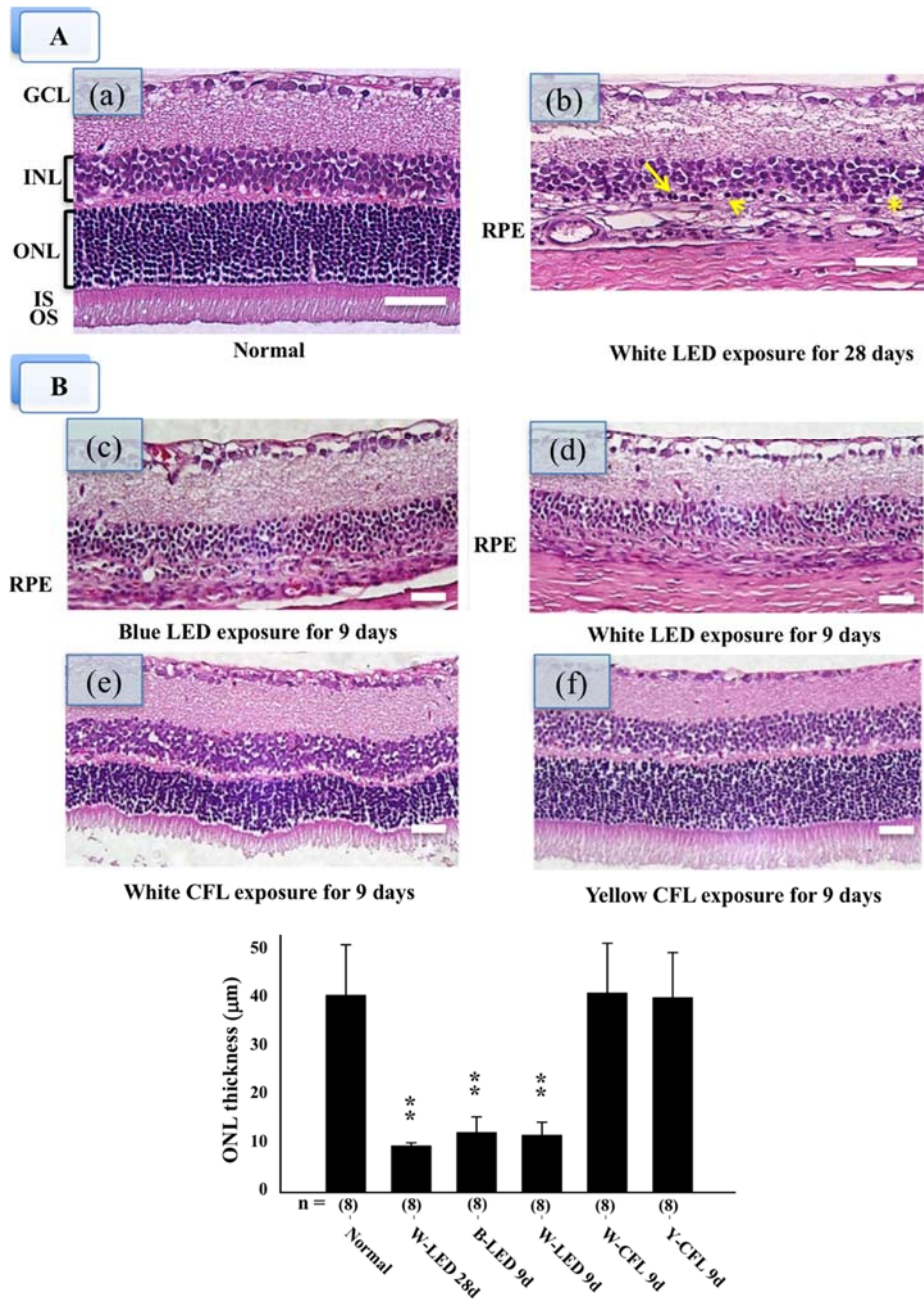


**Figure 30 Retinal light injury after 9 d or 28 d of exposure analyzed by H&E staining**

GCL: ganglion cell layer. INL: inner nuclear layer. ONL: outer nuclear layer. IS: inner segment. OS: outer segment. \*RPE: the retinal pigment epithelium (usually next to the OS layer) is detached and cannot be found within this scope.

(A) (a) Normal retina layers, and (b) light exposure-induced retinal injury, including the absence of photoreceptors and INL degeneration. (B) The ONL thickness of the LED groups decreased significantly at day 9 and day 28 after light exposure, whereas the ONL thickness of white and yellow CFL groups did not decrease significantly at day 9 after light exposure. Both blue (c) and white LED (d) light exposure caused the disappearance of photoreceptors; the white CFL group (e) exhibited distortion of the OS and ONL; and the yellow CFL group (f) exhibited less movement in each layer.  $n = 3$  for controls and  $n = 8$  for each group after 9 or 28 days of exposure (\*\* indicates  $p < 0.01$ , compared to the “normal” group by ANOVA with the Tukey post hoc test; scale bar = 50 µm).

#### 4.1.3 Apoptosis Detection - TUNEL staining detects nuclear apoptosis

The retinal TUNEL stains are shown in Figure 31. Light exposure induced significant retinal cell apoptosis in all groups. However, more apoptotic cells were shown in the retina of the LED groups than in the retina of the CFL lamp groups after 9 d of exposure (ANOVA followed by Tukey post hoc test  $p < 0.001$  for LED groups;  $p < 0.01$  for CFL groups).

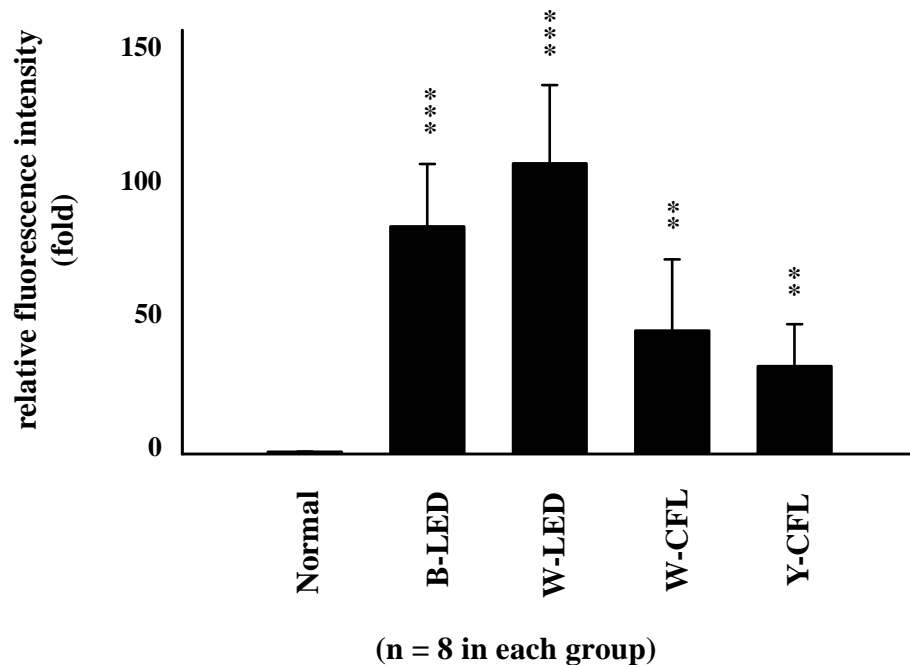
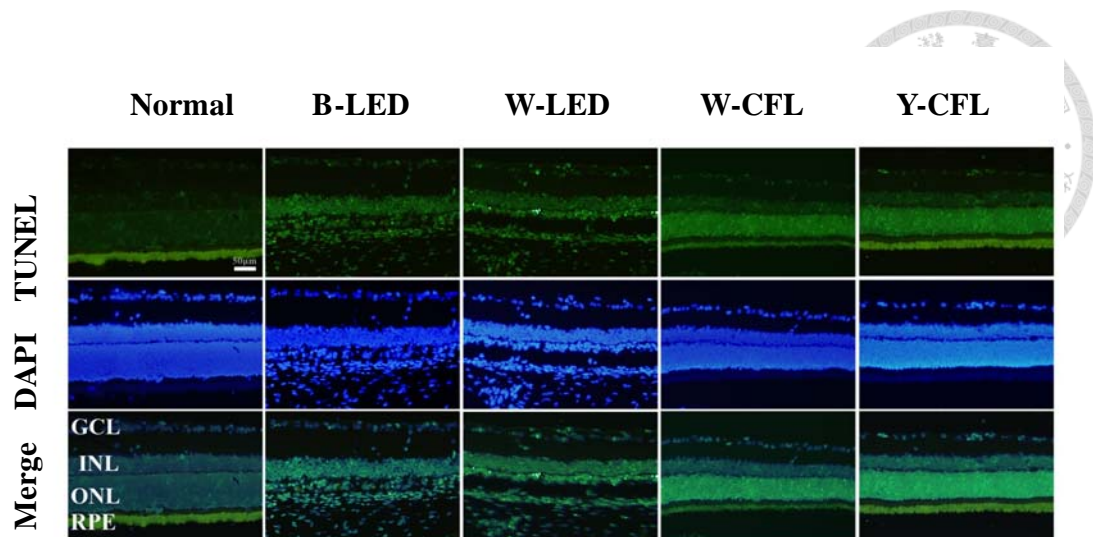


**Figure 31 Light-induced retinal cell apoptosis tested by TUNEL labeling**

GCL: ganglion cell layer. INL: inner nuclear layer. ONL: outer nuclear layer. RPE: the retinal pigment epithelium.

The damaged retina cells correspond to the positive labeling. (A) The result shows that more apoptotic cells (arrows) appear in the retina of the LED groups than that of the CFL groups after 9 days of light exposure. (B) The LED groups exhibit higher fluorescence intensity. n = 3 for controls and n = 8 for each exposure group (\*\*, \*\*\*  $p < 0.01, 0.001$ , respectively, compared to the “normal” group by ANOVA with the Tukey post hoc test; scale bar = 50 μm).

#### 4.1.4 TEM demonstrations on the cellular injury

As shown in Figure 32 (samples were taken after 9 d of white LED light exposure). Nucleolus damage of photoreceptors occurred after exposure including early stage of nucleolus condensation (32b), karyolysis (32c), pyknosis (32d-e), and karyorrhexis (32f). Another crucial observation of photoreceptor injury included disruption of the inner and outer segments, which is shown in Figure 32g-l.





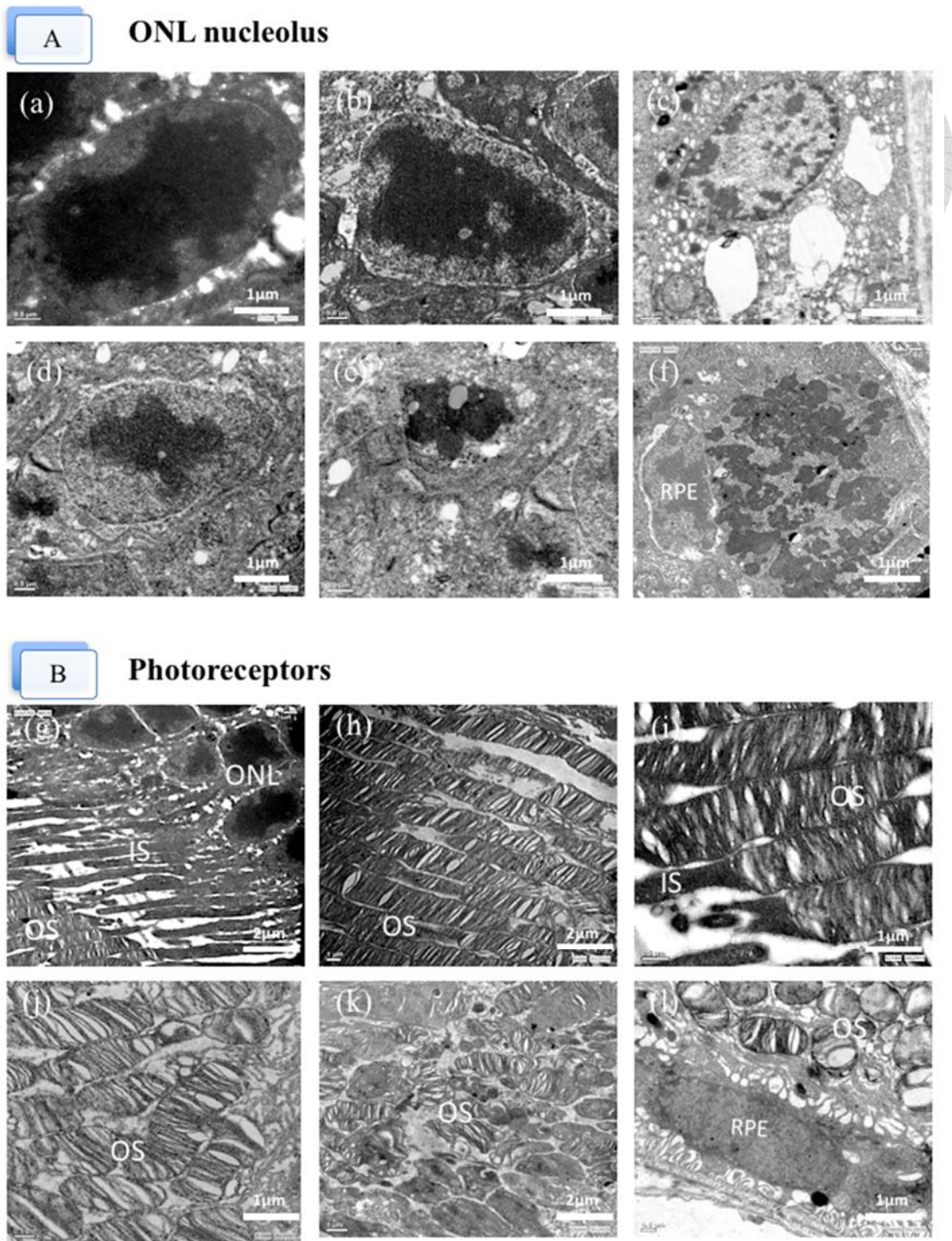


**Figure 32 Retinal cellular injury studied by TEM**

The photoreceptor nucleolus damage after LED light exposure result in (A) ONL nuclear deformations (arrows) shown as (a) normal ONL nucleus; (b) nucleolus condensation; (c) karyolysis; (d and e) pyknosis; (f) karyorrhexis. (B) Photoreceptor deformations and (g) normal photoreceptor, IS and OS; (h and i) showing minor disruption; (j, k, and l) and IS disappearance followed by OS shrinkage and the formation of several small round shapes (scale bar = 2 μm for g, h, and k; scale bar = 1 μm for the rest of others). n = 3 for controls and n = 5 for white LED group after 9 days of exposure. Samples were selected to show their representativeness and photographs were taken from different samples.

#### 4.1.5 Immunohistochemistry (IHC) staining results indicating retinal light injury

Oxidative injury results in adducts on macromolecules that can be detected by immunostaining. The antibodies that specifically recognize these adducts provide evidence of the oxidative injury. Three antibodies were used to detect cell conditions in these experiments after 9 d of light exposure, including acrolein for lipid recognition (Figure 33A), 8-OHdG for DNA detection (Figure 33B), and nitrotyrosine for protein identification (Figure 33C). The results show that LED groups exhibit higher fluorescence intensity with 8-OHdG, acrolein and nitrotyrosine in ONL (ANOVA followed by Tukey post hoc test  $p < 0.001$  for LED groups) and that the fluorescent lamps induced lower fluorescence intensity of 8-OHdG, acrolein and nitrotyrosine in ONL.

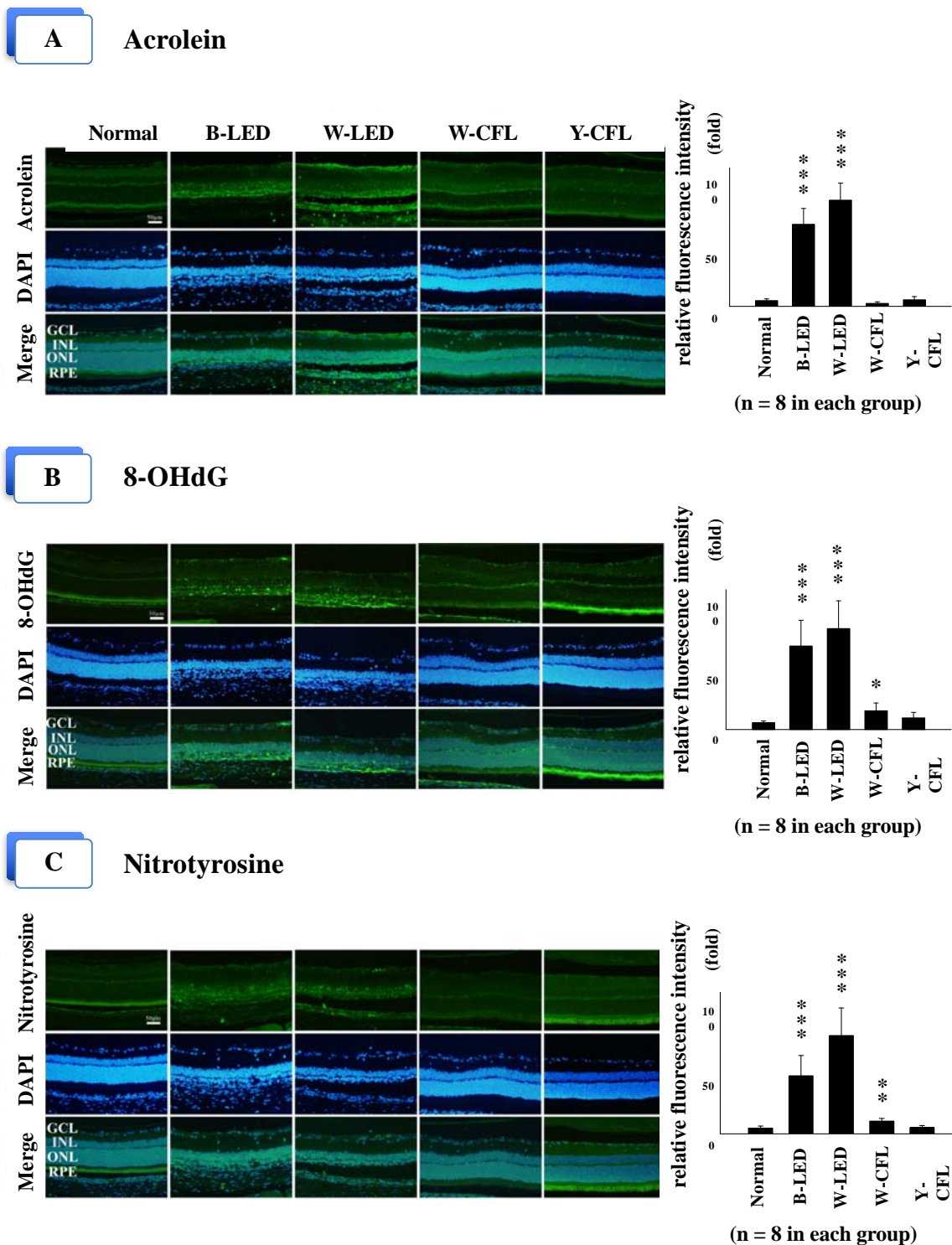
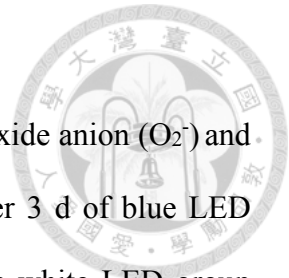


**Figure 33 Retinal light injury labeling after 9 d of exposure by IHC**

(A) Acrolein was used to detect the lipid adducts on macromolecules; (B) 8-OHdG was used to detect the DNA adducts; and (C) Nitrotyrosine was used for protein adduct recognition. The result shows LED groups exhibit higher fluorescence intensity on ONL, and the fluorescent lamp groups respond to lower fluorescence intensity on ONL.  $n = 3$  for controls and  $n = 8$  for each exposure group (\*, \*\*, \*\*\*  $p < 0.05, 0.01, 0.001$ , respectively, compared to the “normal” group by ANOVA with the Tukey post hoc test; scale bar = 50  $\mu\text{m}$ ).

#### 4.1.6 Oxidative Stress -- superoxide anion $O_2^-$ shows the injury

As shown in Figure 34A. Lucigenin-stimulated superoxide anion ( $O_2^-$ ) and total oxidative products were computed for all groups. After 3 d of blue LED light exposure, the retina  $O_2^-$  exceeded 60000 in 8 min, the white LED group exhibited a high total count close to 40000, and the fluorescent groups accumulated smaller total counts from 20000 to 30000. However, the plot exhibited an opposite trend when the exposure duration was increased to 9 d (Figure 34B). This result suggests that retinal oxidative stress may be induced by light exposure in the early stage.



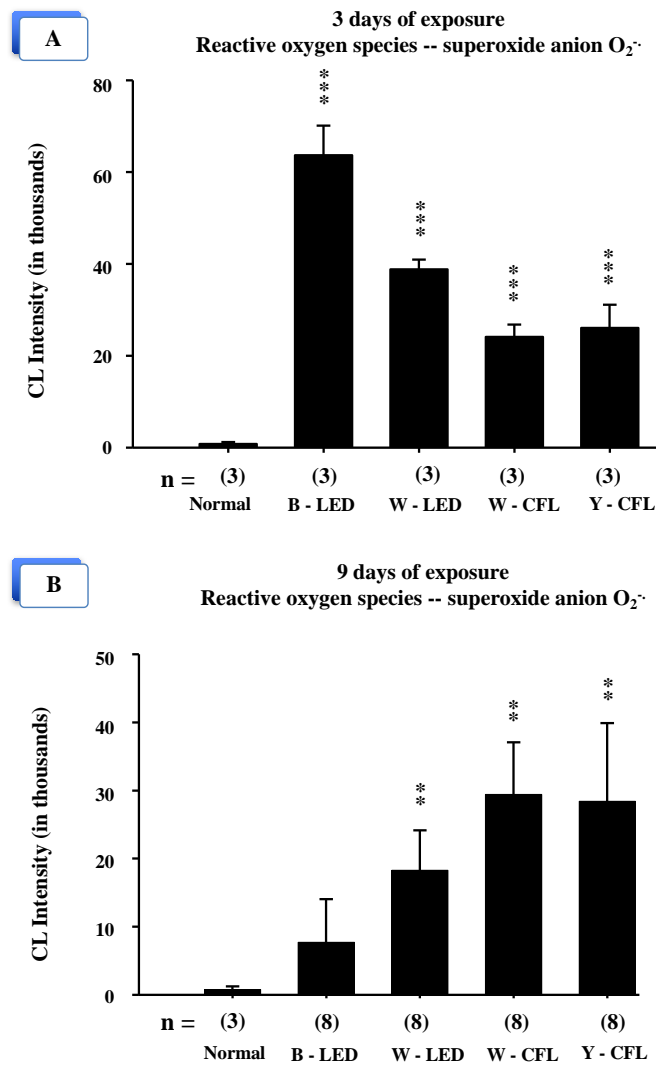


**Figure 34 A reactive oxygen species assay after 3 d and 9 d of light exposure**

CL: chemiluminescence

(A) After 3 d of blue LED light exposure, the lucigenin-stimulated superoxide anion ( $O_2^{\cdot -}$ ) exceeded 60000 in total count; the white LED group had a high total count close to 40000; and the fluorescent groups accumulated less total counts from 20000 to 30000, whereas normal rats exhibited only a count of approximately 1000.  $n = 3$  for controls and  $n = 3$  for each exposure group. (B) After 9 d of exposure, the  $O_2^{\cdot -}$  total count for the blue LED light group decreased to 8000; the white LED light group decreased to 18000; and both fluorescent light groups remained at the same level at 20000 to 30000.  $n = 3$  for controls and  $n = 8$  for each exposure group (\*\*, \*\*\*  $p < 0.01, 0.001$ , respectively, compared to the “normal” group by ANOVA with the Tukey post hoc test).

## 4.2 Mechanism of LED induced retinal injury and its wavelength dependency

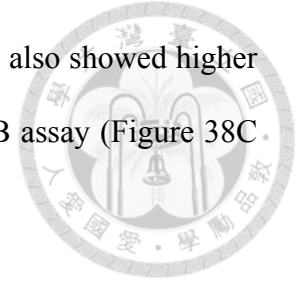
### 4.2.1 Functional and morphological alterations

The representative ERG response curves of the testing animals are shown in Figure 35. Whereas the control group showed normal ERG a- and b-waves, the blue LED significantly weakened the ERG responses after 3 days of exposure. Moreover, the b-wave amplitudes for the blue, green, and red light exposure groups all showed a significant decrease compared with the control group after 9 days of exposure. The H&E images in Figure 36A show an uneven morphological alteration in the rat retinas after 28 days of light exposure. Figure 36B quantifies the thickness of the ONL and shows that the blue LED exposure group has the least thickness.

The TEM histopathology analysis (Figure 37) highlighted that the injury in the RPE and photoreceptors area from blue light could be lethal after 9 days of exposure; more details were described in section 4.1.4. Referring to the retinal remodeling phases <sup>62, 63</sup>, Figure 37A shows the normal ONL nucleolus and its pyknosis in phases 1 and 2. Figure 37B shows the normal photoreceptor outer segment (POS) and its disorganized disks in phase 1 and the round POS in phase 2. Figure 37C displays the normal oval-shaped RPE nucleus and shrinkage in phase 1 and the RPE condensation and deformation in phase 2.

As shown in Figure 38, the apoptotic analysis by TUNEL staining in Figure 38A and 38B shows significant fluorescence response increases after 9 days of light exposure. Both the histological and apoptotic results showed that light exposure may cause RPI for blue, green and red LEDs. However, the blue light had a stronger effect than did the other two groups. It's also worth to mention that TUNEL staining does not always correlate with the eventual cell

death.<sup>69</sup> The caspase-independent apoptotic marker PARP-1 also showed higher activation signals after blue and green light exposure by WB assay (Figure 38C and 38D). \*



---

\* The results in section 4.2 has been accepted for publication by *International Journal of Ophthalmology* under the title of “Light-emitting-diode (LED) induced retinal damage and its wavelength dependency *in vivo*”. It is arranged to be published in the volume 10, number 2, column of basic research in 2017.

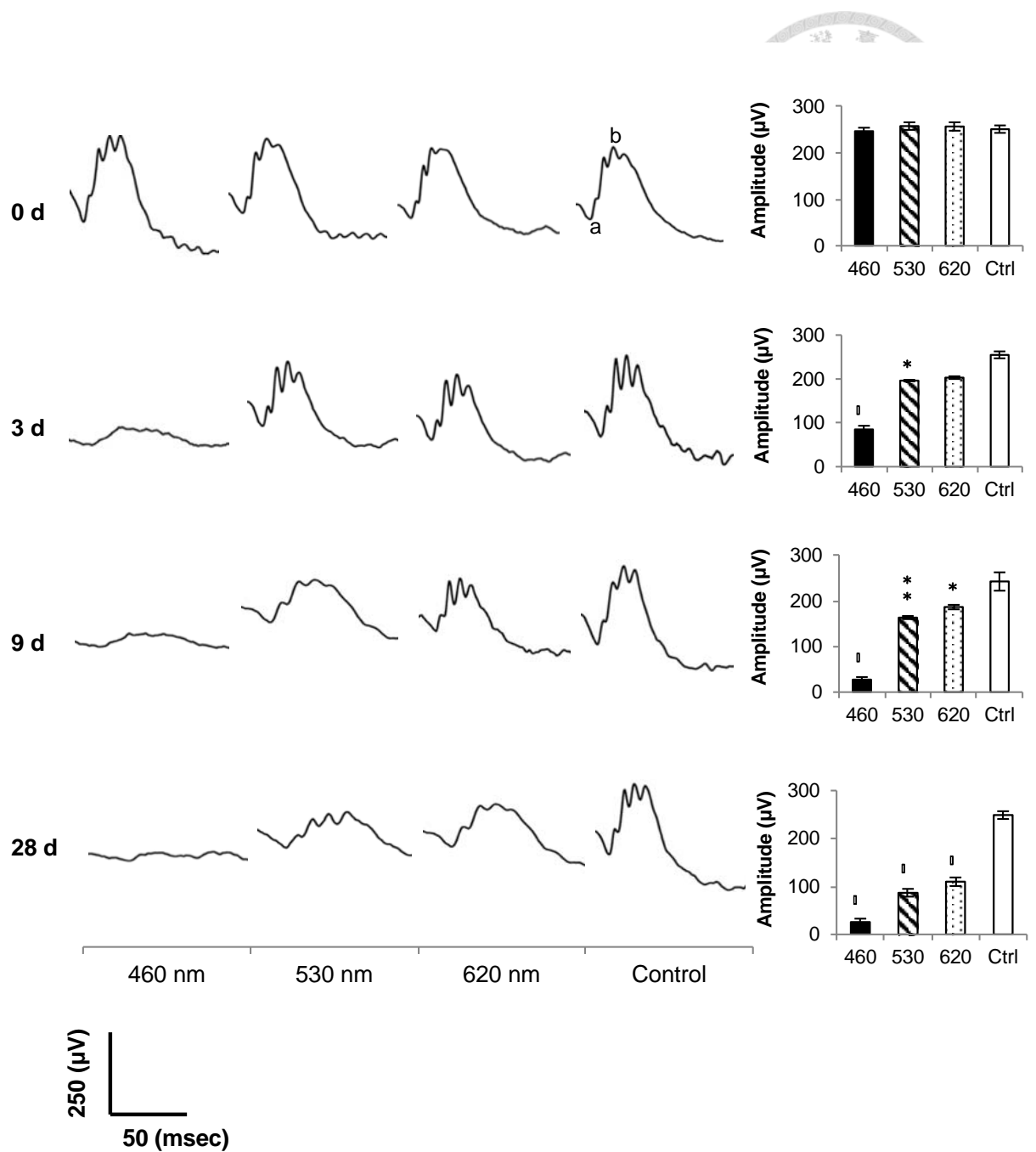


**Figure 35 Electretinography (ERG) responses**

All three LED groups demonstrated a significant decrease in the b-wave amplitude after light exposure. The blue LED group showed the highest function loss;  $n = 40$  for the control group and  $n = 54$  for each exposure group (curve scale: amplitude = 250  $\mu\text{V}$  and stimulation = 50 msec) (\*, \*\*, #  $p < 0.05, 0.01, 0.001$ , respectively, compared with the control group).



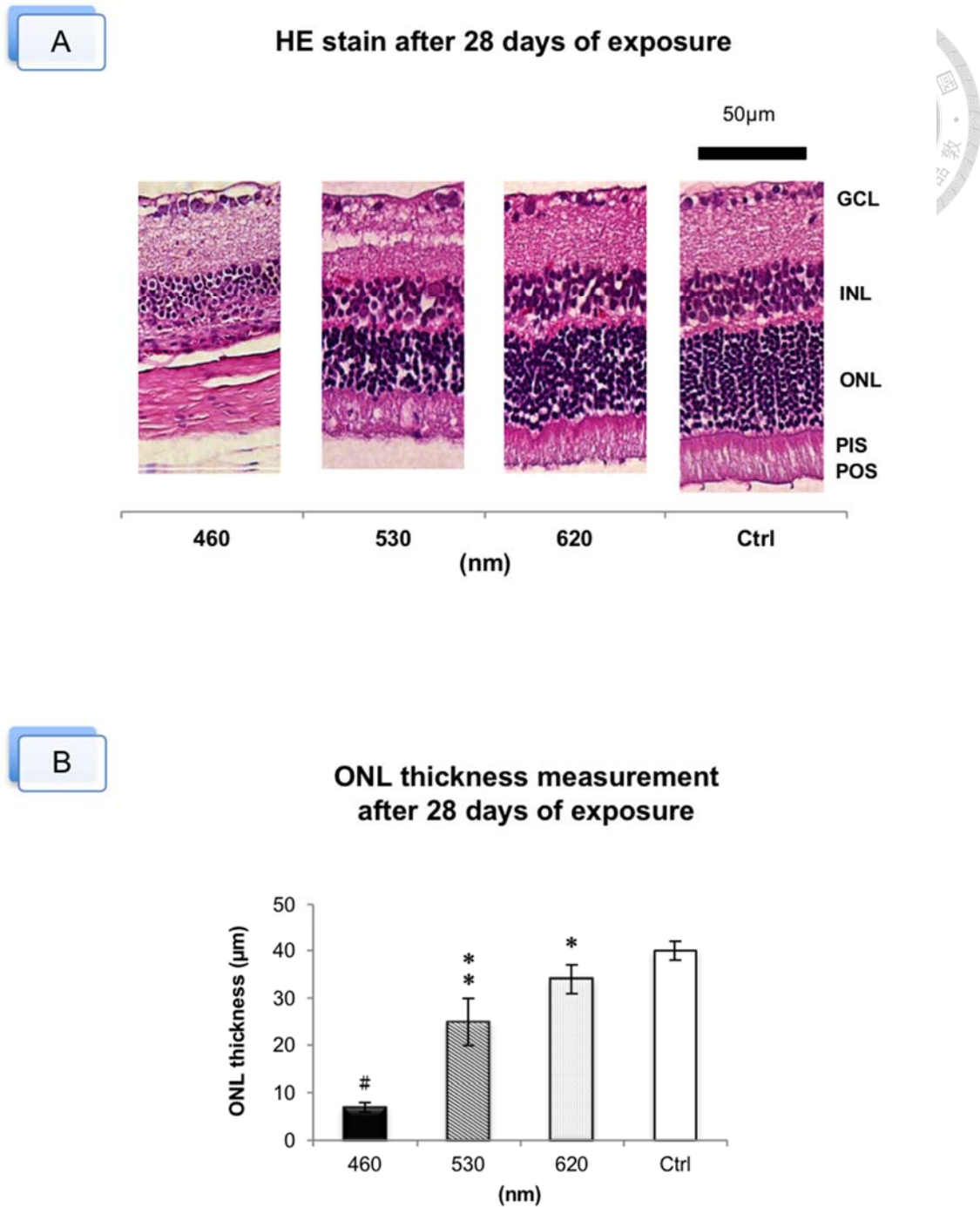


**Figure 36 Histological analysis**

GCL: ganglion cell layer. INL: inner nuclear layer. ONL: outer nuclear layer. PIS: photoreceptor inner segment. POS: photoreceptor outer segment. \*RPE: the retinal pigment epithelium (usually next to the POS layer) is detached and cannot be found within this scope in (A).

(A) Normal retinal layers in the control group compared to different LED light exposure-induced retinal injuries, including the absence of photoreceptors and INL degeneration. (B) The ONL thickness of the exposure groups decreased significantly after 28 days of light exposure. The blue LED group exhibited the strongest loss;  $n = 6$  for the control group and  $n = 8$  for each exposure group. (\*, \*\*, #  $p < 0.05, 0.01, 0.001$ , respectively, compared with the control group; scale bar = 50 μm).

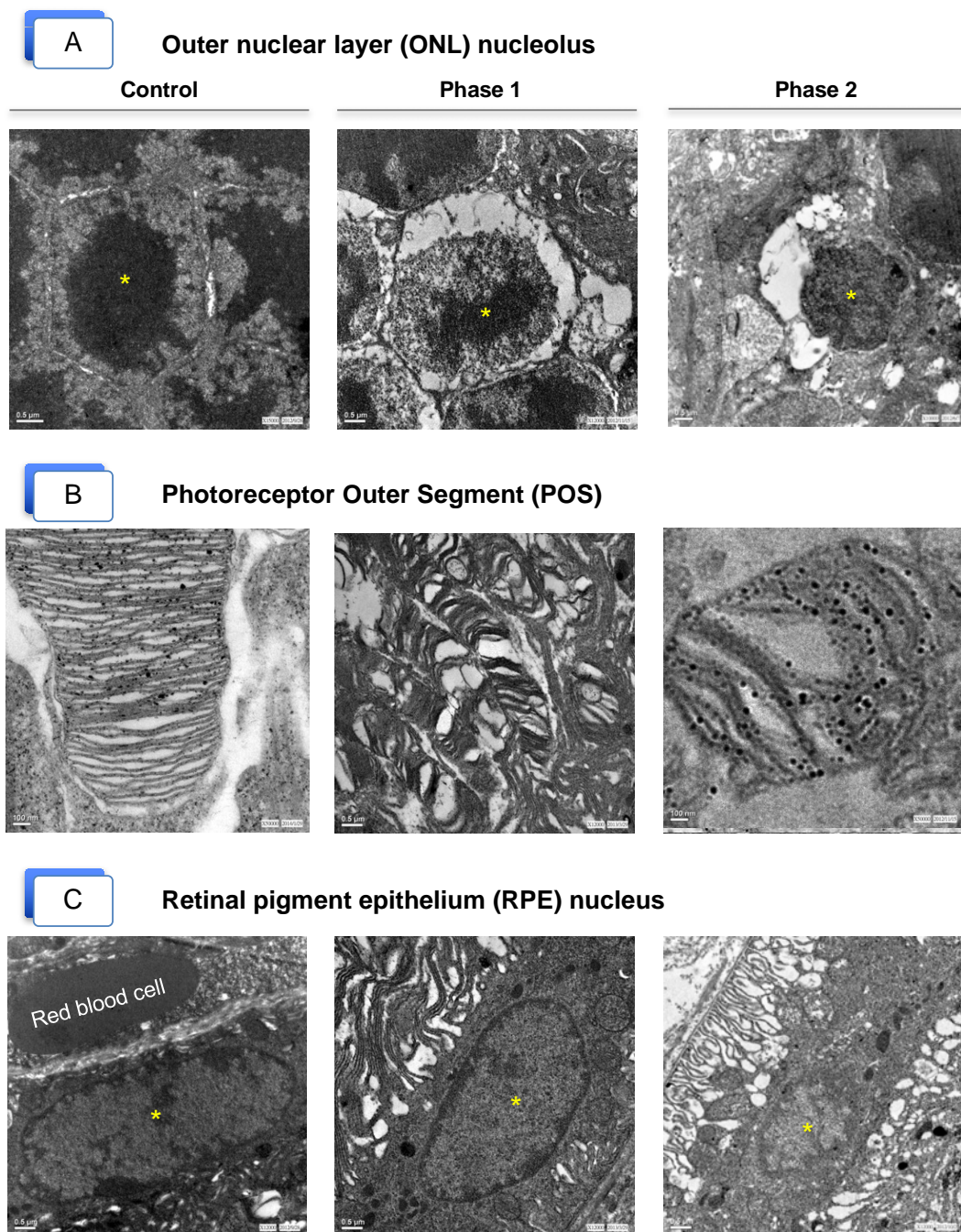
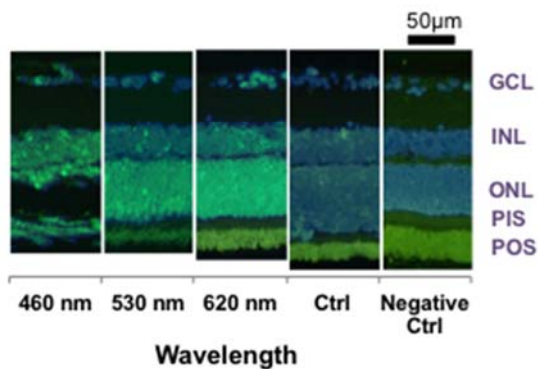


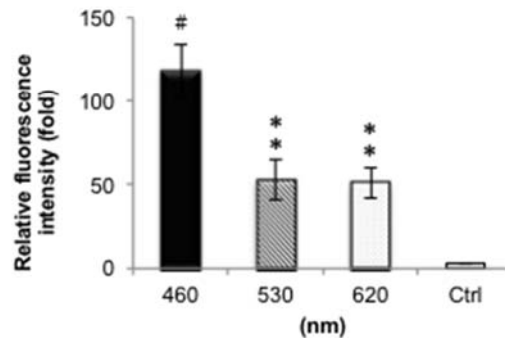
**Figure 37 Retinal cellular injury studied by transmission electron microscopy (TEM)**

(A) Normal ONL nucleolus on the left; nucleolus condensation in phase 1 remodeling and pyknosis in phase 2. (B) Normal photoreceptor outer segment (POS) on the left; POS deformations in phase 1 remodeling and round POS debris in phase 2. (C) Normal retinal pigment epithelium (RPE) nucleus on the left; shrinking RPE nucleus in phase 1 and condensation in phase 2. There are 36 sections analyzed and 244 of pyknotic RPE nuclei observed after the blue light exposure;  $n = 4$  for the control group and  $n = 6$  for the exposure group (Scale bar = 100 nm for the control and phase 2 in (B); scale bar = 0.5  $\mu\text{m}$  for the rest of other images).

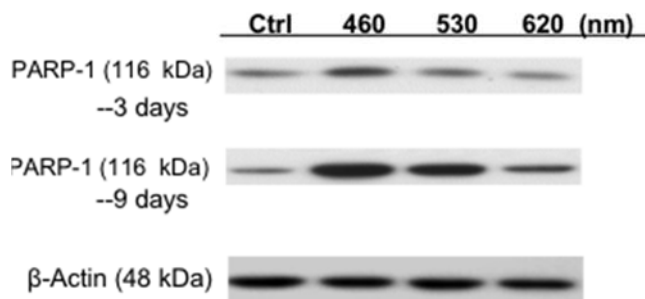
**A** TUNEL labeling after 9 days of exposure



**B** Quantified measurement



**C** Apoptotic marker expression after 3- and 9 days of exposure



**D** Quantified measurement

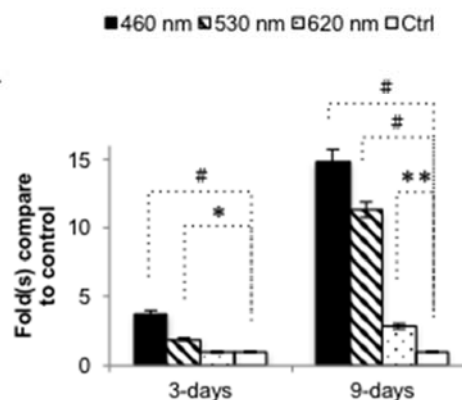


**Figure 38 Molecular apoptotic marker detection**

GCL: ganglion cell layer. INL: inner nuclear layer. ONL: outer nuclear layer. PIS: photoreceptor inner segment. POS: photoreceptor outer segment.

(A) The damaged retinal cells correspond to the positive labeling. The results showed that more apoptotic cells presented in the retina of the exposure groups. (B) The blue LED group exhibited the highest fluorescence intensity. (C) The WB results showed apoptotic marker, PARP-1, had higher activation after 3 days of blue or green light exposure. (D) The PARP-1 expression showed much significant activation after 9 days of exposure;  $n = 4$  for the control group and  $n = 8$  for each exposure group. (\*, \*\*, #  $p < 0.05, 0.01, 0.001$ , respectively, compared with the control group).

#### 4.2.2 RPI oxidative stress markers expression

Three IHC antibodies were used to detect cellular oxidative/nitrative markers after 9 days of light exposure. The 8-OHdG (Figure 39A and 39B), acrolein (Figure 39C and 39D), and nitrotyrosine (Figure 39E and 39F) labels represent the oxidative and nitrative damage to DNA, lipid, and protein, respectively. These three IHC antibodies all showed strong responses. The blue LED caused more cell insults than did the green and red LED based on the highest fluorescence responses ( $p < 0.001$ , by ANOVA followed by Tukey's post hoc test).

As shown in Figure 40A and 40B, the WB results showed that light injury up-regulated the stress protein expression of the antioxidant genes hemeoxygenase-1 (HO-1) and the enzymatic antioxidant GPx1 as an antioxidant response to light insult. The protein expression levels of HO-1 and GPx1 were significantly augmented in the blue light exposure group (15.03 and 6.34 times higher, respectively, compared with the control). The apoptotic marker PARP-1 also showed a 3.8 times higher activation signal after blue light exposure. Overall, the blue light group had the clearest expression in the bands, and the green and red light groups had relatively mild responses after 3 days of exposure. Although the upward trend remained the same among the exposure groups, the intensity factors varied after 9 days of exposure (Figure 40C and 40D). Interestingly (Figure 40E), the manganese superoxide dismutase (MnSOD, SOD2) was down-regulated after 3 or 9 days of blue LED light exposure (0.69 and 0.78 times that of the control group) before reaching a higher expression of 0.99 at day 28 due to the delayed/adaptive antioxidant response<sup>70</sup>.

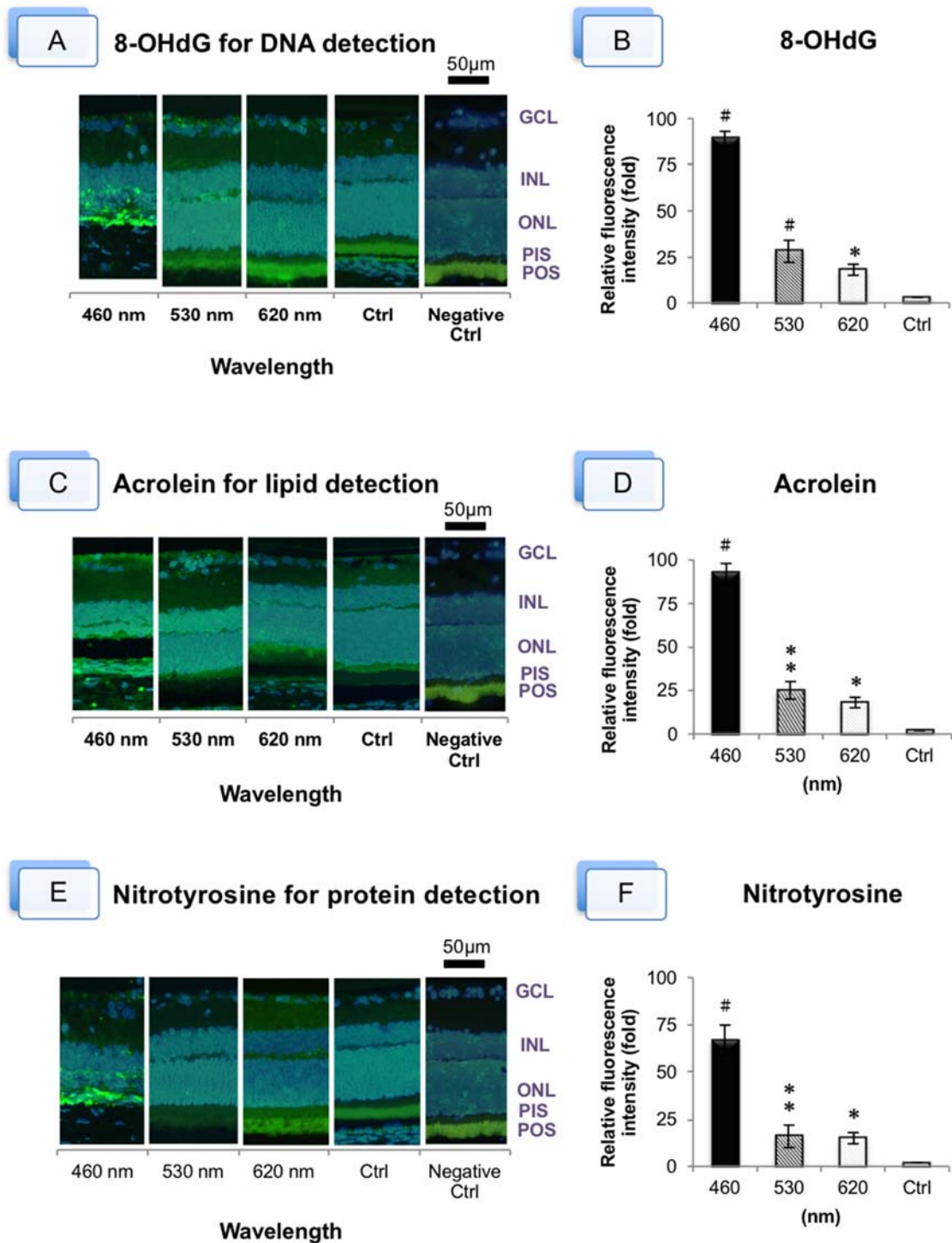


**Figure 39 Retinal light injury molecular labeling by immunohistochemistry (IHC)**

GCL: ganglion cell layer. INL: inner nuclear layer. ONL: outer nuclear layer. PIS: photoreceptor inner segment. POS: photoreceptor outer segment.

(A, B) 8-OHdG was used to detect the DNA adducts, (C, D) acrolein to detect the lipid adducts on macromolecules, and (E, F) nitrotyrosine for protein adduct recognition. The result shows all exposure groups exhibited higher fluorescence intensity in the ONL. The blue LED group exhibited the highest response, whereas the green and red groups' response was lower;  $n = 6$  for the control group and  $n = 8$  for each exposure group. (\*, \*\*, #  $p < 0.05, 0.01, 0.001$ , respectively, compared with the control group; scale bar = 50  $\mu\text{m}$ ).

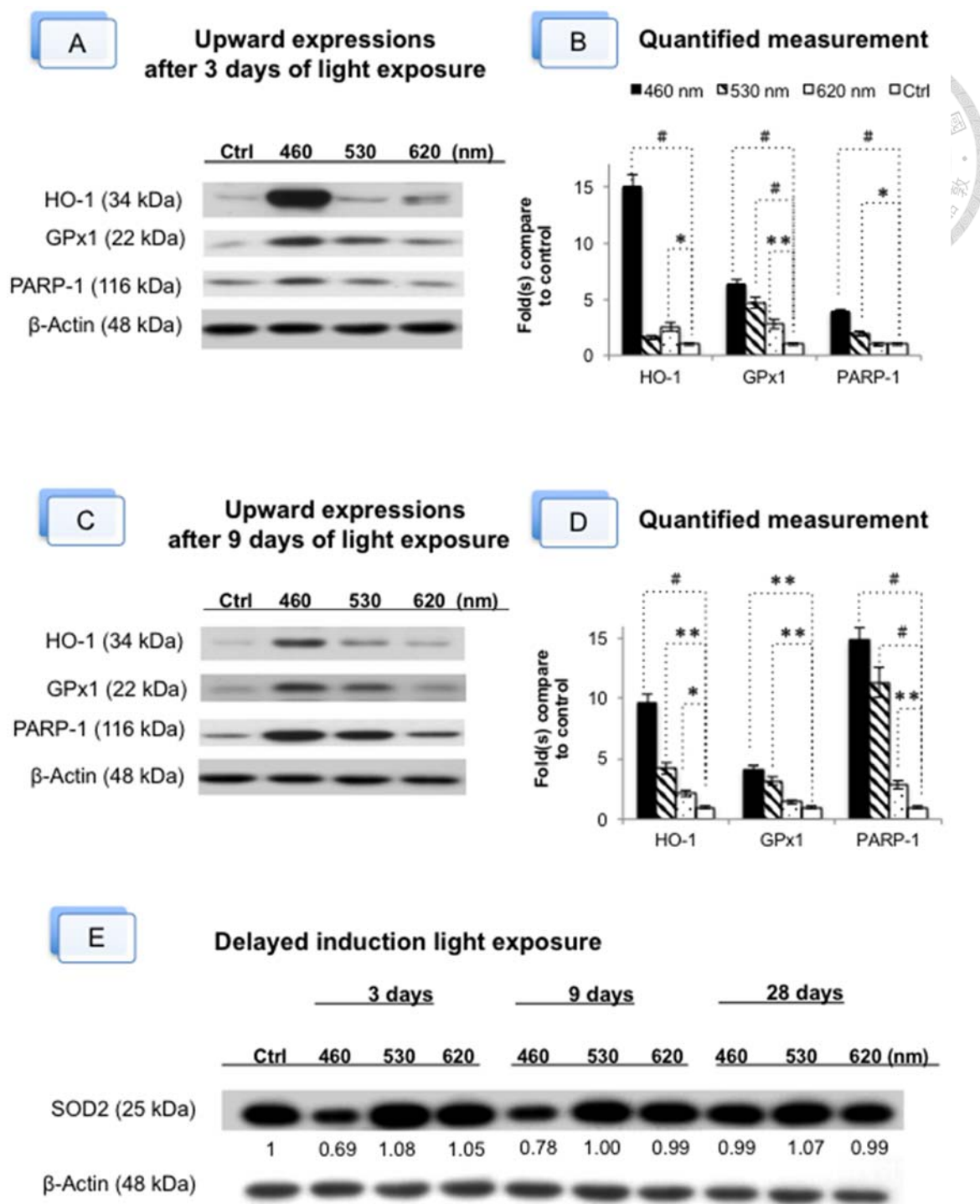


**Figure 40 Western blot (WB) assay of anti-oxidant enzymes**

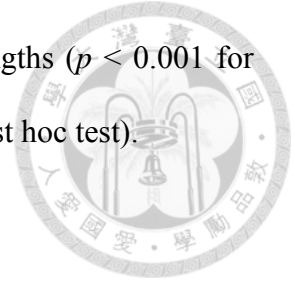
(A and B) After 3 days of light exposure, the antioxidant genes hemoxygenase-1 (HO-1) and cytosolic glutathione peroxidase (GPx1) were up-regulated after blue LED light exposure as an antioxidant response to all LED light insults, but the blue LED showed the strongest expression. The apoptotic marker PARP-1 showed greater densities after blue and green light exposure. (C and D) Clear wavelength-dependent expressions were found after 9 days of light exposure. (E) SOD2 was down-regulated, corresponding to the wavelengths after 3 or 9 days of light exposure, but the blue light activated a higher expression after 28 days of exposure due to the delayed/adaptive antioxidant response;  $n = 6$  for the control group and  $n = 8$  for each exposure group. (\*, \*\*, #  $p < 0.05, 0.01, 0.001$ , respectively, compared with the control group).

### 4.2.3 Iron metabolism and superoxide products

The WB results showed a strong association between iron metabolism and light injury resulting from 3 days of blue LED light exposure, as shown in Figure 41A. The ferroxidase ceruloplasmin (CP) that functions as an antioxidant (Figure 41B) by oxidizing iron from its ferrous ( $\text{Fe}^{2+}$ ) to ferric ( $\text{Fe}^{3+}$ ) form, ferritin (Ft, Figure 41C) for iron storage and ferroportin (Fpn, Figure 41D) for iron transportation were up-regulated, but transferrin (Tf, Figure 41E) and the transferrin receptor (TrfR, Figure 41F) for iron transportation between membranes were down-regulated as the wavelength decreased.

In Figure 42A, the  $\text{O}_2^{\cdot-}$  levels were significantly increased and reached 60,000 after 3 days of blue LED light exposure. The green and red LED light exposure groups accumulated smaller total counts, mostly less than 20,000. In Figure 42B, light exposure increased the  $\text{H}_2\text{O}_2$  concentrations in the retina, which indicates that ROS accumulation is involved in light-induced RPI. Blue LED light stimulated  $\text{H}_2\text{O}_2$  production to the highest concentration of 0.13 nmol/retina, whereas the green and red groups had 0.089 and 0.083 nmol/retina, respectively. In Figure 42C, the total iron concentration in the retina was also dominated by the LED light exposure. All three LED light exposures significantly increased the total iron concentration. Blue LED light exposure significantly increased the total iron concentration to 2 nmol/retina, and the normal retina only contained 0.35 nmol/retina of total iron. The longer wavelength exposures also increased the total iron concentration. The green LED group increased to 1 nmol/retina and the red LED group increased to 0.89 nmol/retina. In Figure 42D, the  $\text{Fe}^{3+}$  concentration in the retina also corresponded to the LED light exposure, which also demonstrated the oxidative

effects from exposure to LED lights with different wavelengths ( $p < 0.001$  for the blue light group by ANOVA followed by the Tukey's post hoc test).





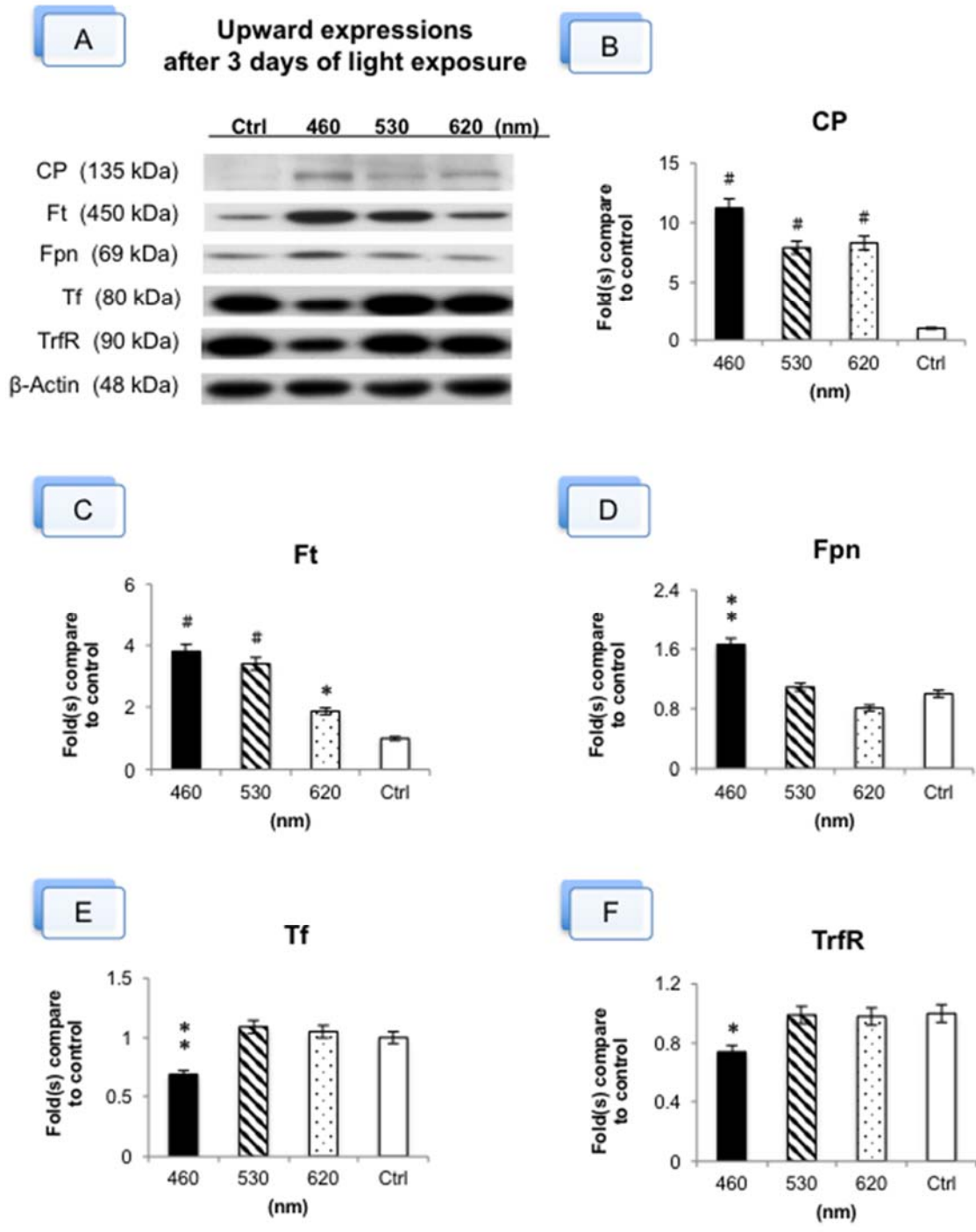


**Figure 41 Western blot (WB) assay of iron metabolism markers**

(A) A strong association between iron metabolism and light injury resulting from 3 days of blue LED light exposure. (B) Ceruloplasmin (CP), (C) ferritin (Ft), and (D) ferroportin (Fpn,) were up-regulated, but (E) transferrin (Tf) and (F) the transferrin receptor (TrfR) were down-regulated as the wavelength decreased; n = 8 for the control group and each exposure group. (\*, \*\*, #  $p < 0.05, 0.01, 0.001$ , respectively, compared with the control group).

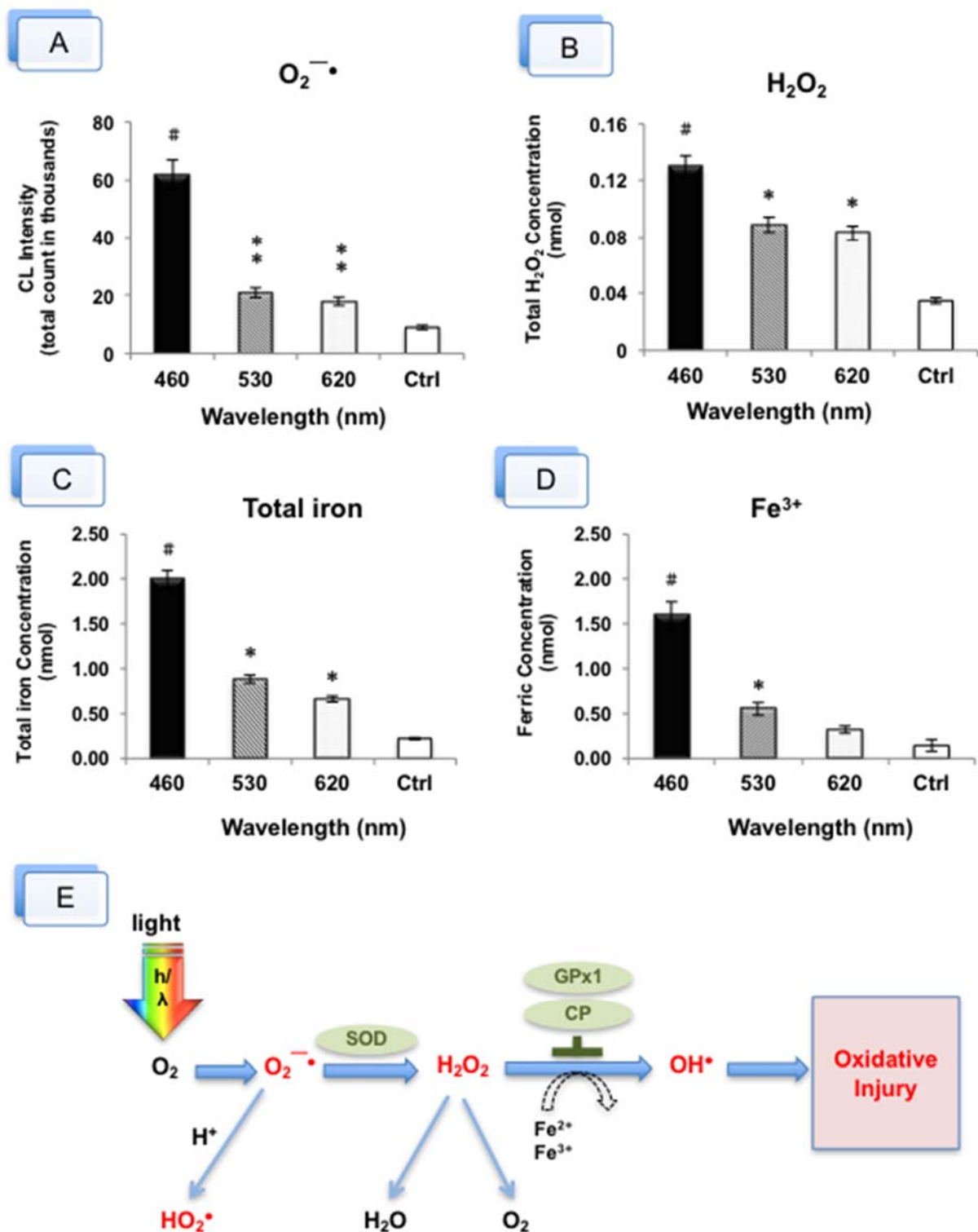


**Figure 42 Iron metabolism and superoxide products**

(A) Lucigenin-stimulated superoxide anion ( $O_2^{\cdot-}$ ) had reached 60,000 of chemiluminescence (CL), and the green and red LED light exposure groups accumulated 10,000 to 20,000 of CL in 8 min after 3 days of blue LED light exposure. (B) Blue light exposure increased hydrogen peroxide ( $H_2O_2$ ) concentrations and reached a high concentration of 0.13 nmol/retina, whereas the green and red

groups contained 0.089 to 0.083 nmol/retina, respectively. (C) Blue LED light exposure significantly increased the total iron concentration to 2 nmol/retina, whereas the normal retina only contains 0.23 nmol/retina of total iron. The longer wavelength exposures also increased the total iron concentration. The green LED group increased to 1 nmol/retina and the red LED group increased to 0.89 nmol/retina. (D) Blue LED light exposure significantly increased the ferric concentration to 1.6 nmol/retina, whereas the normal retina only contains 0.15 nmol/retina. The green LED exposure increased to 0.56 nmol/retina and the red LED exposure increased to 0.33 nmol/retina (\*, \*\*, #  $p < 0.05$ , 0.01, 0.001, respectively, compared with controls).  $n = 6$  for controls and  $n = 8$  for each exposure group. (E) Diagram of the oxidative pathway in the outer retina and RPE. As the retina absorbed the light under a high oxygen ( $O_2$ ) condition, superoxide anion radical ( $O_2^{\cdot-}$ ) is initially generated and converted to  $H_2O_2$ , then ultimately to  $H_2O$ . The  $O_2^{\cdot-}$  could easily convert to a toxic hydroperoxyl radical ( $HO_2$ ) during the process. The abnormal accumulation of  $H_2O_2$  under the high iron condition leads to a ferrous ion ( $Fe^{2+}$ ) being converted to the more injurious ferric ( $Fe^{3+}$ ). Although the  $Fe^{2+}$ -melanin complex is readily oxidized by  $H_2O_2$  and  $O_2$ , few highly noxious hydroxyl radicals ( $OH^{\cdot}$ ) escape the melanin polymer via a Fenton reaction and may develop injurious reactions. (Concept modified from Rozanowska, Malgorzata Barbara, 2009. <http://www.photobiology.info/Rozanowska.html> accessed 18 March 2015).

## 4.3 Discussion

### 4.3.1 Retinal light injury susceptibility between human and experimental animals

Retinal light injury depends on the duration of exposure and light level reaching the retina (retinal irradiance). The pathological process is also wavelength dependent <sup>71</sup>. The experiment results of the present study clearly demonstrate that exposure to LED light can induce retinal injury as evidenced by the functional ERG study, IHC, TUNEL and TEM examinations in an albino rat model. The results also demonstrated that this retinal injury could be related to the blue light-induced oxidative stress within the retinal tissues, as evidenced by the ROS generated in the retina after LED light exposure.

The ERG results clearly indicate functional loss in the retina after LED light exposure. The white and blue LED group demonstrated a significant decrease in the b-wave amplitude at day 9 and day 28 after light exposure. The morphological results show that cyclic white LED light exposure may cause outer retinal injury within 9 d and may cause further deterioration when the exposure duration is extended. ONL, which is usually 12-14 rows of nuclei in normal Sprague-Dawley rats at 2-3 months, was reduced to approximately 4-5 rows. OS and IS were absent, and the RPE appeared to be damaged or missing. However, yellow fluorescent light exposure induced less injury within the photoreceptor, as shown in Figure 30f. Therefore, above functional and morphological results indicate that the wavelength and the spectral power distribution (SPD) rather than total light irradiance, are crucial risk factors that contribute to photochemical retinal injury. The results of the present study also suggest that LED light-induced cell death may occur through the intrinsic apoptotic pathway under oxidative stress. However, Sliney calculated that for

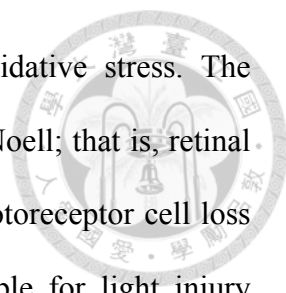
the same lamp brightness, the retinal irradiance in the rat eye would be at least 60% greater than experienced by the human retina <sup>72</sup>. The exposure started at 6:00 PM to match the nocturnal activity pattern may also enhance the light injury susceptibility. Therefore, the careful development of an action spectrum for LED light injury remains an important research goal.

#### 4.3.2 Oxidative stress induced injury

The retina is one of the highest oxygen-consuming tissues in the body and is sensitive to oxidative stress <sup>73</sup>. Oxidative stress is the crucial risk factor for photoreceptor degeneration, which is caused by the generation of toxic reactive oxidative species within retinal tissue. The retina contains enzymes involved in detoxification or synthesis, particularly in OS or RPE <sup>74</sup>. This report is an initial study to compare the phototoxicity with the fluorescent lamps and typical white LEDs. It is clear that typical white LED lights carry higher energy that exceeds the threshold of this stress-induced protection mechanism and results in severe injury to the outer retina. Therefore, some companies are increasing the market segments of lower color-temperature LEDs for domestic lighting selection.

#### 4.3.3 Low-intensity chronic exposure

Photochemical injury is the major cause of low-intensity chronic exposure light-induced injury. Noell indicated that the direct action of light on photoreactive molecules within the damaged cell causes primary injury. Secondary injury, which follows the primary event, can either continue the damaging process in the same cell or expand to other cells <sup>75</sup>. The main concern is that light injury involves oxidative events <sup>76</sup>. As shown in Figure 19, this study was designed to use several exposure durations in the study to analyze cause and effect in a temporal manner. The results of the present study show that LED



lights carry energy that is strong enough to generate oxidative stress. The experimental results are consistent with the observation by Noell; that is, retinal neuronal cell DNA levels and ERG b-wave estimates of photoreceptor cell loss correlate in light-injured rats. Oxidative stress is responsible for light injury pathogenesis, especially when light is sufficient to injury over 80% of photoreceptor cells detected by non-recoverable ERG b-waves. Furthermore, the histological analysis showed that most cell death does not occur immediately after light exposure. The damaged retinal neuronal cells may lose function, yet appear on the retina layers with oxidative modified lipids, nucleic acids, and proteins.

#### 4.3.4 LED-induced RPI is wavelength-dependent

Excessive LED light exposure presents a potential hazard to retinal function<sup>4</sup>. The previous study reported that a white light LED is more likely to induce RPI than is a CFL<sup>77</sup>. In the present study, the same irradiance level (102  $\mu\text{W}/\text{cm}^2$ ) for three light sources was used to conduct a more sophisticated experiment. This study analyzed the three major components of white light. As shown in Figure 35 (ERG), Figure 36 (H&E), and Figure 37 (TEM), the functional and morphological results suggested the blue light contributed the most to the RPI. The wavelength-dependent effect from the recent studies by Jaadane et al.<sup>45</sup> Bennet et al.<sup>37</sup> and Knels et al.<sup>38</sup> have similar results regardless of the different LED exposure intensities, durations, and experimental settings. Furthermore, the results agreed with the claim that wavelength is the determining factor rather than the total light irradiance<sup>38</sup> in terms of RPI.

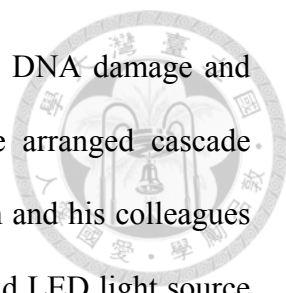
#### 4.3.5 Oxidative stress and photon absorption-stimulated RPI

The retina is a high oxygen environment with high oxygen tensions close

to 70 mmHg<sup>78</sup>, which is ideal for ROS formation. Absorption spectra explain how light absorption changes by wavelength<sup>14</sup>. The exposure of blue light increased the vulnerability to oxidative stress. The defense function in the retina creates high oxidative stress, which makes it extremely susceptible to RPI as reported by many previous studies<sup>23, 37, 38, 41, 43, 45-49, 53, 57, 58, 61, 79-82</sup>.

This study results demonstrated that ROS accumulation was involved in RPI. ROS caused cellular injury by attacking the macromolecules within the cells when the light exposure duration exceeds its threshold<sup>83</sup>. The oxidative stress markers such as 8-OHdG, acrolein and nitrotyrosine noticeably increased in the blue light-exposed retinas. The caspase-independent apoptotic marker, PARP-1, was significantly up-regulated in blue and green light-induced photoreceptor cell apoptosis after light exposure. This indicated the initiation of the retina cell apoptotic pathway. Furthermore, the antioxidant enzymes were produced to defend the insult, and the phagocytosis of toxicants or damaged debris by macrophage leading to the retina thickness decrease.

Apoptosis plays a major role in retinal visual cell loss<sup>57, 84-88</sup>. The caspase-dependent and caspase-independent pathways are the two major apoptotic pathways associated with retinal light injury have been reported<sup>41, 45, 49, 57, 58, 76, 89-96</sup>. There are various reports regarding caspase involvement in retinal light injury. As previously reported, prolonged white light exposure does not activate caspase-3 protein expression<sup>89</sup>, while blue light exposure increases its expression and leads to its activation<sup>95</sup>. The classical caspase did not show a consistent wavelength-dependent expression in the experiment, but the caspase-independent marker has in another report<sup>96</sup>. PARP-1 can induce apoptotic cell death when it is over-stimulated by excessive oxidant-induced DNA damage<sup>58</sup>.



The cleavage of PARP-1 inhibits the enzyme responding to DNA damage and secures substantial energy pools in the cells allowing the arranged cascade activities to occur in this type of apoptotic event<sup>58,93</sup>. Aydin and his colleagues also reported the retinal endoilluminator toxicity of xenon and LED light source in a rabbit model<sup>83</sup>. Although their study did not directly match the experimental setting of this study, it explained the potential effect of LED retinal light injury in different operation conditions.

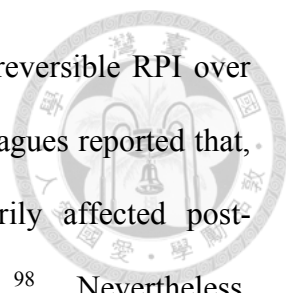
#### 4.3.6 Iron-related RPI oxidative pathway

As the retina absorbed the light under a high oxygen ( $O_2$ ) condition,  $O_2\cdot$  was initially generated and converted by anti-oxidant enzymes to  $H_2O_2$  and then ultimately to  $H_2O$ <sup>78</sup>. However, excessive short-wavelength light causes an imbalance in this conversion. Blue light irradiation accelerates the mitochondrial superoxide radical formation<sup>38</sup>. The  $O_2\cdot$  radicals can be easily converted to toxic hydroperoxyl radicals ( $HO^2\cdot$ ). Under the high iron condition, the abnormal accumulation of  $H_2O_2$  can lead to a  $Fe^{2+}$  oxidation to  $Fe^{3+}$ <sup>60,97</sup>. Although the  $Fe^{2+}$ -melanin complex is readily oxidized by  $H_2O_2$  and  $O_2$ , few highly noxious hydroxyl radicals ( $OH\cdot$ ) may escape from the melanin polymer via the quick interaction of melanin and  $OH\cdot$ ; causing further oxidative injuries. The above-mentioned process is illustrated in Figure 42E.

#### 4.3.7 Wavelength (hue) discrimination and specie differences

The permanent and serious injury from the blue LED exposure but the mild injury from the green and red LED exposure at the same irradiance level could possibly be explained by photoreceptor wavelength discrimination<sup>98</sup>. It is well established that blue light exposure results in irreversible RPI to the S (blue) cones. However, green light exposure is different in nature. Unlike the blue light,





which only affects the blue cones, green light may induce reversible RPI over both the M (green) and L (red) cones. Sperling and his colleagues reported that, in a rhesus monkey study, green light exposure primarily affected post-receptoral processes, not the receptors themselves <sup>98</sup>. Nevertheless, Kokkinopoulos reported that short period of 670 nm LED exposure may regulate innate immunity and alleviate RPI inflammation in a mouse model <sup>99</sup>.

However, the photoreceptor structure and functions are different between pigmented and albino species <sup>100, 101</sup>. It's been reported that albino SD rat has L-cones with a mean density of 2000 cells/mm<sup>2</sup> in their retina <sup>102</sup>. The S-cones are about 133 cells/mm<sup>2</sup> with a ratio of S- to L-cones of 1:15 <sup>103</sup>. Despite the population of S-cones are much less than M- or L-cones, S-cones are extremely sensitive to photons compare to the other two cones. Therefore, S-cones can be triggered instantly and easily result in exhaustion from over-excitement.

#### 4.3.8 Environmental health perspectives

Based on the findings, we understand that the albino strain is approximately twice as susceptible to RPI compared with the pigmented strain <sup>17</sup>, and the experimental results from this study cannot fully describe the injury mechanism and the theories apply to human from a rod dominated albino rats. However, from the environmental health perspective, it is necessary to urge manufactures to disclose the detail product specifications. Government agencies should further arrange that information available to the general public (as shown in Figure 43). Continuous investigations on potential light injuries to animal or human are also required to clarify the exposure risk and determinate the exact threshold.

### 2016 JA8 High Efficacy Lighting

Cancel



*Model Number	
<input type="text" value="SM16-07-10D-930-03"/>	
Manufacturer	Add Date
<input type="text" value="Soraa, Inc."/>	<input type="text" value="11/21/2016"/>
Brand	*Regulatory Status
<input type="text" value="Soraa Vivid"/>	<input type="text" value="N - Non Federally-Regulated"/>
Light Source Technology	Product Type
<input type="text" value="LD - Light Emitting Diode"/>	<input type="text" value="DL - Directional Lamp"/>
Connection Type	Light Source Dimming Type
<input type="text" value="GU - GU Base"/>	<input type="text" value="RPC - Reverse Phase Cut Controls"/>
Light Source Initial Efficacy (lumens/watt)	Rated Correlated Color Temperature (CCT)
<input type="text" value="54.3"/>	<input type="text" value="3000"/>
DUV	Color Rendering Index
<input type="text" value="0.0014"/>	<input type="text" value="95"/>
Color Rendering R9	Start Time (milliseconds)
<input type="text" value="98"/>	<input type="text" value="89"/>
Power Factor	Ambient or Elevated Temperature Test
<input type="text" value="0.91"/>	<input type="text" value="E - Elevated"/>
Rated life (hours)	Lumen Maintenance After 6,000 Hour Test (percent)
<input type="text" value="25000"/>	<input type="text" value="0.96"/>
Survival Rate After 6,000 Hour Test (percent)	IES LM-80 and TM-21 Projected L70 (inseparable SSL luminaires only) (hours)
<input type="text" value="1"/>	<input type="text"/>
Minimum Dimming Level (percent)	Audible Noise at 100% Light Output (dba)
<input type="text" value="0.04"/>	<input type="text" value="20"/>
Audible Noise at 20% Light Output (dba)	Flicker - Percent Amplitude at 100% Light Output (percent)
<input type="text" value="20"/>	<input type="text" value="0.06"/>
Flicker - Percent Amplitude at 100% Light Output and 1000Hz Cutoff Frequency (percent)	Flicker - Percent Amplitude at 100% Light Output and 400Hz Cutoff Frequency (percent)
<input type="text" value="0.05"/>	<input type="text" value="0.04"/>
Flicker - Percent Amplitude at 100% Light Output and 200Hz Cutoff Frequency (percent)	Flicker - Percent Amplitude at 100% Light Output and 90Hz Cutoff Frequency (percent)
<input type="text" value="0.04"/>	<input type="text" value="0"/>
Flicker - Percent Amplitude at 100% Light Output and 40Hz Cutoff Frequency (percent)	Flicker - Percent Amplitude at 20% Light Output (percent)
<input type="text" value="0"/>	<input type="text" value="0.29"/>
Flicker - Percent Amplitude at 20% Light Output and 1000Hz Cutoff Frequency (percent)	Flicker - Percent Amplitude at 20% Light Output and 400Hz Cutoff Frequency (percent)
<input type="text" value="0.22"/>	<input type="text" value="0.21"/>
Flicker - Percent Amplitude at 20% Light Output and 200Hz Cutoff Frequency (percent)	Flicker - Percent Amplitude at 20% Light Output and 90Hz Cutoff Frequency (percent)
<input type="text" value="0.19"/>	<input type="text" value="0.01"/>
Flicker - Percent Amplitude at 20% Light Output and 40Hz Cutoff Frequency (percent)	Flicker - Percent Amplitude at Minimum Light Output (percent)
<input type="text" value="0"/>	<input type="text" value="0"/>
Flicker - Percent Amplitude at Minimum Light Output and 1000Hz Cutoff Frequency (percent)	Flicker - Percent Amplitude at Minimum Light Output and 400Hz Cutoff Frequency (percent)
<input type="text" value="0"/>	<input type="text" value="0"/>
Flicker - Percent Amplitude at Minimum Light Output and 200Hz Cutoff Frequency (percent)	Flicker - Percent Amplitude at Minimum Light Output and 90Hz Cutoff Frequency (percent)
<input type="text" value="0"/>	<input type="text" value="0"/>

Figure 43 Light source registration at California energy commission

## 5 CONCLUSION

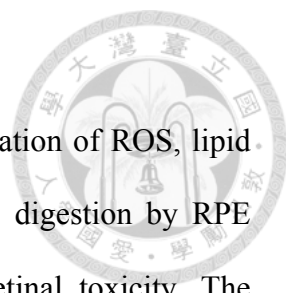


### 5.1 LED lighting induces retinal light injury

LEDs are expected to become the primary domestic light sources in the near future. Certain amounts of LED light exposure may induce retinal injury, and this animal model provides comparative measures of injury from different commercial light sources. Albino rats are commonly used for retinal light injury experiments. It has been reported that retinas from rats maintained in the dark for 14 days are more susceptible to light-induced injury than normal pigmented retinas. As a comparison, the study results show that the SPDs of bluish-white (high CCT) LEDs contain a major fraction of short-wavelength light that causes irreversible retinal neuronal cell death in rats. Furthermore, this model shows that the SPD of white LEDs now being introduced for domestic lighting pose a theoretical risk compared to CFLs (or incandescent lamps that have little blue light). When analyzing blue-light hazards, the risk of chronic effects from daily exposure cannot be excluded considering photochemical injury may not induce an acute syndrome; instead, blue light exposure may cumulatively induce photoreceptor loss.

Regardless of whether the initial injury is caused by a photochemical effect, LED light injury is dependent on wavelength and duration. The entire retinal neuronal cell is affected, regardless of whether the injury is localized in the outer segment, mitochondria, or other subcellular organelles. Because illuminance levels of LED domestic light sources may induce retinal degeneration in experimental albino rats, the exact risks for the pigmented human retina require further investigation.

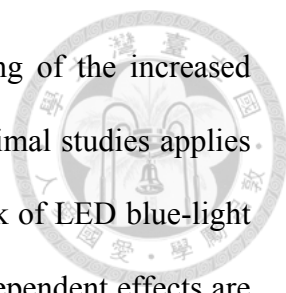
## 5.2 Blue light makes the most contribution to retinal light injury



There have been several investigations into the formation of ROS, lipid peroxidation, and the weakening of phagocytosis and POS digestion by RPE cells are thought to be the mechanism of iron-induced retinal toxicity. The increased Ft, Fpn, and CP (Figure 41) suggest that the retinal cells detected an increase in intracellular iron, which could be a sign for iron accumulation in all exposure groups. The strong expression of HO-1 in the blue light exposure group indicates its anti-oxidative function as reported by several publications previously. In contrast, HO-1 could also catalyze  $\text{Fe}^{2+}$  and carbon monoxide production, which may potentially exacerbate oxidative stress by generating free radicals. Moreover, SOD2 encoded by distinctive nuclear gene is localized in the mitochondrial matrix and converts the  $\text{O}_2^-$  generated by aerobic respiration to  $\text{H}_2\text{O}_2$ . This is the critical cell defense mechanism against the oxidative stress as reported previously. The activation of cytosolic glutathione peroxidase (GPx1) in the outer retina may also be an important factor in the response to photo-oxidative stress mitigating retinal lipid peroxidation, and CP acts as an antioxidant by oxidizing iron from its  $\text{Fe}^{2+}$  to  $\text{Fe}^{3+}$  form. The concomitant activation of several antioxidants in the same detoxification pathway could possibly be an indicator of short wavelength cytotoxicity superinduction. These defense gene expressions support that light-induced retinal degeneration involves oxidative stress. This study thus proposes that an iron-related RPI pathway, as shown in Figure 42E, based on these findings.

## 5.3 The way ahead

The continual development of blue light-based electrical panels and much brighter lighting environments pose concerns for retinal safety. The



experimental results have confirmed that the general finding of the increased RPI from blue light found from *in vitro* and anesthetized-animal studies applies to a free-running animal model. It also showed a greater risk of LED blue-light injury in awake, task-oriented rod-dominant animals. Four dependent effects are considered with light-induced retinal injury, including wavelength-, oxygen-, iron- (site-specific), and time/dose-dependent effects, which indicate a cumulative effect and a possible association with chronic ocular diseases. The associated oxidatively damaged biomolecules, cell destruction, and chronic inflammation should be carefully considered when switching to LED lighting. However, the exact mechanism underlying these effects will be the subject of ongoing investigation with more analytical methods. The interpretation from the animal study to human applications should also be carefully considered based on the risk assessment perspective.

Base on the study findings, this study proposes the following suggestions for LED domestic lighting application.

1. Manufacturers are advised to design LED lamps with less portion of short wavelengths.
2. Consumers should be educated to select yellow LED lamps (CCT < 4000) and reduce the brightness by applying dimmable fixtures for domestic lighting.
3. Reduce the total exposure time or allow a short break in between.
4. Consult with ophthalmologists before switching to LED lamps for domestic lighting, if a person has any pre-existing retinal diseases or special ocular conditions.
5. Governmental regulations should be reevaluated frequently

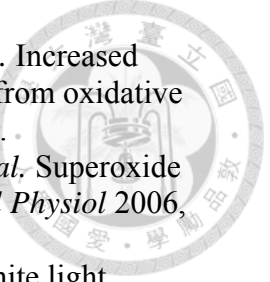
conforming the rapid improvement of the LED lighting technology. Proper certification and labeling of cautions are required before LED lamps being launched to the market.

6. Detail product specifications of all LED lamps should be disclosed by manufacturers which are approved by the government agencies. This product information can be accessed by the general public.
7. Future studies are suggested to focus on the pigmented species or occupational exposures to determine the exact risk and injury threshold to human.

## 6 REFERENCES

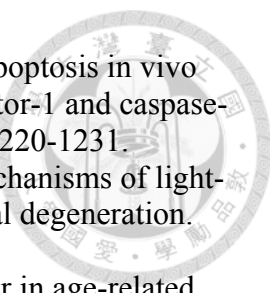


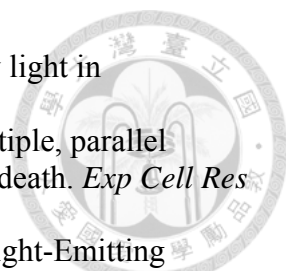
1. Mitchell TV, Maslin MT. How vision matters for individuals with hearing loss. *Int J Audiol* 2007, **46**(9): 500-511.
2. Youssef PN, Sheibani N, Albert DM. Retinal light toxicity. *Eye* 2011, **25**(1): 1-14.
3. Mattsson M-O, Jung T, Proykova A. Health effects of artificial light: Scientific Committee on Emerging and Newly Identified Health Risks (SCENIHR); 2012.
4. Behar-Cohen F, Martinsons C, Vienot F, Zissis G, Barlier-Salsi A, Cesarini JP, *et al.* Light-emitting diodes (LED) for domestic lighting: any risks for the eye? *Prog Retin Eye Res* 2011, **30**(4): 239-257.
5. Boyce PR. *Human Factors in Lighting*, 3rd edn. CRC press: New York, 2014, pp 458-488.
6. Mills E, Borg N. Trends in Recommended Lighting Levels: An International Comparison. *Journal of the Illuminating Engineering Society of North America* 1999, **28**(1): 155-163.
7. Held G. *Introduction to Light Emitting Diode Technology and Applications*, 1st edn. Auerbach Publications: New York, 2008, pp 79-102.
8. DiLaura D, Houser K, Mistrick R, Steffy G. *IES Lighting Handbook*, 10th edn. Illuminating Engineering Society: New York, 2011.
9. Vienot F. Quality of white light from LEDs. In: Mottier P, editor. *LEDs for lighting applications*. Hoboken, NJ: Wiley; 2010. p. 208.
10. Navigant Consulting I. Energy Savings Forecast of Solid-State Lighting in General Illumination Applications. Washington, D.C.: U.S. Department of Energy; 2014.
11. Kim JK, Schubert EF. Transcending the replacement paradigm of solid-state lighting. *Opt Express* 2008, **16**(26): 21835-21842.
12. Schubert EF, Kim JK, Luo H, Xi JQ. Solid-state lighting—a benevolent technology. *Reports on Progress in Physics* 2006, **69**(12): 3069-3099.
13. U.S. Department of Energy. LED-color-characteristics-factsheet. In: Energy Do, editor. Washington D.C.; 2012.
14. Sliney DH. How light reaches the eye and its components. *Int J Toxicol* 2002, **21**(6): 501-509.
15. Zrenner E. The role of electrophysiology and psychophysics in ocular toxicology. In: Fraunfelder TF, Fraunfelder WF, Chambers AW (eds). *Clinical Ocular Toxicology*. Elsevier: Portland OR, 2008, pp 21-38.
16. Wu J, Seregard S, Algyvere PV. Photochemical damage of the retina. *Surv Ophthalmol* 2006, **51**(5): 461-481.
17. Organisciak D, Zarbin M. Retinal photic injury. In: Levin LA, Albert DM (eds). *Ocular Disease Mechanisms and Management*. Elsevier London, 2010, pp 499-505.
18. Sliney DH. Photoprotection of the eye - UV radiation and sunglasses. *J Photochem Photobiol B* 2001, **64**(2-3): 166-175.
19. Sliney HD. Optical radiation hazard analysis; 2006.
20. Noell WK, Walker VS, Kang BS, Berman S. Retinal damage by light in rats. *Invest Ophthalmol* 1966, **5**(5): 450-473.
21. Glickman RD. Phototoxicity to the retina: mechanisms of damage. *Int J Toxicol* 2002, **21**(6): 473-490.

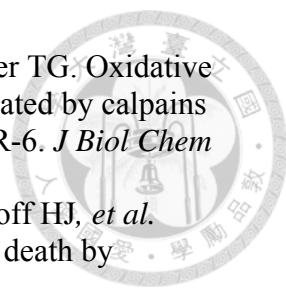
- 
22. Lu L, Oveson BC, Jo YJ, Lauer TW, Usui S, Komeima K, *et al.* Increased expression of glutathione peroxidase 4 strongly protects retina from oxidative damage. *Antioxidants & Redox Signaling* 2009, **11**(4): 715-724.
23. Dong A, Shen J, Krause M, Akiyama H, Hackett SF, Lai H, *et al.* Superoxide dismutase 1 protects retinal cells from oxidative damage. *J Cell Physiol* 2006, **208**(3): 516-526.
24. Kremers JJ, van Norren D. Retinal damage in macaque after white light exposures lasting ten minutes to twelve hours. *Invest Ophthalmol Vis Sci* 1989, **30**(6): 1032-1040.
25. Kuwabara T, Gorn RA. Retinal damage by visible light. An electron microscopic study. *Arch Ophthalmol* 1968, **79**(1): 69-78.
26. Albarracin R, Valter K. 670 nm red light preconditioning supports Muller cell function: evidence from the white light-induced damage model in the rat retina. *Photochem Photobiol* 2012, **88**(6): 1418-1427.
27. Mandal NA, Anderson RE, Ash JD. Injury and Repair: Light Damage. vol. 392-399. Elsevier, 2010.
28. Ham WT, Jr., Mueller HA, Sliney DH. Retinal sensitivity to damage from short wavelength light. *Nature* 1976, **260**(5547): 153-155.
29. Hunter JJ, Morgan JI, Merigan WH, Sliney DH, Sparrow JR, Williams DR. The susceptibility of the retina to photochemical damage from visible light. *Prog Retin Eye Res* 2012, **31**(1): 28-42.
30. Peng ML, Tsai CY, Chien CL, Hsiao JCJ, Huang SY, Lee CJ. The Influence of Low-powered Family LED Lighting on Eyes in Mice Experimental Model. *Life Sci J* 2012, **9**(1): 477.
31. Spivey A. The mixed blessing of phosphor-based white LED. *Environ Health Perspect* 2011, **119**(11): A472-473.
32. Holzman DC. What's in a color? The unique human health effect of blue light. *Environ Health Perspect* 2010, **118**(1): A22-27.
33. U.S. Department of Energy. Lifetime of white LED. In: Energy Do, editor. Washington D.C.; 2009.
34. Boulton M, Rozanowska M, Rozanowski B. Retinal photodamage. *Journal of photochemistry and photobiology B, Biology* 2001, **64**(2-3): 144-161.
35. Beatty S, Koh H, Phil M, Henson D, Boulton M. The role of oxidative stress in the pathogenesis of age-related macular degeneration. *Surv Ophthalmol* 2000, **45**(2): 115-134.
36. van Norren D, Gorgels TG. The action spectrum of photochemical damage to the retina: a review of monochromatic threshold data. *Photochem Photobiol* 2011, **87**(4): 747-753.
37. Bennet D, Kim MG, Kim S. Light-induced anatomical alterations in retinal cells. *Anal Biochem* 2013, **436**(2): 84-92.
38. Knels L, Valtink M, Roehlecke C, Lupp A, de la Vega J, Mehner M, *et al.* Blue light stress in retinal neuronal (R28) cells is dependent on wavelength range and irradiance. *Eur J Neurosci* 2011, **34**(4): 548-558.
39. Ueda T, Nakanishi-Ueda T, Yasuhara H, Koide R, Dawson WW. Eye damage control by reduced blue illumination. *Exp Eye Res* 2009, **89**(6): 863-868.
40. Osborne NN, Li GY, Ji D, Mortiboys HJ, Jackson S. Light affects mitochondria to cause apoptosis to cultured cells: possible relevance to ganglion cell death in certain optic neuropathies. *J Neurochem* 2008, **105**(5): 2013-2028.



- 
41. Seko Y, Pang J, Tokoro T, Ichinose S, Mochizuki M. Blue light-induced apoptosis in cultured retinal pigment epithelium cells of the rat. *Graefes Arch Clin Exp Ophthalmol* 2001, **239**(1): 47-52.
  42. Pang J, Seko Y, Tokoro T, Ichinose S, Yamamoto H. Observation of ultrastructural changes in cultured retinal pigment epithelium following exposure to blue light. *Graefes Arch Clin Exp Ophthalmol* 1998, **236**(9): 696-701.
  43. Kuse Y, Ogawa K, Tsuruma K, Shimazawa M, Hara H. Damage of photoreceptor-derived cells in culture induced by light emitting diode-derived blue light. *Sci Rep* 2014, **4**: 5223.
  44. Ogawa K, Kuse Y, Tsuruma K, Kobayashi S, Shimazawa M, Hara H. Protective effects of bilberry and lingonberry extracts against blue light-emitting diode light-induced retinal photoreceptor cell damage in vitro. *BMC Complement Altern Med* 2014, **14**: 120.
  45. Jaadane I, Boulenguez P, Chahory S, Carre S, Savoldelli M, Jonet L, *et al.* Retinal damage induced by commercial light emitting Diodes (LED). *Free Radic Biol Med* 2015, **84**: 373–384.
  46. Geiger P, Barben M, Grimm C, Samardzija M. Blue light-induced retinal lesions, intraretinal vascular leakage and edema formation in the all-cone mouse retina. *Cell Death Dis* 2015, **6**: e1985.
  47. Narimatsu T, Negishi K, Miyake S, Hirasawa M, Osada H, Kurihara T, *et al.* Blue light-induced inflammatory marker expression in the retinal pigment epithelium-choroid of mice and the protective effect of a yellow intraocular lens material in vivo. *Exp Eye Res* 2015, **132**: 48-51.
  48. Yu ZL, Qiu S, Chen XC, Dai ZH, Huang YC, Li YN, *et al.* Neuroglobin - A potential biological marker of retinal damage induced by LED light. *Neuroscience* 2014, **270**: 158-167.
  49. Kim GH, Kim HI, Paik SS, Jung SW, Kang S, Kim IB. Functional and morphological evaluation of blue light-emitting diode-induced retinal degeneration in mice. *Graefes Arch Clin Exp Ophthalmol* 2016, **254**(4): 705-716.
  50. Wu J, Chen E, Soderberg PG. Failure of ascorbate to protect against broadband blue light-induced retinal damage in rat. *Graefes Arch Clin Exp Ophthalmol* 1999, **237**(10): 855-860.
  51. Roehlecke C, Schaller A, Knels L, Funk RH. The influence of sublethal blue light exposure on human RPE cells. *Mol Vis* 2009, **15**: 1929-1938.
  52. Chamorro E, Bonnin-Arias C, Perez-Carrasco MJ, Munoz de Luna J, Vazquez D, Sanchez-Ramos C. Effects of light-emitting diode radiations on human retinal pigment epithelial cells in vitro. *Photochem Photobiol* 2013, **89**(2): 468-473.
  53. King A, Gottlieb E, Brooks DG, Murphy MP, Dunaief JL. Mitochondria-derived reactive oxygen species mediate blue light-induced death of retinal pigment epithelial cells. *Photochem Photobiol* 2004, **79**(5): 470-475.
  54. Lascaratos G, Ji D, Wood JP, Osborne NN. Visible light affects mitochondrial function and induces neuronal death in retinal cell cultures. *Vision Res* 2007, **47**(9): 1191-1201.
  55. Bravo-Nuevo A, Williams N, Geller S, Stone J. Mitochondrial deletions in normal and degenerating rat retina. *Adv Exp Med Biol* 2003, **533**: 241-248.
  56. Huang H, Li F, Alvarez RA, Ash JD, Anderson RE. Downregulation of ATP synthase subunit-6, cytochrome c oxidase-III, and NADH dehydrogenase-3 by bright cyclic light in the rat retina. *Invest Ophthalmol Vis Sci* 2004, **45**(8): 2489-2496.

- 
57. Donovan M, Cotter TG. Caspase-independent photoreceptor apoptosis in vivo and differential expression of apoptotic protease activating factor-1 and caspase-3 during retinal development. *Cell Death Differ* 2002, **9**(11): 1220-1231.
58. Wenzel A, Grimm C, Samardzija M, Reme CE. Molecular mechanisms of light-induced photoreceptor apoptosis and neuroprotection for retinal degeneration. *Prog Retin Eye Res* 2005, **24**(2): 275-306.
59. Dunaief JL. Iron induced oxidative damage as a potential factor in age-related macular degeneration: the Cogan Lecture. *Invest Ophthalmol Vis Sci* 2006, **47**(11): 4660-4664.
60. Ugarte M, Osborne NN, Brown LA, Bishop PN. Iron, zinc, and copper in retinal physiology and disease. *Surv Ophthalmol* 2013, **58**(6): 585-609.
61. Hadziahmetovic M, Kumar U, Song Y, Grieco S, Song D, Li Y, *et al.* Microarray analysis of murine retinal light damage reveals changes in iron regulatory, complement, and antioxidant genes in the neurosensory retina and isolated RPE. *Invest Ophthalmol Vis Sci* 2012, **53**(9): 5231-5241.
62. Marc RE, Jones BW, Watt CB, Vazquez-Chona F, Vaughan DK, Organisciak DT. Extreme retinal remodeling triggered by light damage: implications for age related macular degeneration. *Mol Vis* 2008, **14**: 782-806.
63. Jones BW, Marc RE. Retinal remodeling during retinal degeneration. *Exp Eye Res* 2005, **81**(2): 123-137.
64. Hafezi F, Marti A, Munz K, Reme CE. Light-induced apoptosis: differential timing in the retina and pigment epithelium. *Exp Cell Res* 1997, **64**(6): 963-970.
65. Hsu YJ, Wang LC, Yang WS, Yang CM, Yang CH. Effects of fenofibrate on adiponectin expression in retinas of streptozotocin-induced diabetic rats. *Journal of diabetes research* 2014, **2014**: 540326.
66. Schatz A, Arango-Gonzalez B, Fischer D, Enderle H, Bolz S, Röck T, *et al.* Transcorneal electrical stimulation shows neuroprotective effects in retinas of light-exposed rats. *Invest Ophthalmol Vis Sci* 2012, **53**(9): 5552-5561.
67. Collier RJ, Wang Y, Smith SS, Martin E, Ornberg R, Rhoades K, *et al.* Complement deposition and microglial activation in the outer retina in light-induced retinopathy: inhibition by a 5-HT<sub>1A</sub> agonist. *Invest Ophthalmol Vis Sci* 2011, **52**(11): 8108-8116.
68. Fang IM, Yang CM, Yang CH, Chiou SH, Chen MS. Transplantation of induced pluripotent stem cells without C-Myc attenuates retinal ischemia and reperfusion injury in rats. *Exp Eye Res* 2013, **113**: 49-59.
69. Gordon WC, Casey DM, Lukiw WJ, Bazan NG. DNA damage and repair in light-induced photoreceptor degeneration. *Invest Ophthalmol Vis Sci* 2002, **43**(11): 3511-3521.
70. Meewes C, Brenneisen P, Wenk J, Kuhr L, Ma W, Alikoski J, *et al.* Adaptive antioxidant response protects dermal fibroblasts from UVA-induced phototoxicity. *Free Radic Biol Med* 2001, **30**(3): 238-247.
71. Organisciak DT, Vaughan DK. Retinal light damage: mechanisms and protection. *Prog Retin Eye Res* 2010, **29**(2): 113-134.
72. Sliney DH. Quantifying retinal irradiance levels in light damage experiments. *Curr Eye Res* 1984, **3**(1): 175-179.
73. Yu DY, Cringle SJ. Retinal degeneration and local oxygen metabolism. *Exp Eye Res* 2005, **80**(6): 745-751.
74. Newsome DA, Dobard EP, Liles MR, Oliver PD. Human retinal pigment epithelium contains two distinct species of superoxide dismutase. *Invest Ophthalmol Vis Sci* 1990, **31**(12): 2508-2513.

- 
75. Noell WK. Possible mechanisms of photoreceptor damage by light in mammalian eyes. *Vision Res* 1980, **20**(12): 1163-1171.
76. Lohr HR, Kuntchithapautham K, Sharma AK, Rohrer B. Multiple, parallel cellular suicide mechanisms participate in photoreceptor cell death. *Exp Cell Res* 2006, **83**(2): 380-389.
77. Shang YM, Wang GS, Sliney D, Yang CH, Lee LL. White Light-Emitting Diodes (LEDs) at Domestic Lighting Levels and Retinal Injury in a Rat Model. *Environ Health Perspect* 2014, **122**(3): 269-276.
78. Boulton M, Rozanowska M, Rozanowski B. Retinal photodamage. *J Photochem Photobiol B* 2001, **64**(2-3): 144-161.
79. Organisciak DT, Darrow RM, Rapp CM, Smuts JP, Armstrong DW, Lang JC. Prevention of retinal light damage by zinc oxide combined with rosemary extract. *Mol Vis* 2013, **19**: 1433-1445.
80. Organisciak DT, Wong P, Rapp C, Darrow R, Ziesel A, Rangarajan R, *et al.* Light-induced retinal degeneration is prevented by zinc, a component in the age-related eye disease study formulation. *Photochem Photobiol* 2012, **88**(6): 1396-1407.
81. Zhang TZ, Fan B, Chen X, Wang WJ, Jiao YY, Su GF, *et al.* Suppressing autophagy protects photoreceptor cells from light-induced injury. *Biochem Biophys Res Commun* 2014, **450**(2): 966-972.
82. Hahn P, Lindsten T, Lyubarsky A, Ying GS, Pugh EN, Jr., Thompson CB, *et al.* Deficiency of Bax and Bak protects photoreceptors from light damage in vivo. *Cell Death Differ* 2004, **11**(11): 1192-1197.
83. Aydin B, Dinc E, Yilmaz SN, Altiparmak UE, Yulek F, Ertekin S, *et al.* Retinal endoilluminator toxicity of xenon and light-emitting diode (LED) light source: rabbit model. *Cutan Ocul Toxicol* 2014, **33**(3): 192-196.
84. Chang GQ, Hao Y, Wong F. Apoptosis: final common pathway of photoreceptor death in rd, rds, and rhodopsin mutant mice. *Neuron* 1993, **11**(4): 595-605.
85. Portera-Cailliau C, Sung CH, Nathans J, Adler R. Apoptotic photoreceptor cell death in mouse models of retinitis pigmentosa. *Proc Natl Acad Sci U S A* 1994, **91**(3): 974-978.
86. van Soest S, Westerveld A, de Jong PT, Bleeker-Wagemakers EM, Bergen AA. Retinitis pigmentosa: defined from a molecular point of view. *Surv Ophthalmol* 1999, **43**(4): 321-334.
87. Dunaief JL, Dentchev T, Ying GS, Milam AH. The role of apoptosis in age-related macular degeneration. *Arch Ophthalmol* 2002, **120**(11): 1435-1442.
88. Boulton ME, Mitter SK, Rao HV, Dunn WA. Cell Death, Apoptosis, and Autophagy in Retinal Injury. In: Ryan SJ, Schachat AP, Wilkinson CP, Hinton DR, Sadda S, Wiedemann P (eds). *Retina*, 5th edn, vol. 1. Elsevier: London, 2013, pp 537-552.
89. Li F, Cao W, Anderson RE. Alleviation of constant-light-induced photoreceptor degeneration by adaptation of adult albino rat to bright cyclic light. *Invest Ophthalmol Vis Sci* 2003, **44**(11): 4968-4975.
90. Chahory S, Keller N, Martin E, Omri B, Crisanti P, Torriglia A. Light induced retinal degeneration activates a caspase-independent pathway involving cathepsin D. *Neurochem Int* 2010, **57**(3): 278-287.
91. Tomita H, Kotake Y, Anderson RE. Mechanism of protection from light-induced retinal degeneration by the synthetic antioxidant phenyl-N-tert-butyl nitron. *Invest Ophthalmol Vis Sci* 2005, **46**(2): 427-434.

- 
92. Sanvicens N, Gomez-Vicente V, Masip I, Messeguer A, Cotter TG. Oxidative stress-induced apoptosis in retinal photoreceptor cells is mediated by calpains and caspases and blocked by the oxygen radical scavenger CR-6. *J Biol Chem* 2004, **279**(38): 39268-39278.
93. Yu SW, Wang H, Poitras MF, Coombs C, Bowers WJ, Federoff HJ, *et al.* Mediation of poly(ADP-ribose) polymerase-1-dependent cell death by apoptosis-inducing factor. *Science* 2002, **297**(5579): 259-263.
94. Sparrow JR, Cai B. Blue light-induced apoptosis of A2E-containing RPE: involvement of caspase-3 and protection by Bcl-2. *Invest Ophthalmol Vis Sci* 2001, **42**(6): 1356-1362.
95. Wu J, Gorman A, Zhou X, Sandra C, Chen E. Involvement of caspase-3 in photoreceptor cell apoptosis induced by in vivo blue light exposure. *Invest Ophthalmol Vis Sci* 2002, **43**(10): 3349-3354.
96. Li GY, Osborne NN. Oxidative-induced apoptosis to an immortalized ganglion cell line is caspase independent but involves the activation of poly(ADP-ribose)polymerase and apoptosis-inducing factor. *Brain Res* 2008, **1188**: 35-43.
97. Rozanowski B, Burke JM, Boulton ME, Sarna T, Rozanowska M. Human RPE melanosomes protect from photosensitized and iron-mediated oxidation but become pro-oxidant in the presence of iron upon photodegradation. *Invest Ophthalmol Vis Sci* 2008, **49**(7): 2838-2847.
98. Sperling HG, Wright AA, Mills SL. Color vision following intense green light exposure: data and a model. *Vision Res* 1991, **31**(10): 1797-1812.
99. Kokkinopoulos I. 670 nm LED ameliorates inflammation in the CFH(-/-) mouse neural retina. *J Photochem Photobiol B* 2013, **122**: 24-31.
100. Wasowicz M, Morice C, Ferrari P, Callebert J, Versaux-Botteri C. Long-term effects of light damage on the retina of albino and pigmented rats. *Invest Ophthalmol Vis Sci* 2002, **43**(3): 813-820.
101. Ortin-Martinez A, Jimenez-Lopez M, Nadal-Nicolas FM, Salinas-Navarro M, Alarcon-Martinez L, Sauve Y, *et al.* Automated quantification and topographical distribution of the whole population of S- and L-cones in adult albino and pigmented rats. *Invest Ophthalmol Vis Sci* 2010, **51**(6): 3171-3183.
102. Chrysostomou V, Stone J, Valter K. Life history of cones in the rhodopsin-mutant P23H-3 rat: evidence of long-term survival. *Invest Ophthalmol Vis Sci* 2009, **50**(5): 2407-2416.
103. Szel A, Rohlich P. Two cone types of rat retina detected by anti-visual pigment antibodies. *Exp Eye Res* 1992, **55**(1): 47-52.

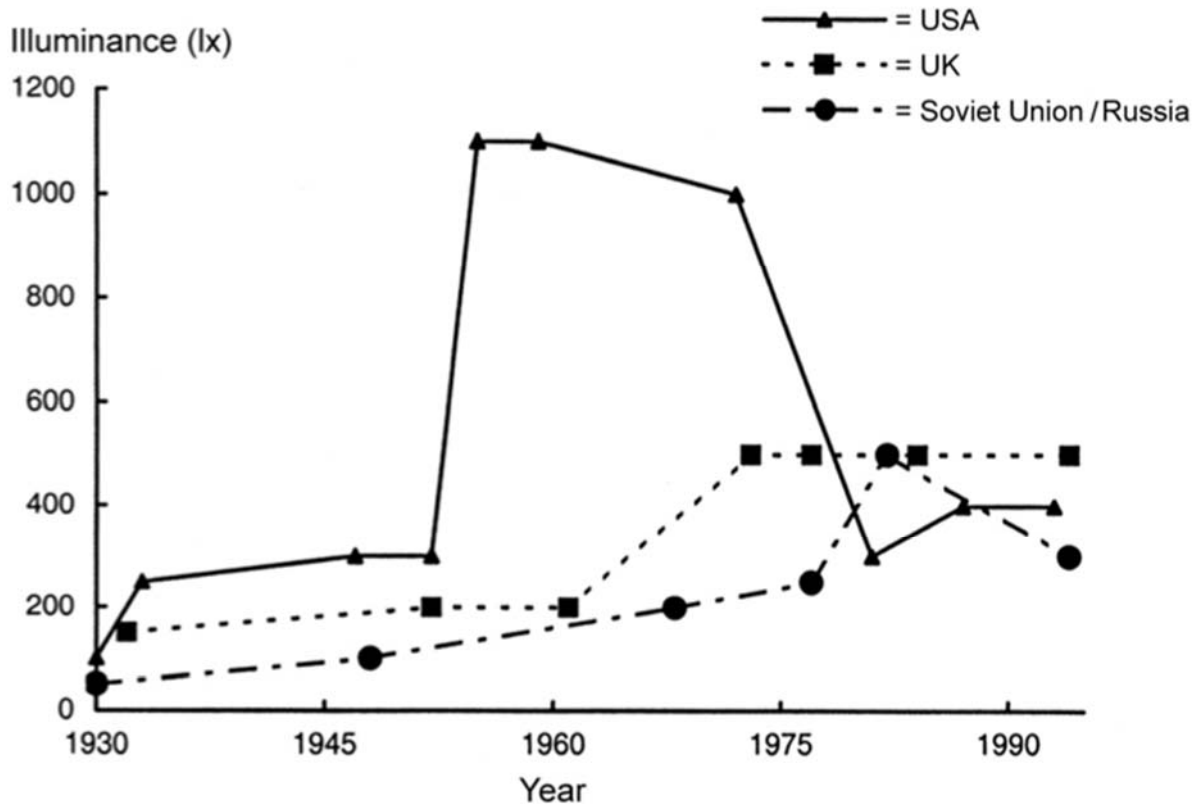


**Fig. 2** Illuminance recommendations fluctuations since 1930

Mills and Borg (1999) have reviewed the illuminance recommendations made in 19 different countries. Above figure shows the changes in illuminance on a horizontal plane recommended for general offices at different times in the US, UK, and the Soviet Union/Russia. Clearly, there are wide differences between different countries in the illuminance recommended for the same application. From their review, Mills and Borg (1999) conclude that the historical pattern has been for recommended illuminances to increase over time by up to a factor of 10 until the early 1970s after which there was stabilization or a decline. The current trend in illuminance recommendations is towards a convergence to similar values in different countries, values that are significantly lower than in earlier decades.

The changes in lighting recommendations over time reveal a fact about all lighting recommendations that should always be remembered. Lighting recommendations are not immutable. They are not like the laws of physics, nor are they written on tablets of stone. Rather, they represent the best efforts of people to decide on reasonable lighting recommendations in the prevailing conditions. To

reach this decision for any particular application, a number of factors have to be considered.

First, there is what might be called the aims of the lighting. For each application it is necessary to consider the relative weights to be given to task visibility, task performance, observer comfort, and perceived impression. Once the aims of the lighting have been specified the necessary lighting conditions can be derived from any available experimental evidence and from practical experience. Second, there is the extent to which the lighting desired could be achieved with available equipment. There is little point in recommending lighting that cannot be achieved. Third, the economics need to be assessed. What does it cost to produce and operate the recommended lighting from the available equipment? There is little point in recommending lighting that is not economically viable.

These three factors: the desired lighting, its technical possibility, and its cost to produce and operate are all considered before making a decision about lighting criteria. The point to grasp from all this is that recommended illuminances, and all other quantitative lighting criteria, are matters of judgment, involving the balancing of several factors. Therefore, they inevitably represent a consensus view of what is reasonable for the conditions prevailing when they are written (Boyce, 1996). That consensus will be different in different countries, and vary at different times in the same country, depending on the state of knowledge about lighting, the technical and most importantly social-economic situation, and the interests of the people contributing to the consensus.

**\* This appendix is adapted and edited from Boyce PR. *Human Factors in Lighting*, 2nd edn. CRC press: New York, 2003, pp 494-497.**